

ABSTRACT

In the light of the increasing terrorist SAMs threat to civil and military aircraft, the need of a high-fidelity, low-cost, IR signature scene modelling and simulation capability that could be used for development, testing and evaluation of IRCM systems cannot be overlooked.

The performance evaluation, training and testing of IR missiles or other IR based weapon systems, is very expensive and is also dependent upon atmospheric factors. Whereas, the computer based non-destructive simulation can provide a cost-effective alternative to field trials.

An effort has been made to model the IR scene signature using virtual reality modelling tools and integrating this model into the missile-target engagement and countermeasure simulator. The developed algorithm can simulate passive IR imaging seeker engagements with aerial targets. The presented algorithm uses the developed models for IR signature of the target, the background, the flare spectral and temporal responses and the flare ballistic trajectory. The missile guidance, auto-pilot and tracker algorithms have also been developed. The atmospheric conditions have been modelled, using LOWTRAN, as “good”, “typical” or “bad” to account for atmospheric transmittance and the sky-radiance. The results were analysed and validated through four test scenarios. The code is written in MATLAB which gives it openness for user verification/validation and also flexibility for any future modifications.

The work presented may help the IRCM designer and pilots to evaluate potential strategies to defeat the imaging seeker threat.

DEDICATION

Specially dedicated with love and prayers to my mother who is suffering from “Pulmonary Fibrosis” disease.

Secondly, dedicated to my father, sisters and brother who have always prayed and guided me throughout my life.

Finally, dedicated to my gorgeous wife and lovely children for their patience and support during my PhD.

ACKNOWLEDGEMENTS

I was able to accomplish this immense task mainly because of the whole hearted support, valuable guidance, professional critic and moral support extended to me by Dr. Mark A. Richardson, who has supervised this research, leading to PhD thesis, in a very friendly and encouraging atmosphere. I am extremely thankful to Dr Mark for all his support and the time he devoted for in depth review of my thesis.

Many of the ideas explored in this research were contributed by individuals who gave their time and supported me at different stages of this work. In particular, I would like to thank Professor Richard Ormondroyd, Dr. Martin L. Fair of DSTL (UK), Dr Evan Hughes, Dr. Robin Jenkin, Dr. John Coath, Mr. Roy Walmsley of Chemring Countermeasures, High Post, UK and Dr. Peter Silson.

I would like to thank my departmental staff for their support. Also, I would like to thank fellow research students at Post Graduated Centre for staying long hours together and sharing ideas.

Finally, I would like to thank the NUST, Pakistan for sponsoring me and Pakistan Air Force for sparing me for this research work.

TABLE OF CONTENTS

ABSTRACT	ii
DEDICATION	iii
ACKNOWLEDGEMENTS	iv
TABLE OF CONTENTS	v
LIST OF TABLES	xv
LIST OF FIGURES	xvii
ACRONYMS	xxiii
1 INTRODUCTION	1
1.1 Background	1
1.2 Aim	1
1.3 Objectives	1
1.4 Need of IR Signature Modelling and Simulation	2
1.5 Why Commercial Off-the-Shelf?.....	2
1.6 Future Utility.....	3
1.7 Summary	3
2 IR Radiations and Signature	5
2.1 Introduction.....	5
2.2 Infrared Radiations.....	6
2.2.1 Plank’s Law for Blackbody Radiations	6
2.2.2 Radiant Properties of Materials	7
2.2.3 Emissivity	8
2.2.4 Spectral Radiance.....	8
2.2.5 Power	9
2.2.6 Solid Angle	10
2.2.7 Projected Area.....	11
2.3 Sources of Radiation	11
2.3.1 Sources of Radiation on Jet Aircraft.....	12
2.3.2 Sources of Radiation on Ground Vehicles.....	14
2.4 Transmission of Infrared Radiation through Earth’s Atmosphere.....	15
2.4.1 Atmospheric Transmittance Calculation Software	15
2.4.2 Atmospheric Transmittance	17

2.4.3	Atmospheric Path-radiance	18
2.5	IR Signature Scene Model Ingredients	19
2.5.1	Targets.....	19
2.5.2	Background as Clutter or Source	20
2.5.3	Thermally Static IR Background	20
2.6	Low and High-Fidelity IR Signature Models	21
2.7	Conclusion	21
3	IR Guided Missiles.....	23
3.1	Introduction.....	23
3.2	Evolution of Heat Seeking Missiles.....	23
3.2.1	First Generation Seekers	23
3.2.2	Second Generation Seekers.....	26
3.2.3	Third Generation Seekers	29
3.2.4	Fourth Generation Seekers.....	31
3.3	Missile Tracking Techniques.....	33
3.3.1	Gated Video Tracker.....	33
3.3.2	Correlation Tracker.....	34
3.4	Missile Guidance	35
3.4.1	Line-of-Sight Guidance	35
3.4.2	Homing Guidance	36
3.4.3	Navigational Guidance.....	36
3.4.4	Compound Guidance	36
3.4.5	Guided Missile Trajectories.....	37
3.4.6	Proportional Navigation Guidance	40
3.4.7	Pursuit Course Guidance.....	42
3.5	Missile Controls	43
3.6	Missile Aerodynamics	44
3.6.1	Aerodynamics Drag	44
3.6.2	Lateral Acceleration of the Missile.....	45
3.7	Missile Fuses.....	46
3.8	Summary	46
3.9	Conclusion	47
4	Infrared countermeasures.....	49

4.1	Introduction.....	49
4.2	Defence against Heat Seeking Missiles	49
4.2.1	Pre-Launch Defence.....	49
4.2.2	Post Launch Defence	49
4.3	Infrared Signature Suppression.....	50
4.3.1	Suppressing Heat Source	51
4.3.2	Reducing Emissivity	51
4.4	Infrared Countermeasures.....	51
4.5	Off-board IRCM Flares.....	52
4.5.1	Conventional Flares	53
4.5.2	Multi-spectral Flares	53
4.5.3	Special Material Decoy.....	54
4.5.4	Electronically Configurable IR Towed Decoy	55
4.5.5	Kinematics or Fly-along Flares.....	55
4.5.6	Flare Performance Factors	55
4.5.7	Flare Limitations.....	58
4.5.8	Flight Guard Self Protection System	58
4.5.9	Wide-body Integrated Platform Protection System.....	58
4.5.10	Comet IRCM Pod	58
4.6	Active IR Countermeasures	59
4.6.1	Advanced Threat Infrared Countermeasures	59
4.6.2	Directional IRCM	60
4.6.3	Large Aircraft Infrared Countermeasures	60
4.6.4	Tactical Aircraft Directional IRCM.....	61
4.6.5	Closed-loop IR Countermeasures	61
4.6.6	Mobile Tactical High-energy Laser.....	61
4.7	Missile Approach Warning System	62
4.8	IR Counter-countermeasures against IRCM Flares.....	63
4.9	Improvements in Flares Design	64
4.10	Terrorist Missile Threat to Commercial Airlines.....	64
4.11	IRSS and IRCM System Analysis and Evaluation Software.....	66
4.11.1	DSTL Fly-in 2000 Model	66
4.11.2	Tactical Engagement Simulation Software.....	67

4.11.3	Chemring Countermeasures CounterSim	67
4.12	Summary	68
4.13	Conclusion	69
5	Simulation and Modelling	71
5.1	Introduction.....	71
5.2	Simulation and Modelling.....	71
5.2.1	Types of Simulation.....	71
5.2.2	Uses of Simulation and Modelling	72
5.2.3	Application of Modelling and Simulation in Military Systems.....	73
5.2.4	Low cost PC Based Systems.....	74
5.2.5	Military Simulators Developed around COTS Software	74
5.2.6	Commercial Modelling Tools	76
5.3	Computer Graphics Hardware	76
5.3.1	Applications of Hardware Graphics.....	76
5.3.2	Advantages of Hardware Graphics	77
5.3.3	Computer Graphics Card	77
5.3.4	Integrated Graphics Processor	79
5.3.5	Graphics Hardware Manufacturers	80
5.3.6	AGP and PCI Express	80
5.3.7	Nvidia® SLI Technology	81
5.4	Graphics APIs	81
5.4.1	OpenGL®	81
5.4.2	Architecture Review Board.....	82
5.4.3	Difference between Direct3D and OpenGL	82
5.5	Realism	83
5.5.1	Physical Realism.....	83
5.5.2	Photo Realism	83
5.5.3	Functional Realism	84
5.6	Computer Graphics Rendering	84
5.6.1	Rendering Pipeline Stages	84
5.6.2	Types of Rendering.....	85
5.6.3	Illumination Techniques	87
5.7	Virtual Reality Modelling Language	87

5.7.1	Military Vehicles 3D Virtual Reality Models.....	88
5.7.2	Open Inventor™ vs VRML	89
5.8	Virtual Reality Toolbox	89
5.8.1	V-Realm™ Builder/Editor	90
5.8.2	Virtual Reality Viewer	90
5.8.3	MATLAB VRML Interface	90
5.9	MATLAB® Aerospace Blockset.....	91
5.10	Microsoft Flight Simulator	91
5.11	Unmanned Dynamics AeroSim Blockset	92
5.12	FlightGear Flight Simulator.....	92
5.13	Conclusion	93
6	Development of an IR Signature Model.....	95
6.1	Introduction.....	95
6.2	IR Signature Modelling of the Background.....	95
6.2.1	Background Input Parameters.....	95
6.2.2	Sky-radiance Data Sets	96
6.2.3	Calculating Background Radiance.....	98
6.2.4	Multiple Backgrounds or Sub-backgrounds	99
6.3	IR Signature Modelling of the Targets	100
6.3.1	Target Input Parameters	100
6.3.2	Calculating Radiance of the Target.....	101
6.3.3	More Realistic Targets with Different Temperature Zones.....	102
6.3.4	Adding Reflection Effects to the Model	103
6.3.5	Modelling IR Signature of the Exhaust Gas Plume.....	105
6.4	IR Signature Modelling of IRCM (Flares).....	109
6.4.1	Input Data Required for Flare IR Signature Modelling	109
6.4.2	Assumptions for Modelling Flare IR Signature.....	110
6.4.3	Modelling IR Spectral Response of Flare	110
6.4.4	Modelling Temporal Response of IR Flare	111
6.5	Modelling Atmospheric Effects on IR Signature.....	113
6.5.1	Inputs Required to Generate Atmospheric Transmission Data.....	114
6.5.2	Transmittance to Atmospheric Attenuation Coefficient Conversion.....	115
6.5.3	Wave-numbers to Micrometers Conversion	116

6.5.4	Calculating Atmospheric Transmittance for each Target	117
6.5.5	Scattering Effects of the Atmosphere	117
6.5.6	Modelling Atmospheric Path-radiance	118
6.6	Modelling Missile IR Detector and Optics	119
6.6.1	Missile Input Parameters.....	119
6.7	Calculating Power Received at the Detector	120
6.7.1	Calculating Projected Area of the Detector	121
6.7.2	Calculating Solid-angle of Seeker Optics	121
6.7.3	Exposed Area of Targets as Projected on Background.....	122
6.7.4	Point Source or Extended Source Target.....	123
6.7.5	Background Area	123
6.7.6	Power received at the Detector Due to Target and Background.....	124
6.7.7	Lock-on Range or Maximum Range Prediction	126
6.7.8	Fidelity of the Model	126
6.8	Data Stored in Excel Spreadsheets	127
6.9	Source Code of the Main Algorithm.....	128
6.10	Conclusion	128
7	Modelling the IR Scene in a 3D Virtual World.....	131
7.1	Introduction.....	131
7.2	Why VRML	131
7.3	Developing the 3D Virtual World.....	131
7.4	Military Targets 3D VRML Models	132
7.4.1	F-16 Fighting Falcon 3D VRML Model.....	132
7.4.2	C-130 Hercules 3D VRML Model	133
7.4.3	T-62 Tank 3D VRML Model.....	135
7.4.4	Boeing B-737 3D VRML Model	136
7.4.5	Helicopter 3D VRML Model.....	137
7.5	Altering Target VRML Model for IR Signature Modelling	137
7.5.1	Grouping Parts as Sub-targets.....	138
7.5.2	Modelling Appearance of Sub-targets	139
7.5.3	Controlling the Translation and Rotation fields of the Target.....	145
7.5.4	Adding Leading-edge Geometry.....	146
7.5.5	Adding Exhaust Gas Plume Geometry	147

7.6	Modelling IR Background	148
7.7	Modelling IR Atmosphere as “Fog” in VRML.....	150
7.8	Modelling Multiple Viewpoints.....	151
7.9	Modelling Missile Optics and Seeker-head	152
7.9.1	Missile Optics Field-of-View	153
7.9.2	FOV to Focal Length Conversion.....	155
7.9.3	Modelling “NavigationInfo” Node for Missile Seeker View	155
7.10	Modelling IR Flare Geometry and Aerodynamics.....	157
7.10.1	Inputs for Flare Modelling	157
7.10.2	Assumptions for Flare Modelling	158
7.10.3	Modelling Flare Pallet Geometry.....	159
7.10.4	Modelling Flare IR Plume 3D Geometry.....	160
7.10.5	Modelling Flare Dispenser.....	162
7.10.6	Modelling Flare Plume Appearance	164
7.10.7	Modelling Flare Trajectory in 3D	165
7.11	VRML vs IR Comparrision Summary.....	172
7.12	Conclusion	174
8	Target Manoeuvrability and Missile Guidance and Control Modelling	175
8.1	Introduction.....	175
8.2	VR World Fields for Target and Missile Movement.....	175
8.3	Assumptions for Missile and Target Movement.....	177
8.3.1	Target Degree-of-freedom	177
8.3.2	Missile Degree-of-freedom.....	178
8.3.3	Targets Initial Position.....	178
8.3.4	Information about Missile Launch.....	178
8.4	User Inputs and Typical Data Ranges.....	179
8.5	An Aircraft in a Level Turn	180
8.5.1	Effects of Turn-radius and Rate-of-turn on Aircraft Performance	182
8.6	Target and Missile Increment in one Time Frame.....	184
8.7	Rate-of-Climb or Rate-of-Descent.....	185
8.8	Target Manoeuvrability	186
8.8.1	Straight-and-Level Modes	186
8.8.2	Level-Turn Modes	188

8.8.3	Take-off and Landing Modes.....	189
8.8.4	Spiral Descent Mode.....	189
8.8.5	Complex Manoeuvres	190
8.8.6	Modelling Level Flight Modes	190
8.8.7	Modelling Turn Modes	191
8.9	Cartesian Coordinates and Axis Angle.....	194
8.10	Missile Guidance and Control Modelling.....	196
8.10.1	Missile Gimbal Initial Direction Modelling	196
8.10.2	Capturing Frame from 3D VR Viewer	200
8.10.3	Converting RGB Image into Gray-scale Image and Binary Image ...	201
8.10.4	Centroid Tracking as Target Location Estimation.....	202
8.10.5	Calculating Target Error from Bore-sight.....	206
8.10.6	Sign Conversions in VRML and MATLAB.....	208
8.10.7	Updating Gimbal Rotation Field.....	209
8.10.8	Gimballed Seeker Head Maximum Angle Limit.....	211
8.10.9	Updating Missile Translation Fields.....	212
8.10.10	Modelling Missile Lateral Acceleration Limit	213
8.10.11	Updating Missile_LOS Rotation Field	216
8.11	Missile Miss-distance and Hit-Criterion.....	217
8.12	Conclusion	218
9	Simulation Results, Analysis and Validation	219
9.1	Introduction.....	219
9.2	System Requirements.....	219
9.2.1	Hardware Requirements.....	219
9.2.2	Software Requirements.....	220
9.2.3	Software Control.....	220
9.3	Presenting Simulation Results	220
9.3.1	Numerical Data	220
9.3.2	Graphical Representation.....	221
9.3.3	3D Virtual Reality.....	221
9.4	Modelling and Simulation Steps.....	221
9.5	Explanation of the Test Scenario No. 1	222
9.5.1	Input Data for Test Scenario No. 1	223

9.5.2	Results of Test Scenario No. 1.....	224
9.5.3	Discussion on Results of Test Scenario No. 1	231
9.6	Explanation of the Test Scenario No. 2	233
9.6.1	Input Data for Test Scenario No. 2	233
9.6.2	Results of Test Scenario No. 2.....	235
9.6.3	Discussion on Results of Test Scenario No. 2.....	243
9.7	Explanation of the Test Scenario No. 3	245
9.7.1	Inputs Data for Test Scenario No. 3.....	246
9.7.2	Results of Test Scenario No. 3.....	247
9.7.3	Discussion on Results of Test Scenario No. 3	252
9.8	Explanation of the Test Scenario No. 4	254
9.8.1	Input Data for Test Scenario No. 4	255
9.8.2	Results of Test Scenario No. 4.....	256
9.8.3	Discussion on Results of Test Scenario No. 4.....	261
9.9	Validation of Results.....	262
9.9.1	Need for Validation.....	262
9.9.2	Validation Methods.....	263
9.9.3	Flare Trajectory Validation.....	263
9.9.4	Missile LATAX and Centroid Tracking Algorithm Validation	266
9.9.5	Validations of Code	267
9.10	IRCM Analysis and Validation using Published Results	268
9.10.1	IRCM Analysis Scenario Generation and Input Parameters.....	268
9.10.2	Comparison of Results of First IRCM Analysis Approach	268
9.10.3	Adding Kinematic CCM Module in Seeker Algorithm.....	275
9.10.4	Changes in Target Aircraft Manoeuvrability Algorithm	277
9.10.5	Missile Orientated to Look Directly at Target at Launch	279
9.10.6	IRCM analysis with Kinematic CCM Seeker.....	280
9.10.7	Discussion on Results of IRCM Analysis with Kinematic CCM.....	284
9.11	Summary	287
10	Conclusions and Recommendations.....	289
10.1	Introduction.....	289
10.2	Research Objectives.....	289
10.3	Thesis Conclusions	289

10.3.1	IR Signature Modelling.....	290
10.3.2	Missile Modelling	291
10.3.3	IRCM Modelling.....	291
10.3.4	Missile-target Engagement Simulation.....	292
10.3.5	Extracts form IRCM Analysis	292
10.3.6	Fidelity of the Model and the Assumptions Made.....	293
10.4	Contributions.....	296
10.5	Limitations	297
10.6	Recommendations for Future Research Work.....	298
10.6.1	IR Signature Modelling.....	298
10.6.2	Missile Modelling	299
10.6.3	Target Modelling	300
10.6.4	IRCM Flare modelling.....	301
10.6.5	Running Simulation	301
10.6.6	IRCM Further Analysis.....	302
10.6.7	Directional-IRCM Modelling and Analysis.....	302
10.7	Further Validation.....	303
10.8	Conclusions.....	304
	REFERENCES.....	305
	ANNEX “I” VRML Light Model	
	ANNEX “II” VRML nodes and Fields for IR Signature Modelling	

LIST OF TABLES

Table 2-1 : Composition of atmospheric constituent gases	16
Table 2-2 : Radiant properties of various sources.	19
Table 4-1 : Typical signature levels of airborne platforms	58
Table 4-2 : Active IR countermeasure systems for military aircraft	59
Table 4-3 : IRCM systems developed for the protection of commercial airliners.....	66
Table 5-1 : Virtual Reality Models available on the internet.....	89
Table 6-1 : Background input parameters.....	96
Table 6-2 : Typical LOWTRAN input parameters for calculating sky-radiance	97
Table 6-3 : Target input parameters.....	101
Table 6-4 : LOWTRAN inputs for three weather conditions	114
Table 6-5 : LOWTRAN inputs to calculate atmospheric transmittance.....	115
Table 6-6 : Missile input parameters	120
Table 7-1 : Material fields to model different material types	143
Table 7-2: Atmospheric Parameters as function of height.....	166
Table 7-3 : Summary of VRML nodes and fields used for IR signature scene modelling	173
Table 8-1 : Typical input data ranges	179
Table 8-2 : Rate-of-turn and Turn-radius Calculated Values	183
Table 8-3 : Summary of ROT and TR for different cases	184
Table 8-4 : Target manoeuvrability different modes	191
Table 8-5 : Aircraft translation and rotation fields for turned flight modes	193
Table 8-6 : VR Toolbox functions used for capturing 2D image	200
Table 9-1: Numerical results of Test Scenario No. 1 for “good” weather.....	225
Table 9-2: Numerical results of Test Scenario No. 1 for “typical” weather.....	226
Table 9-3: Numerical results Test Scenario No. 1 for “bad” weather	227
Table 9-4 : Target input parameters for test scenario No 2	234
Table 9-5 : Input material properties of the sub-targets for test scenario No. 2	235
Table 9-6 : Outputs of test scenario No. 2 for 3 to 5 micron waveband.....	236
Table 9-7 : Outputs of test scenario No. 2 for 8 to 12 micron waveband.....	237
Table 9-8 : Summary of Colour-map response in 3-5 and 8-12 micron wavebands .	243
Table 9-9 : Input material properties of the flare for test scenario No. 4	255

Table 9-10 : Outputs of test scenario No. 4 for 3 to 5 micron waveband.....	256
Table 9-11 : Outputs of test scenario No. 4 for 8 to 12 micron waveband.....	256
Table 9-12: List of validation of code.....	267
Table 9-13 : Input parameters for IRCM Analysis	269
Table 9-14 : Summary of simulation results of fast jet deploying flare	274
Table 9-15 : Modified aircraft translation and rotation fields for level-turn modes..	279
Table 9-16 : Summary of the IRCM analysis results of the CounterSim and my simulator	284
Table 10-1: List of features available in the model and the assumptions made	294

LIST OF FIGURES

Figure 2-1 : The Electromagnetic Spectrum	5
Figure 2-2 : Spectral radiant exitance of blackbody	7
Figure 2-3 : Spectral emissivity of three types of radiators	8
Figure 2-4 : Geometry used in power definition.....	10
Figure 2-5 : Geometry used in solid angle definition	11
Figure 2-6 : Projected area calculations.....	11
Figure 2-7 : Sources of radiations on an aircraft.....	12
Figure 2-8 : Exhaust temperature contours for Turbo-jet engine with and without afterburner	13
Figure 2-9 : Transmittance of atmosphere at sea level	18
Figure 3-1: Block Diagram of First Generation (Spin-Scan) Seeker.....	23
Figure 3-2 : Rising-Sun Reticle showing Amplitude Modulation and Null-Phase Sector	24
Figure 3-3: Typically Atmospheric Transmission with IR Emitters	25
Figure 3-4: Improved First Generation Reticle.....	25
Figure 3-5: SA-7 a First Generation Seeker System.....	26
Figure 3-6: Second Generation Seeker Schematic.....	27
Figure 3-7: Wagon Wheel Reticle Showing Frequency Modulation Outputs.....	28
Figure 3-8: AIM-9L a Second Generation Seeker System	28
Figure 3-9: Open-Cross Detector Showing Frequency Modulation Outputs	29
Figure 3-10: Risley Prisms to Generate Pseudo Image Scanning.....	29
Figure 3-11 : Resley Scan Patterns	30
Figure 3-12: Stinger-RMP a Third Generation Seeker System	30
Figure 3-13: Illustration of a Typical Target on a Staring Array.....	31
Figure 3-14: Spectral Output of a Typical Plume	32
Figure 3-15 : Binary centroid of target image	34
Figure 3-16 : Straight-line Trajectory	37
Figure 3-17 : Line-of-sight Trajectory	38
Figure 3-18 : Proportional Navigation Trajectory	38
Figure 3-19 : Pure Pursuit Course Trajectory	39

Figure 3-20 : Pure pursuit and Proportional navigation explained.....	41
Figure 3-21 : Pure Pursuit Course Guidance	42
Figure 3-22 : Missile six degrees-of-freedom.....	44
Figure 4-1 : Spectrally balanced array Flares	54
Figure 4-2 : Liquid Pyrophoric Infrared Flares.....	55
Figure 4-3 : Typical flare decoy/target spectra	57
Figure 4-4 : MANPAD Threat Area on Takeoff and Landing	65
Figure 5-1: Functional block diagram of graphics card.....	78
Figure 5-2 : MATLAB VRML Coordinates System	91
Figure 6-1 : Sky-radiance in good weather for various altitudes.....	98
Figure 6-2 : Sub-backgrounds or multiple-background.....	100
Figure 6-3 : Aircraft thermal radiation sources.....	103
Figure 6-4 : IR signature elements of an aircraft	104
Figure 6-5 : Transmission, reflection and absorption of thermal radiations.....	105
Figure 6-6 : Exhaust plume modelled as Co-centric cylindrical regions.....	106
Figure 6-7 : simplified aircraft jet engine exhaust plume	107
Figure 6-8 : Spectral emissivity of the exhaust gas plume	109
Figure 6-9 : IR flare plume modelled as co-centric cones	111
Figure 6-10 : Temporal response of flare	113
Figure 6-11 : Atmospheric transmission of 1 km path length	114
Figure 6-12 : LOWTRAN actual data vs. interpolated data	117
Figure 6-13 : Scenario with three targets at different ranges from seeker.....	121
Figure 6-14 : Target exposed area on the background.....	123
Figure 6-15 : Explaining background area.....	124
Figure 7-1 : Orthographic projection of F-16 model	133
Figure 7-2 : VRML 3D model of F-16 before modifications	133
Figure 7-3 : C-130 Hercules Orthographic projection.....	134
Figure 7-4 : VRML 3D model of C-130 Hercules aircraft	134
Figure 7-5 : T-62 tank 3D VRML model.....	135
Figure 7-6 : Boeing-737 3D VRML model	136
Figure 7-7 : 3D VRML model of a military helicopter	137
Figure 7-8 : Different colour-maps supported by MATLAB	145
Figure 7-9 : F-16 3D VRML model after modifications	147

Figure 7-10 : Exhaust gas plume modelled as co-centric cones	147
Figure 7-11 : F-16 3D VRML model with exhaust gas plume	148
Figure 7-12 : Instantaneous field-of-view.....	154
Figure 7-13 : Horizontal and Vertical Field-of-view	155
Figure 7-14 : Flare pallet 3D geometry.....	160
Figure 7-15 : Flare plume 3D geometry	161
Figure 7-16 : Modelling Flare ejection direction.....	163
Figure 7-17 : Drag Coefficient of different shapes	167
Figure 7-18 : Aircraft and flare velocity Vectors in 3D world coordinates.....	168
Figure 7-19 : Aircraft and Flare velocity components.....	170
Figure 8-1 : Target translation and rotation Fields	176
Figure 8-2 : Missile and gimbals translation and rotation Fields.....	177
Figure 8-3 : Aircraft six degree-of-freedom	178
Figure 8-4 : An aircraft in level turn.....	182
Figure 8-5 : Rate-of-climb explanation.....	186
Figure 8-6 : Target Manoeuvres straight-and-level modes.....	187
Figure 8-7 : Target manoeuvres level turn modes	188
Figure 8-8 : Target take-off and landing modes	189
Figure 8-9 : Target manoeuvre spiral descent mode.....	189
Figure 8-10 : Direction Cosines of a Unit vector.....	194
Figure 8-11 : Cartesian coordinates and direction cosines	196
Figure 8-12 : Target and missile relative positions in 3D view	197
Figure 8-13 : 2D views of target and missile relative positions	199
Figure 8-14 : Explaining binary centroid.....	203
Figure 8-15 : Explaining intensity centroid	205
Figure 8-16 : Flow diagram of centroid tracking algorithm	206
Figure 8-17 : Error signals from bore sight	207
Figure 8-18 : Geometry explaining size of one pixel in meters.....	207
Figure 8-19 : Sign for translation and rotation fields as per four quadrants	209
Figure 8-20 : Total error vector magnitude and direction.....	211
Figure 8-21 : Flow diagram explaining gambal maximum angle limit	212
Figure 8-22 : Calculating missile angle	213
Figure 8-23 : Flow chart explaining missile ROT limit logic.....	214

Figure 8-24 : Explaining missile new position in next frame	216
Figure 8-25 : Considering Hit-criterion as a cylindrical region in front of missile ...	218
Figure 9-1: Window for entering targets locations	224
Figure 9-2: Lock-on range of five targets for different weather conditions	228
Figure 9-3 : Atmospheric transmission for 3 to 5 micron waveband	228
Figure 9-4 : Atmospheric transmission data for 8 to 12 micron waveband.....	229
Figure 9-5: Sky radiance for 3 to 5 micron waveband.....	229
Figure 9-6: Sky radiance for 8 to 12 micron waveband.....	230
Figure 9-7: Image showing 5 targets at different ranges for “good” weather conditions	230
Figure 9-8: Image showing 5 targets at different ranges for “typical” weather conditions.....	231
Figure 9-9: Image showing 5 targets at different ranges for “bad” weather conditions	231
Figure 9-10 : The spectral emissivity of the exhaust gas plume.....	234
Figure 9-11 : Dimensions of the exhaust gas plume geometry.....	235
Figure 9-12 : 256x256 image of target aircraft at 0.75 km range from beam aspect.	238
Figure 9-13 : 256x256 image of target aircraft at 0.75 km range from nose aspect..	238
Figure 9-14 : 256x256 image of target aircraft at 0.75 km range from tail aspect	239
Figure 9-15 : 256x256 image of target aircraft without background from beam aspect	239
Figure 9-16 : target aircraft image without background captured from nose aspect .	240
Figure 9-17 : Target aircraft image without background captured from tail aspect ..	240
Figure 9-18 : target image in 3 to 5 micron band with and without reflection effects	241
Figure 9-19 : Target image in 3 to 5 micron band without background	241
Figure 9-20 : Target/background image in 8 to 12 micron band showing reflection effects.....	242
Figure 9-21 : Target image in 8 to 12 micron band without background	242
Figure 9-22 : Air-to-air Missile chasing straight and level target aircraft	248
Figure 9-23 : XZ-view of missile chasing straight and level target.....	248
Figure 9-24 : Air-to-air missile chasing the target aircraft in level turn.....	249
Figure 9-25 : XZ-view of air-to-air missile chasing the target aircraft in level turn .	249

Figure 9-26 : Surface-to-air Missile chasing a target in level-turn	250
Figure 9-27 : XZ-view of surface-to-air missile chasing target in level-turn	250
Figure 9-28 : YZ-view of surface-to-air missile chasing target in level-turn	251
Figure 9-29 : XY-view of the surface-to-air missile chasing target in level-turn.....	251
Figure 9-30 : Centroid output of Binary and Intensity centroid trackers.....	252
Figure 9-31 : Centroid output of Binary and Intensity centroid trackers with flare ..	252
Figure 9-32 : 256x256 image of aircraft with flare at 1.5 km range from beam aspect	257
Figure 9-33 : 256x256 image of aircraft with flare at 1.5 km range without background.....	257
Figure 9-34 : Flare temporal response	258
Figure 9-35 : Affect of C_D on 300 gm flare eject downward.....	258
Figure 9-36 : Affect of C_D on 300 gm flare ejected forward	259
Figure 9-37 : Affect of pallet mass on trajectory for flare fired downward	259
Figure 9-38 : Affect of pallet mass on trajectory for flare fired forward.....	260
Figure 9-39 : Flare trajectory for different eject angles	260
Figure 9-40 : Flare separation for selected airspeeds at 1500 meters altitude	265
Figure 9-41 : Simulated flare separation for selected airspeeds at 1500 meters altitude	265
Figure 9-42 : Typical fast jet deploying standard flare fired backward.....	270
Figure 9-43 : Fast jet deploying standard flare fired straight forward.....	270
Figure 9-44 : Fast jet deploying standard flare fired downward.....	271
Figure 9-45 : Aerodynamic flare C_D 1.0 fired forward @ -30° pitch	271
Figure 9-46 : Fast jet deploying standard flare C_D 2.4 fired in different directions ..	272
Figure 9-47 : Fast jet deploying aerodynamic flare C_D 1.0 in different directions....	273
Figure 9-48 : Fast jet deploying aerodynamic flare C_D 0.1 fired in different directions	274
Figure 9-49 : Explaining missile CCM maximum separation	276
Figure 9-50 : Flow diagram explaining the missile kinematics CCM algorithm	277
Figure 9-51 : Standard flare C_D 10.0 fired backward	281
Figure 9-52 : Standard flare C_D 10.0 fired downward	281
Figure 9-53 : Standard flare C_D 10.0 fired forward	282
Figure 9-54 : Aerodynamic flare C_D 1.0 fired forward @ -30 deg pitch.....	282

Figure 9-55 : Aerodynamic flare C_D 1 fired forward @-30 deg pitch from aircraft in-
turn283
Figure 9-56 : Aerodynamic flare C_D 0.1 fired forward @ -30 deg pitch.....284

ACRONYMS

6DOF	Six degree-of-freedom
AAMs	Air-to-air missile
AB	After burner
ACM	Association of Computing Machinery
ADAM	Aircraft decoy Assessment Model
ADAM	Aircraft Decoy Assessment Model
AFIWC	Airforce Information Warfare Centre
AFRL	Airforce Research Laboratory
AGC	Automatic Gain Control
AGP	Accelerated Graphics Port
AH	Attack Helicopter
AIRCMM	Advance IRCM Munition
AIRSAM	Advanced IRCM Assessment Model
AJEM	Advance Joint Effectiveness Model
AM	Amplitude Modulation
AMCOM	U.S. Army Aviation and Missile Command
AMRAAMs	Advanced Medium-range Air-to-air Missiles
AMRDEC	Aviation and Missile Research, Engineering and Development Centre
API	Application Programmers Interface
APNG	Augmented Proportional Navigation Guidance
ARB	Architectural Review Board
ASE	Aircraft Survivability Equipment
ASRAAM	Airborne Short-range Air-to-air Missile
ASTE	Advanced Strategic and Tactical Infrared Expendables
ATAGS	Automatic Target Acquisition and Guidance System
ATD	Advance Technology Demonstrator
ATIRCM	Advanced Threat Infrared Countermeasures
BRDF	Bidirectional Reflectance Distribution Function
CAD	Computer Aided Design
CFD	Chaff and Flare Dispensation
CLIRCM	Closed-loop IRCM
CLOS	Command to LOS Guidance
CMD&V	Countermeasures Development and Validation
CMT	Mercury Cadmium Telluride (HgCdTe)
CMWS	Common Missile Warning System
CO ₂	Carbon dioxide
COTS	Commercial off-the-shelf
CPU	Central Processing Unit
DAS	Defensive Aids Suits
DHS	Department of Homeland Security (USA)
DIRCM	Directional IRCM

DISP	Dynamic Infrared Scene Projector
DMA	Direct memory access
DOF	Degree of freedom
EGT	Exhaust Gas Temperature
FASCODE	Fast Atmospheric Signature Code
FLIR	Forward Looking Infrared
FM	Frequency modulation
FMS	Flight Motion Simulator
FOM	Figure of merit
FOR	Field-of-regard
FOV	Field-of-view
ftp	File transfer protocol
GLU	Graphical Language Utility (OpenGL)
GMA	Graphics Media Accelerator
GOT	Guide-on-the-target
GOTS	Government off-the-shelf
GPS	Global Positioning System
GPU	Graphics processing unit
GSE	Ground Support Equipment
GSMVT	Ground Systems modeling validation and testing conference
GVT	Gated Video Tracker
H ₂ O	Di-hydrogen monoxide (water)
HgCdTe	Mercury Cadmium Telluride (CMT)
HITL	Human-in-the-loop
HITRAN	High Resolution Transmission Molecular Absorbance Database
HORNET	Hazardous Ordinance engagement Toolkit
HWIL	Hardware-in-the-Loop
I ² R	Imaging Infrared
IAI	Israel Aircraft Industry
ICMD	Improved Countermeasures Dispenser
IFOV	Instantaneous FOV
IFS	Integrated flight simulation
IIR	Imaging infrared (I ² R)
IN	Inertial Navigation
InSb	Indium Antimonide
IR	Infrared
IR/EO	Infrared Electro-optical
IRCCM	Infrared Counter-Countermeasures
IRCM	Infrared countermeasures
IRSG	IR scene generator
IRSP	IR Scene Projector
IRSS	Infrared Signature Suppression
IRTG	IR Target Generator

ISO	International Standard Organization
JT	Joule Thomson
KHILS	Kinetic Kill Vehicle Hardware-In-the-Loop Simulator
KSMD	Kinematic Special material Decoy
LADAR	Laser Detection And Ranging
LAIRCM	Large aircraft IRCMs
LATAx	Lateral Acceleration
LIDAR	Light Detection and Ranging
LIFE	Laser IR Fly-out Experiment
LOS	Line-of-sight
LOSBR	LOS Beam Rider
LOWTRAN	Low Resolution Transmission (model)
LWIR	Long-wave IR
LWR	Line of Weapon Release
MANPAD	Man-portable Air Defence System
MAT	MOSART Atmospheric Tool
MAWS	Missile Approach Warning System
MFOT	Missile Fine Optical tracker
MLE	Missile Launch Envelop
MODTRAN	Moderate Resolution Atmospheric Radiance and Transmittance Model
MOSART	Moderate Spectral Atmospheric Radiance and Transmittance
MOTS	Either modified or modifiable off-the-shelf, or military off-the-shelf
MSCM	Multi spectral countermeasures
MTHEL	Mobile Tactical High Energy Laser
MTV	Magnesium Teflon Viton
MuSES	Multi-Service Electro-optics Signature Code
MW	Mega watt
MWIR	Mid-wave IR
NASA	National Aeronautics and Space Administration (USA)
NATO	North Atlantic Treaty Organization
NEP	Noise Equivalent Power
NIRATAM	NATO IR Airborne Target Model
nm	Nano-meter
NOTS	NATO off-the-shelf
NRL	Naval Research Laboratories USA
NTCS	Naval Target and Countermeasures Simulator
NUCS	Nonuniformity correction subsystem
NURBS	Non-uniform Rational B-Spline
OBL	Optical Break Lock
OpenGL	Open Graphical Library
PbS	Lead Sulphide
PbSe	Lead Selenide
PC	Personal Computer
PCI	peripheral computer interface

PentA	Advance Anti-air Acquisition Algorithm
PIRATE	passive infrared airborne tracking equipment
PN	Proportional Navigation
PTN	Paint-the-Night
RADAR	RAdio Detection And Ranging
RF	Radio Frequency
RISS	Real-time IR/EO Scene Simulator
SAMs	Surface-to-air Missiles
SBUV	Solar-blind Ultra-Violet
SGI	Silicon Graphics Incorporated
SHARC	Synthetic High-Altitude Radiance Code
SHORAD	Army Short Range Air Defence
SIG	Special Interest Groups
SIGCAS	Special Interest Group on Computers and Society Special Interest Group on Computer Graphics and Interactive
SIGGRAPH	Techniques
SIGIR	Special Interest Group on Information Retrieval
SIGSIM	Special Interest Group on Simulation and Modelling
SLSAM	Shoulder Launched Surface-to-air Missile
SNR	Signal-to-noise Ratio
SPIRITS	Spectral and In-band Radiometric Imaging of Targets and Scenes
SRAAM	Short range Air-to-air Missile
SRF	spectral response filter
SSKP	Single Short Kill Probability
SUT	System under test
TADIRCM	Tactical aircraft Directional IRCM
TCP/IP	Transmission Control Protocol/ Internet Protocol
TEAM	Threat Engagement Analysis Model
TERTEM	Terrain temperature
TESS	Tactical Engagement Simulation Software
TIRS	Target IR Simulator
TMM	Texture material mapper
TOMACS	ACM Transactions on Modeling and Computer Simulation
TTI	Tactical Technologies Institute
UMA	Unified Memory Architecture
UV	Ultra Violet
WIPPS	Wide-body Integrated platform Protection System
WISP	Wideband Infrared Scene Projector
ZR2	Zone Rendering 2 technology

1 INTRODUCTION

1.1 Background

The capabilities of personal computers (PCs) have increased dramatically in the recent past. This is mainly due to the vast gaming and entertainment market. With ever growing gaming and entertainment technology, there is no end in sight to the growing list of features and performance available in PC based graphics systems. Generally, military simulators are developed around expensive workstations and minicomputers. However, the advancements in the low-cost PCs have opened a new front for the researchers to develop cheap, but fast, close to reality simulators for military applications. In the recent past, the special effects such as exhaust gas plume, clouds, smoke and dust were difficult to produce even on expensive workstations, but now it seems possible even with PC technology [SIM00].

1.2 Aim

The area of my research is Infrared and Electro-Optics (IR/EO) signature modelling and simulation. The aim is to develop a low-cost PC based high-fidelity Infrared (IR) signature model of missile seekers and to simulate radiometrically accurate scenes, utilizing fast speed and high resolution computer graphic hardware and software technology.

1.3 Objectives

The leading objectives of my research are:

- (a) To develop high-fidelity IR signature models from first-principles.
- (b) To generate photo-realistic target IR signature.
- (c) To generate photo-realistic background textures in the IR waveband.
- (d) To integrate LOWTRAN atmospheric transmission code data to add in the effects of the atmosphere.
- (e) To model Infrared Countermeasures (IRCM's) and Infrared Signature Suppression (IRSS).
- (f) To simulate a target-missile engagement sequence in air-to-air and surface-to-air modes.

- (g) To render an IR signature scene rich in fidelity and close to reality to generate special effects such as exhaust plume, leading-edge reflections and clouds.
- (h) To use a standard PC in a simple, easy to use and computationally inexpensive way.
- (i) To keep source code open for verification, validation and modification of algorithms and subsystems for specific applications.
- (j) To analyse IRCM against heat-seeking missiles and the IRCCM techniques used by them.

1.4 Need of IR Signature Modelling and Simulation

Most objects constantly emit IR radiation as a function of their temperature. As an object gets hotter, it gives off more intense IR radiation and it radiates at shorter wavelengths in the IR spectrum. The energy received at the sensitive IR detector is mainly due to the background, the targets and other sources. This energy travels through the air and, of course, gets attenuated due to the atmospheric effects. The performance evaluation, training and testing of IR missiles or other IR based weapon systems, if performed with live firing in the open air environment, is very expensive and also dependent on atmospheric factors which are difficult to control. Whereas, the computer based non-destructive simulation can provide a cost-effective alternative to field trials in which numerous scenarios can be simulated in a short time span and with controlled environmental conditions. However, field trials are considered essential for the validation of the IR signature model results [EIC89].

1.5 Why Commercial Off-the-Shelf?

A commercial off-the-shelf (COTS) product's major advantage is its relatively low cost which reduces the development cost. Also, using COTS software may cause less time on programming issues and more on domain-specific problem solving. Along with the cost advantage, the COTS software is easy to maintain and support. However, one stage towards customization is a MOTS (either modified or modifiable off-the-shelf, or military off-the-shelf, depending on the context). A MOTS product is typically a COTS product whose source code can be modified to meet the customized requirements. The aim of this work is to utilize COTS scene rendering software and three-dimensional (3D) object modelling tools to render the scene in the IR

waveband. Commercial tools are now available for building a virtual 3D scene for use in flight simulators and computer games. The ever growing commercial market has made these tools enormously sophisticated but relatively more user friendly [WRI01].

1.6 Future Utility

The PC based IR missile seeker simulator may be used for operational analysis, training, testing and prediction of air-to-air, air-to-ground, surface-to-air and surface-to-surface IR guided weapon engagements. Also, the IR seeker model and scene simulator could be used for target susceptibility to IR guided missile, aircraft and missile design, Infrared Countermeasures (IRCM) and Infrared Signature Suppression (IRSS) evaluation and analysis. The simulator may also be used for cost effective design and analysis, of Large Aircraft Infrared Countermeasures (LAIRCM), against terrorist missile threats to commercial airliners.

1.7 Summary

The IR Seeker model must include realistic radiometric targets, backgrounds, atmospheric effects and IRCMs. It should be compatible with a wide range of high-fidelity phenomenology models. The user can build high-fidelity, first-principle models using one integrated tool. The output IR simulated scene can be rendered in 3D graphical images and allow animation of targets along with backgrounds under a wide range of operational, atmospheric, observer and spectral conditions. The IR signature model and simulation will provide a very cost effective means to examine a wide range of scenarios which can not be tested or measured in the real world. The use of low cost COTS software such as the MATLAB and Virtual Reality toolbox may give it openness for user verification/validation and also flexibility for any future up-grading or modifications.

2 IR RADIATIONS AND SIGNATURE

2.1 Introduction

Electromagnetic radiation ranges from Gamma-rays to Radio-waves. The Infrared (IR) radiation comes between visible light and microwaves as shown in Figure 2-1 which depicts the major divisions of the electromagnetic spectrum.

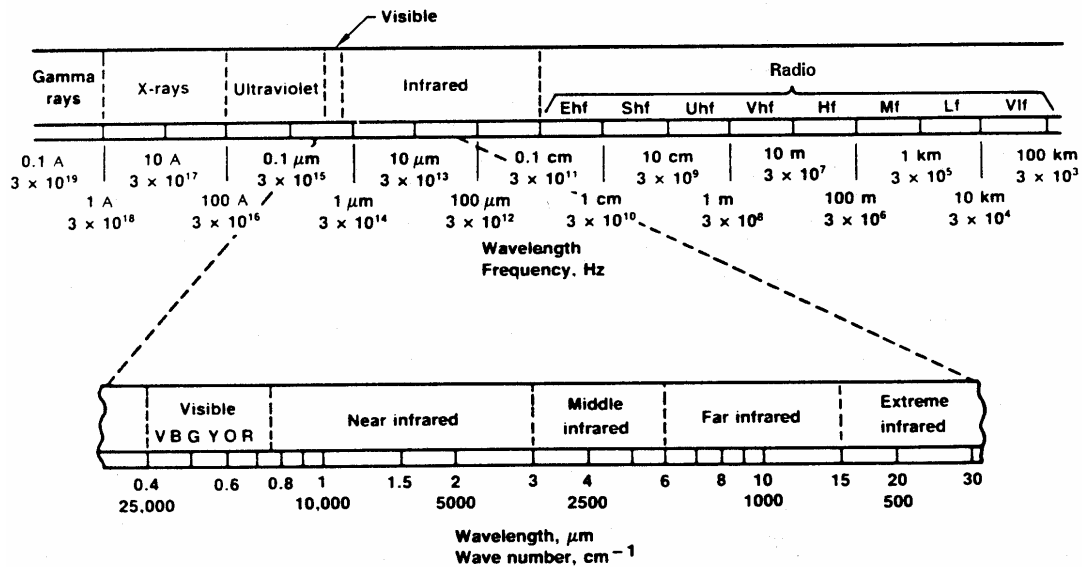


Figure 2-1 : The Electromagnetic Spectrum (source [SCH95])

All objects emit IR radiation as a function of their temperature. As an object gets hotter, it gives off more intense infrared radiation, and it radiates at shorter wavelengths. At very high temperatures, the objects get red-hot and the thermal radiations can be observed visually. But even at moderate temperature, the radiation can be detected or observed as heat but not visible. Below a certain temperature the human being cannot sense (see or feel) the IR radiation, but the radiations are still present. Even at low temperature (for example room temperature), the objects radiate IR energy with different wavelengths and intensities. The IR energy was detected by Sir William Herschel in 1800 while doing experiment with a prism and sun light [SCH95]. Although, IR is invisible to the naked eye, it may be observed using IR detectors and images can then be displayed on TV screens.

2.2 Infrared Radiations

The difference between visible and infrared is that in visible scenes the important parameters are the reflection and external source irradiance, whereas, the infrared radiation emitted by objects are dependent heavily on the body temperature and the surface physical characteristics mainly the emissivity and reflectivity of the material. A hotter object emits more radiation than a cooler one. A rough surface object emits more radiation than a smooth surface. For detection of a target against the background, it should either have higher-temperature differential or higher emissivity differential or a combination of the both.

2.2.1 Planck's Law for Blackbody Radiations

The Planck's Law describes the spectral distribution of the radiation from a blackbody which is usually written as [HUD69].

$$M_{\lambda}(T) = \frac{c_1}{\lambda^5} \frac{1}{e^{c_2/\lambda T} - 1} \quad (2-1)$$

where,

- M_{λ} is the spectral radiant exitance, $\text{W m}^{-2} \mu\text{m}^{-1}$
- T is the absolute temperature, Kelvin
- λ is the wavelength, μm
- c_1 is the first radiation constant, $3.7418 \times 10^8 \text{ Wm}^{-2} \mu\text{m}^4$
- c_2 is the second radiation constant, $1.4388 \times 10^4 \mu\text{mK}$

The spectral radiant exitance of a blackbody at temperatures ranging from 200K to 6000K is shown in Figure 2-2. The total radiant exitance, which is proportional to the area under the curve, increases rapidly with temperature. The wavelength of maximum spectral radiant exitance shifts towards shorter wavelength as the temperature increases. The individual curves never cross one another; hence the higher the temperature, the higher the spectral radiant exitance at all wavelengths.

Integrating Planck's Law over wavelength limits extending from zero to infinity gives an expression for the radiant exitance, the flux radiated into a hemisphere above a blackbody 1 cm^2 in area. This is commonly known as the Stephan-Boltzmann Law. The Stephan-Boltzmann Law applies only to blackbody and graybody sources [DRI99].

$$M(T) = \epsilon \cdot \sigma \cdot T^4 \quad (2-2)$$

where, ϵ is the emissivity of the blackbody or graybody

σ is the Stephan-Boltzmann's constant, 5.6697×10^{-12} , $\text{Wcm}^{-2}\text{K}^{-4}$

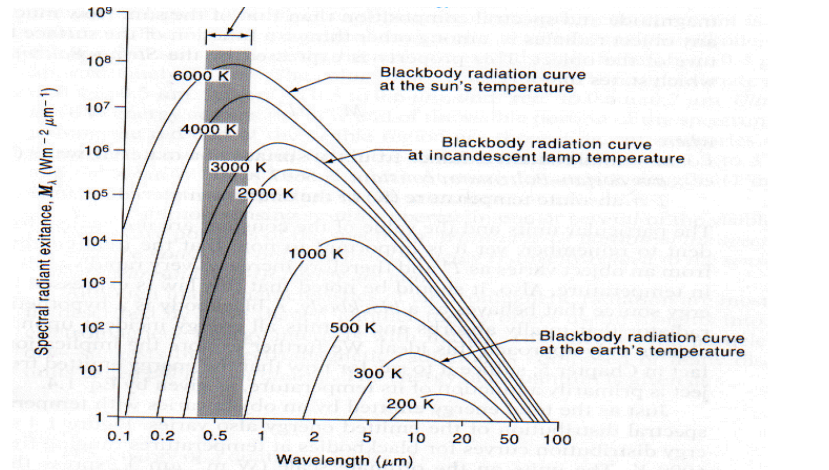


Figure 2-2 : Spectral radiant exitance of blackbody (source [SCH95])

2.2.2 Radiant Properties of Materials

Radiant properties of a material are its ability to absorb, reflect and transmit optical radiation. The quantities that characterize these actions are absorptance (α), reflectivity (ρ) and transmissivity (τ). By the conservation of energy, the sum of all three properties must be equal to one at the same wavelength as all three are functions of wavelength [SCH95].

$$\alpha(\lambda) + \rho(\lambda) + \tau(\lambda) = 1 \quad (2-3)$$

Typically, most solid materials are not transmissive in the IR region. For opaque materials ($\tau(\lambda)=0$) the above relation reduces as.

$$\alpha(\lambda) + \rho(\lambda) = 1 \quad (2-4)$$

In the IR, the objects provide most of the radiant signal seen by the sensor through emission while there is low reflectivity. In fact, for an object at thermal equilibrium (neither gaining nor losing heat) the absorptance (α) and emissivity (ϵ) are identical [DRI99].

$$\alpha(\lambda) = \epsilon(\lambda) \quad (2-5)$$

Therefore, Equation 2-4 can be written as

$$\varepsilon(\lambda) = 1 - \rho(\lambda) \quad (2-6)$$

That implies a higher emissive IR sources has a low reflectivity [DRI99].

2.2.3 Emissivity

The emissivity (ε) of an object can at best be that of a blackbody. The ratio of the emission of an object to that of a blackbody at the same temperature and in the same spectral interval is defined as its emissivity. The weighted emissivity is defined over a spectral region and the total emissivity refers to the emissivity over entire spectrum. A perfect emitter is called a blackbody. It has a constant emissivity of one at all wavelengths. A graybody has a constant emissivity of less than 1. Emission of real materials is always lower than that of an ideal blackbody. Figure 2-3 shows the spectral radiant exitance for a blackbody, a graybody and a selective radiator. A selective radiator as seen in Figure 2-3 has a value that is wavelength dependant [ZIS93].

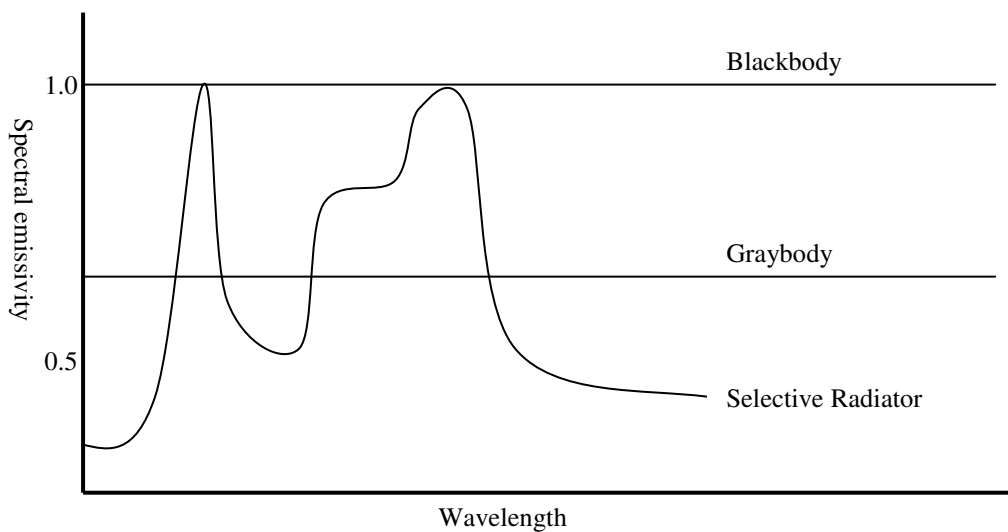


Figure 2-3 : Spectral emissivity of three types of radiators (source [HUD69])

2.2.4 Spectral Radiance

The basic building element, on which all other radiometric quantities are based, is the spectral radiance. It is the radiant flux per unit area, per unit solid angle and per unit bandwidth of wavelength. Assuming that the object is a Lambertian radiator, its radiance (N) can be evaluated from a simple modification to Planck's radiation Law

[RIC02b]. The total radiance within a spectral band is found by integrating the radiance over the appropriate wavelength [DRI99].

$$N = \frac{1}{\pi} \int_{\lambda_1}^{\lambda_2} \frac{\epsilon_{\lambda} \cdot c_1}{\lambda^5 \left(e^{\left[\frac{c_2}{\lambda T} \right]} - 1 \right)} d\lambda \quad (2-7)$$

where, N is the radiance, $\text{Wm}^{-2}\text{sr}^{-1}$
 λ wavelength in μm with λ_1 and λ_2 represents spectral limits
 c_1 first radiation constant, $3.7418 \times 10^8 \text{ Wm}^{-2}\mu\text{m}^4$
 c_2 second radiation constant, $1.4388 \times 10^4 \mu\text{mK}$
 T absolute temperature of object, Kelvin
 ϵ_{λ} spectral emissivity of the object.

2.2.5 Power

Power is the product of radiance times the area times the solid angle to the adjacent area. The power received at the detector is equal to the product of the target radiance times the area of the target and the solid angle of the optics as seen from the target. From Figure 2-4, the power may be equated for different combinations as shown in the following equation [SCH95].

Error! Objects cannot be created from editing field codes. (2-8)

Where,

P Power received at the detector,
 N Radiance,
 A_T area of target,
 A_O area of optics,
 A_D area of detector,
 $\Omega_{O,T}$ solid angle of optics as seen from the target,
 $\Omega_{D,O}$ solid angle of detector as seen from the optics,
 $\omega_{T,O}$ solid angle of target as seen from the optics,
 $\omega_{O,D}$ solid angle of optics as seen from the detector.

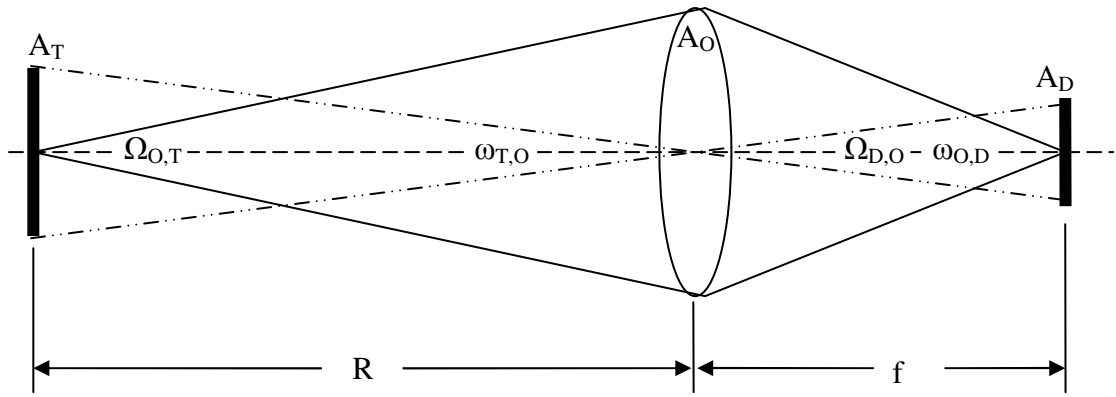


Figure 2-4 : Geometry used in power definition (Source [SCH95])

2.2.6 Solid Angle

The solid-angle (Ω) is the angle subtended at the centre of a sphere by an area on the surface of the sphere. The solid-angle is the area on the sphere surface (A_o) divided by the square of the radius of the sphere (R) [DRI99]. Solid-angle has the units of steradian (sr). Many radiometric units are given with respect to the solid-angle. In Figure 2-5, the solid-angle of optics as seen from the target ($\Omega_{O,T}$) can approximately be given as.

$$\Omega_{O,T} \approx \frac{A_o}{R^2} \quad (2-9)$$

where, radius of the sphere R may represent the distance between target and seeker, and A_o the area of the seeker optics. Equation 2-9 is a good approximation as R is usually large and hence A_o is a good approximation to the cross-sectional area. The area A_o may be written in terms of seeker optics diameter (D_o) as,

$$A_o = \pi \cdot R^2 = \pi \left(\frac{D_o}{2} \right)^2 = \pi/4 \cdot D_o^2 \quad (2-10)$$

Therefore, Equation 2-9 may be written as,

$$\Omega_{O,T} \approx \pi/4 \cdot \frac{D_o^2}{R^2} \quad (2-11)$$

Similarly, in Figure 2-5,

$$\Omega_{O,D} \approx \pi/4 \cdot \frac{D_o^2}{f^2} = \pi/4 \cdot \left(\frac{1}{F\#} \right)^2 \quad (2-12)$$

where, $F\# = f/D_o$ and “ f ” is the focal length of the seeker optics.

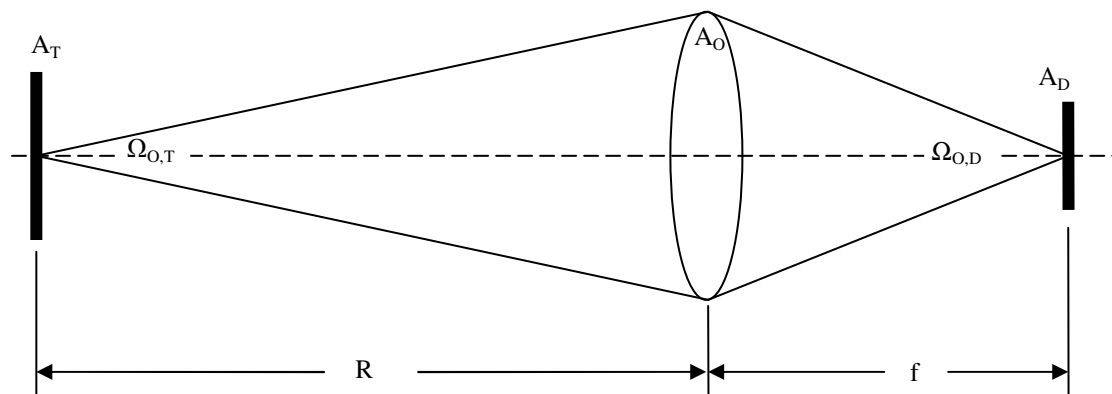


Figure 2-5 : Geometry used in solid angle definition (source [DRI99])

2.2.7 Projected Area

The projected area (A_p) is the area seen by the detector. It depends upon the optics and the range of the target.

$$A_p = a'b' = a.b.\left(\frac{R}{f}\right)^2 \quad (2-13)$$

Where, a and b are detector dimensions and a' and b' are their projection. Equation 2-13 can be derived using the similar triangles shown in Figure 2-6 by the dotted lines.

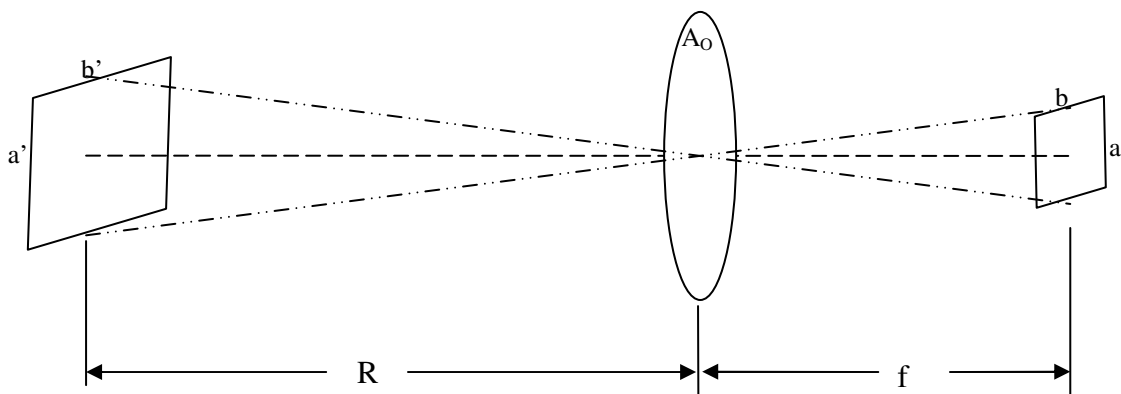


Figure 2-6 : Projected area calculations (source [RIC02b])

2.3 Sources of Radiation

In any IR seeker missile or imaging system, the main sources of radiation are the targets and the backgrounds. The targets are the sources which are of main interest.

For military systems, generally the targets are aircraft, missiles, ships, ground vehicles, tanks etc. Depending upon the application, the buildings or even people could be considered as targets.

Most military targets are man-made sources. The other dominant sources are the natural sources such as the sun, moon, skylight and star light. The sun is the primary source of radiation with a temperature of about 6000 K [DRI99]. The solar irradiance on a target surface changes with a diurnal cycle. Also, the earth, sky and clouds provide thermal emission and solar reflections (in day time only). The sources of radiation on military targets are mainly the hot engine parts and the exhaust plume and the high emissivity metal skin. The engine and exhaust plume produce a large amount of heat and makes the exhaust section a big source of thermal radiation. Figure 2-7 shows the various sources of radiation on an aircraft. Similarly, other military targets also have different sources of radiation.

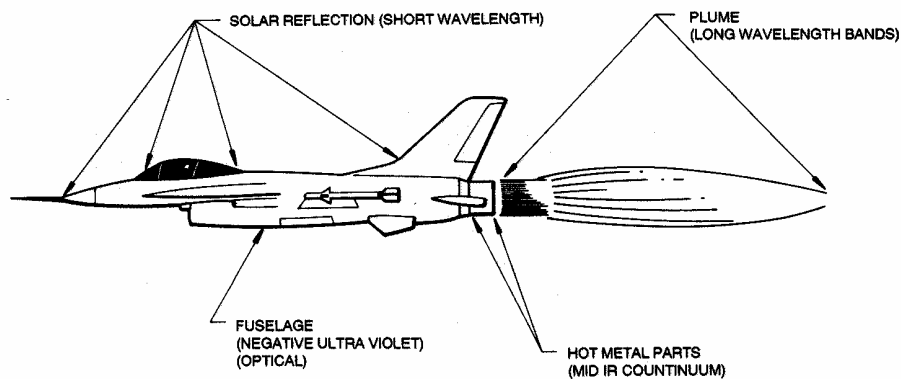


Figure 2-7 : Sources of radiations on an aircraft (source [POL93])

2.3.1 Sources of Radiation on Jet Aircraft

On a target, the IR signature appears as series of hotter and colder regions. The typical sources of radiation on jet aircraft are the hot-metal tail-pipe, the exhaust gas plume, metallic skin and the aerodynamic heating (in case of fast-jet aircraft).

2.3.1.1 Hot Metal Tailpipe and Exhaust Nozzle

Typically there are two sources of radiation from a turbojet engine: the hot metal tailpipe and the stream of hot exhaust gases known as the plume. The tail pipe behaves typically as a gray-body with total emissivity of about 0.9 with an exhaust gas temperature (EGT) up to 900° C and an area equal to that of the exhaust nozzle.

The hottest part of the engine is inside the tail-pipe and, therefore, the tail-pipe radiations are only visible from about 60° cone from the tail aspect. For a non-afterburning engine viewed from the tail aspect, the radiation from the tailpipe is far greater than that from the plume. Consequently, the less sensitive seeker heads of earlier missiles (Sidewinders AIM-9B to 9J and SA-7 etc.) could track only from the tail aspect while the modern missiles (AIM-9L, Mistral, Magic 2 and Darter etc.) with more sensitive seeker heads possess an all aspect capability.

2.3.1.2 Hot Exhaust Gas Plume

The exhaust gas plume extends about 130 feet behind the aircraft. The radiation of the tailpipe is about 25 times that of the plume [HUD69]. The weak plume radiance is due to several reasons. Firstly, the expansion of its constituent gases upon exit through the exhaust nozzle leads to its lower temperature in comparison with that of the tail pipe itself. Secondly, the gas plume is not a blackbody radiator because it is not infinitely thick and there is no temperature equilibrium within the volume of the gas. Thirdly, the atmosphere absorbs the same wavelengths as the plume emits. The spectral distribution of a plume radiation is similar to that of a Bunsen Flame which exhibits strong spectral emissions in the 2.7 μm wavelength (due to CO_2 and H_2O) and 4.4 μm wavelength (due to CO_2). The plume principal combustion products also are CO_2 and

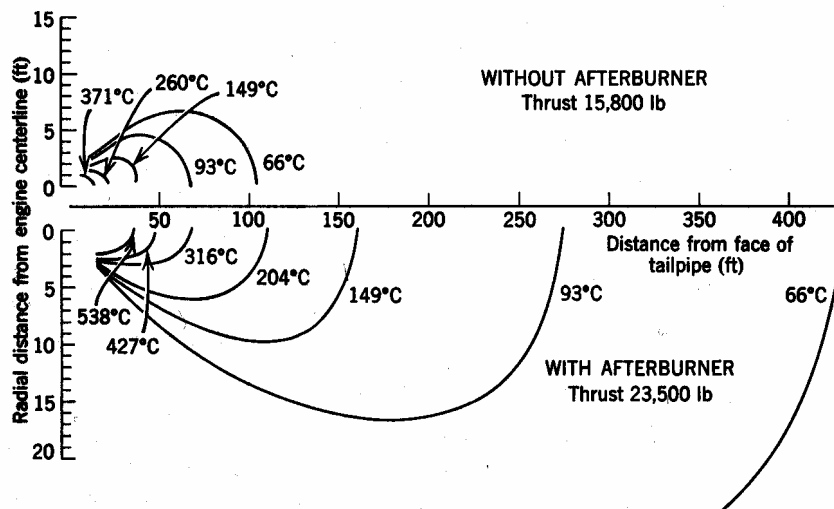


Figure 2-8 : Exhaust temperature contours for Turbo-jet engine with and without afterburner (source [HUD69])

H_2O , which, unfortunately, are also present in the atmosphere; the plume's radiation, therefore, is readily absorbed by the atmosphere. In comparison with the 2.7 and 4.3 μm wavelength, however, the emissions around 4.4-4.6 μm do not suffer from heavy

absorptions and contribute to some heat radiation from the plume itself. Consequently, in comparison with the tailpipe radiation, the exhaust gas plume has diminishing temperatures as shown in Figure 2-8 (about 760°C at the exhaust nozzle and reduce to about 66°C at 400 feet). The plume has lower emissivity and poor transmission through the atmosphere. It is emphasized that the absorption and emission depends on temperature, pressure, size and the shape of the volume. The plume's radiance depends upon the concentration and the temperature of the exhaust gas molecules which, in turn, depends upon the aircraft's fuel consumption; therefore, the radiance of the plume at an altitude of 35,000 feet is only one half of its value at sea level [WOL78].

2.3.1.3 The After-burner Plume

With afterburner (AB) turned on, the temperature and size of the plume increases appreciably. Figure 2-8 shows the exhaust temperature contours of a turbojet engine at full takeoff thrust with and without AB turned on. With AB on the exhaust plume becomes the dominant IR signature of the turbo-jet aircraft and is viewable from much large aspect angles [HUD69].

2.3.1.4 Aerodynamic Heating

An object moving at high speed through the atmosphere gets heated. At speeds above Mach 2, when airflow over a body it often becomes turbulent towards the rear of the body. Any point on the body where the air stream comes to a complete rest is called a stagnation point. At stagnation point, the kinetic energy of the moving air is converted into potential energy in the form of high temperature and pressure the resulting high temperature produces sufficient radiation to be of interest to the IR system designer. At speeds above Mach 2, for head-on aspects, the aerodynamic heating becomes the dominant source of radiation on the aircraft [HUD69].

2.3.2 Sources of Radiation on Ground Vehicles

Military ground vehicles include trucks, tanks, command and communication equipment and mobile power generating units etc. One of the main threats posed to the ground vehicles is detection by the Forward Looking IR (FLIRs) systems and attacked by the IR guided sub-munitions. Because of their high temperature, exhaust pipes and mufflers may radiate several times as much energy as the rest of the vehicle

does. The drive train and the exhaust plume may also radiate sufficient energy to be of interest as targets. The tyres and tracks may cause secondary heating in the ground which may contribute to the overall IR signature of the scene. Most ground vehicles are made of metals and are coated with paints of emissivity of around 0.85 or greater. In daytime, the IR signature of ground vehicle may also be modified by solar heating [HUD69].

2.4 Transmission of Infrared Radiation through Earth's Atmosphere

The energy radiated from the target or source has to pass through some medium before reaching the sensor. Generally, this medium is the atmosphere. In the visible region, our ability to view a distant object is not constant and depends upon the weather conditions. Similarly, the EO/IR sensors are adversely affected by the changing atmosphere. The influence of the atmosphere on thermal radiation is a complex process. The earth's atmosphere is a mixture of many gases and the existence of these gases in the atmosphere varies with altitude, time and space. The contents of a typical atmosphere are shown in Table 2-1. The largest constituents are the Nitrogen, Oxygen and Argon. The other molecules such as Carbon-dioxide, water vapours, Ozone, Nitrous-oxide and Methane are the key absorbers in the 2-15 micron band even though they have very minor concentrations [SMI93]. The existence of water vapours is highly variable from day to day, from season to season, with altitude and for different geographical locations. Also, the Carbon-dioxide concentration varies seasonally and is high over vegetation and industrial areas as compare to over oceans and deserts. The variable nature of these atmospheric gases makes the prediction of atmospheric propagation at IR frequencies a challenge [SIM93].

2.4.1 Atmospheric Transmittance Calculation Software

The atmospheric transmittance and path-radiance are calculated by using various numerical models. These models are contained in several atmospheric transmission codes. The most commonly used codes are LOWTRAN, MODTRAN and FASCODE. These were developed by Air Force Geophysics Laboratory in Cambridge, Massachusetts, USA. These codes calculate atmospheric transmittance and path-radiance based on absorption and scattering phenomena for a variety of path geometries. All these models developed are only predicting the amount of absorption

and scattering in an atmospheric path and are not the exact means of describing the effects of the atmosphere on infrared energy at any one time and place [SIM93].

Table 2-1 : Composition of atmospheric constituent gases (source [HUD69])

Constituent	Chemical Formula	Contents (% by volume)	Absorbs between 2-15 micron
Nitrogen	N ₂	78.084	No
Oxygen	O ₂	20.946	No
Argon	Ar	0.934	No
Carbon dioxide	CO ₂	0.032	Yes
Neon	Ne	1.818x10 ⁻³	No
Helium	He	5.24x10 ⁻⁴	No
Methane	CH ₄	2.0x10 ⁻⁴	Yes
Krypton	Kr	1.14x10 ⁻⁴	No
Nitrous oxide	N ₂ O	5.0x10 ⁻⁵	Yes
Hydrogen	H ₂	5.0x10 ⁻⁵	No
Xenon	Xe	8.7x10 ⁻⁶	No
Ozone (in troposphere) (20-30km altitude)	O ₃	0-0.3x10 ⁻⁴ 1x10 ⁻⁴ -7x10 ⁻⁴	YES
Water vapours	H ₂ O	0-2	YES

2.4.1.1 LOWTRAN

In 1972, LOWTRAN-2 code was first written to calculate the transmittance and radiance of the atmosphere. LOWTRAN-7 is the most recent version and was made available in 1989. Based on the absorption and scattering phenomena for a variety of path geometries, LOWTRAN calculates the atmospheric transmittance and path-radiance over a wide spectral range from 0.25 μm to 28.5 μm . The spectral resolution of LOWTRAN is 20 cm^{-1} (wave number) with step size of 5 cm^{-1} . Before the introduction of MODTRAN, LOWTRAN-7 was the most widely used and accepted code for atmospheric transmittance [DRI99]. The commercial version was developed by Ontar Corporation, North Andover, MA, USA. LOWTRAN has been validated against field measurements. It is suitable for low altitudes (less than 40 km) and at moderate temperatures. Due to limited spectral resolution, it should not be used for Laser applications [SIM93].

2.4.1.2 MODTRAN

MODTRAN stands for “MODerate spectral resolution atmospheric TRANsmittance” or in some text as “MODerate resolution LOWTRAN code” [BER89]. It covers the infrared, visible and the near-ultraviolet regions and also the microwave region. The MODTRAN is similar to LOWTRAN but with moderate resolution of 2 cm^{-1} . In January 2000, MODTRAN-4 was released for public use. Ontar Corporation MA, USA has developed PcModWin4.0, the WindowsTM based commercial version of MODTRAN-4. PcModWin4.0 is easy to use and calculates the atmospheric transmittance and path-radiance at medium spectral resolution [ONT89].

2.4.1.3 HITRAN

HITRAN stands for High Resolution Transmission Molecular Absorption Database. It is a molecular database with spectral resolution of about 0.001 cm^{-1} . It calculates only the atmospheric transmittance and does not include aerosols and weather conditions and is only suitable for calculating molecular absorption in the atmosphere.

2.4.1.4 FASCODE

FASCODE is a line-by-line model that computes the transmission of each absorption line using the spectroscopic parameters in the HITRAN database. It computes the atmospheric transmittance and path-radiance with spectral resolution of 0.001 cm^{-1} . Generally, it is used for very narrow optical bandwidth radiation, such as Lasers and LIDARs. PcLnWin is Ontar’s WindowsTM based commercial version of FASCODE [ONT89].

2.4.2 Atmospheric Transmittance

The transmission of the atmosphere present in between the scene and the sensor is calculated on the basis of the absorption, scattering and refractive-index fluctuations or turbulence. The turbulence in the atmosphere is due to the temperature, pressure and density in-homogeneities which may result in blurring and distortion of images. It is noticeable only when viewing small objects at long distances and has little effect on near objects [DRI99]. The absorption and scattering are usually grouped together under the topic of extinction which causes attenuation in the amount of radiant flux passing through the atmosphere. The transmittance of a path through the atmosphere can be expressed as

$$\tau(\lambda) = e^{-\sigma(\lambda)x} \quad (2-14)$$

Where, τ represents the transmittance of the atmosphere
 σ is the extinction coefficient, and
 x is the path length of the atmosphere

This principle is known as Beer-Lambert Law [DRI99]. Under most conditions the extinction coefficient (σ) is made up of two components.

$$\sigma(\lambda) = \alpha(\lambda) + \gamma(\lambda) \quad (2-15)$$

Where, α is the absorption coefficient account for the absorption by the gas molecules of the atmosphere and γ is the scattering coefficient, accounts for scattering by small particles suspended in the atmosphere. In IR region of the spectrum, the absorption poses a far more serious problem than does the scattering poses [HUD69]. The spectral transmittance measured over a 6000 feet horizontal path at sea level is shown in Figure 2-9. This curve may be characterized by several regions of high transmission called atmospheric windows.

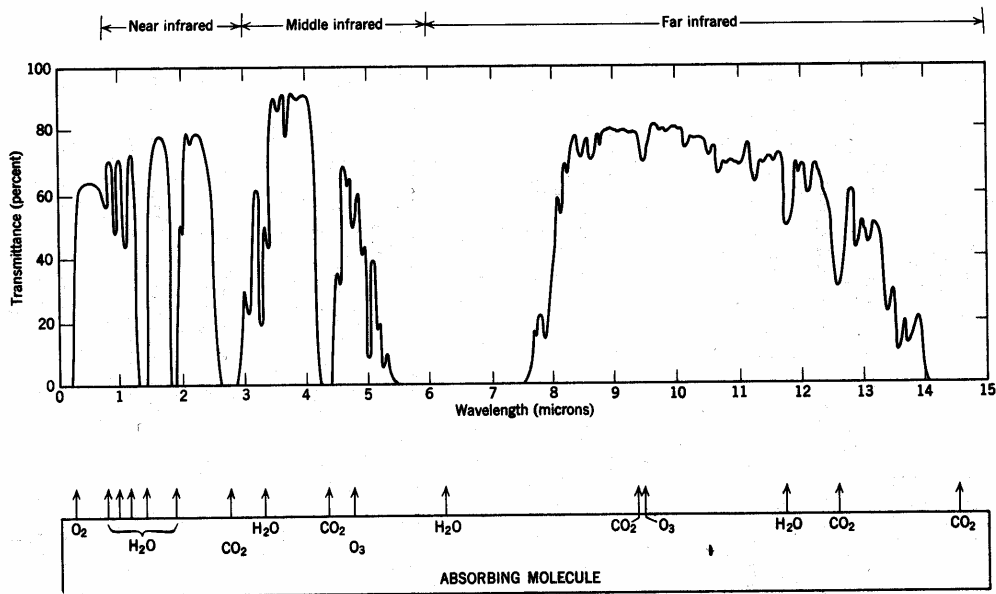


Figure 2-9 : Transmittance of atmosphere over a 6000 feet horizontal path at sea level (source [HUD69])

2.4.3 Atmospheric Path-radiance

As the atmosphere comprises of particles, they thermally emit radiation along the path in LOS of the source to the detector. The path-radiance of the atmosphere may be

calculated by considering atmospheric particles as blackbodies at a particular temperature. The path radiance becomes negligible as the path transmittance gets higher (closer to one). Therefore, with a cold clear sky, the path radiance can usually be neglected but at high temperatures it can cause noticeable effects. Similarly, the path radiance can be negligible for short path distances [DRI99].

2.5 IR Signature Scene Model Ingredients

The basic building block of the IR signature scene model is the total radiance of each visible point in the field-of-view of the sensor. The radiance of points hidden behind any other object will not reach the sensor provided the object obscuring the field-of-view is opaque. The radiance of any point can have contributions from emission, transmission and reflection (scattering). Depending upon the material characteristics, the radiant properties may vary. The opaque surfaces (like an aircraft body or solid background) have no transmission of thermal radiation through them but they emit thermally and reflect energy received from the environment. On the other hand, the non-solids or gases are considered to emit thermally and to transmit but the scattering may be considered as neglected. Table 2-2 summarizes the effects of various ingredients of the IR signature scene model. The same are explained in the following paragraphs.

Table 2-2 : Radiant properties of various sources.

SOURCE	EMISSIVITY	REFLECTIVITY	TRANSMISSION	SCATTERING *
Target (Metal)	YES	YES	NO	NO
Plume (gases)	YES	NO	YES	NO
Background	YES	YES	NO	NO
Sky	YES	YES	YES	YES
Clouds	YES	YES	YES	YES
Glass	YES	YES	NO	NO

* or diffused reflections

2.5.1 Targets

The detection of target by IR sensor is based on the thermal contrast between the target and the background. Although, in opaque objects, in the near and mid-IR bands, both the reflective and emissive properties are generally equally important, however, in the far-IR region the contribution due to reflected radiation is usually much smaller

and the emissive property of target and background are dominant. The IR radiation emitted from various direct and indirect sources in the scene, reaches the sensor through the following mechanisms.

- (a) Thermal emission from target corresponding to the body temperature and in the selected spectral band,
- (b) Thermal emission from background corresponding to the background temperature and in the selected spectral band,
- (c) Transmission of thermal radiation from the objects behind the source (in the case of non-opaque objects),
- (d) Reflection of thermal radiation from the target surface. The environmental sources of reflected radiation are the sun, the earth, the sky and the clouds,
- (e) Inter-reflections caused by very close by targets (in the case of ground or sea targets only),
- (f) Path-radiance of the intervening atmosphere between target and sensor.

2.5.2 Background as Clutter or Source

Depending upon the application, the background may be considered as non-required clutter or a useful source. In the case of aerial targets (air-to-air or surface-to-air missile engagements) the background is primarily sky and usually located quite far from the target. Therefore, the actual background radiance is not as important as the relative radiance between targets or flares. Whereas, in the case of ground targets (air-to-ground or surface-to-surface mode) the background radiance is much higher and in line with the ground target's radiance. For thermal imaging systems (like FLIR), the background may also be considered as a source and not clutter. In the case of ground target, the background is generally earth terrain or man-made structures.

2.5.3 Thermally Static IR Background

The missile-target engagement has a very short flight time (may be a few seconds or minutes). Therefore, for this short duration, the background temperature or radiance may be assumed as constant for the simulation. Therefore, the temperature of each background may be computed for the specific time of the day for which the simulation is to be performed.

2.5.3.1 Clouds

The clouds are non-opaque bodies and behave differently than solid targets and backgrounds. The clouds can have effects in the foreground as well as in the background. In foreground, when in the LOS of the target to the sensor, they attenuate the energy of the target as it passes through the clouds. The transmission of energy through the cloud depends upon the cloud's absorption and scattering ability. When in the background, the clouds themselves act as thermal sources and their emitting properties are considered.

2.6 Low and High-Fidelity IR Signature Models

Various IR signature models have been presented in the past. Some are low-fidelity and others are high-fidelity. The fidelity of a model is dependent on its intended application. Developing a higher fidelity model for a low-fidelity application is not an appropriate solution. Although, simple first-order straight forward equations could not determine the exact performance of a system, it is considered sufficient for evaluating the lock-on range of a point source target. The models presented in references [KIN00],[RIC02b],[YAN02],[RIC03] and [BEN04] are simple and easy to use for low fidelity models. On the other hand, high-fidelity IR signature models presented are time consuming and heavy on computations. The IR signature scene fidelity improves in pace with the increase in the computational capabilities [GON03]. Unlike point source based seekers, the modern image based missile seeker needs high-fidelity modelling with more accurate and realistic imagery. These high-fidelity models contain highly detailed terrains, man-made structures, atmospheric effects, detailed target geometry and thermal signature models [MUU95]. To make it more realistic, the "special effects" such as exhaust gas plume, dust, smoke and clouds are added in these models [HOO91]. The NATO Infrared Air Target Model (NIRATAM) and NATO's NPLUME are the examples of high-fidelity modelling [BAK99], [DEV01] and [CUR02].

2.7 Conclusion

All objects emit energy in the IR portion of the electromagnetic spectrum. The energy radiated from any object depends upon its property to absorb, reflect and transmit radiation. The temperature of the body, emissivity and reflectivity of the surface are the dominant factors for IR signature modelling. The IR energy attenuates as it passes

through the atmosphere. The IR energy received at the detector comprises of radiations from target, background radiations and reflected energy from other sources. Knowledge of IR signatures is fundamental to any development and analysis in the fields of heat seeking missiles and infrared countermeasures. For IR signature modelling the radiometric properties of the material, the temperature of each sub part of the objects present in the scene, the spectral radiance and the total power received at the detector after atmospheric attenuation are the important parameters which needs to be considered. The details of these parameters are given in Chapter-6.

3 IR GUIDED MISSILES

3.1 Introduction

Infrared guided missiles have been among the most deadly threats in all recent conflicts. Also they have been responsible for most of the military and civilian aircraft downed in the last several decades. Since the birth of the first un-cooled reticle seeker, missile technology has advanced considerably to the latest multi-colour array imaging seekers.

3.2 Evolution of Heat Seeking Missiles

The early heat seeking missile used un-cooled detector technology, operating in the near-IR waveband. These missiles typically see high temperature targets or central regions of the exhaust plume. Whereas, the next generation cooled detectors have higher sensitivity in the mid-IR band and can detect warm skin of an aircraft or the hot exhaust gas plume. The latest missiles have imaging seekers working in the mid-IR or the far-IR wave band. The following paragraphs explain the evolution of heat seeking missiles.

3.2.1 First Generation Seekers

Figure 3-1 is a block diagram showing the basic layout of a first generation seeker system. This type of system is often referred to as a *spin-scan* seeker.

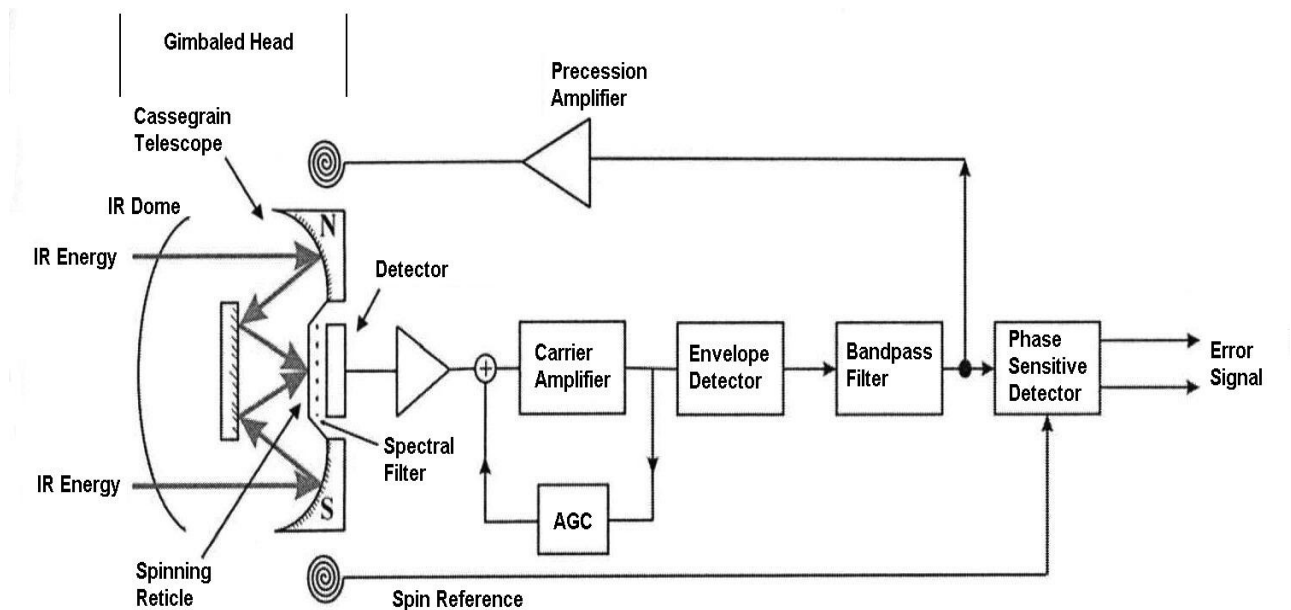


Figure 3-1: Block Diagram of First Generation (Spin-Scan) Seeker

Infrared radiation from the scene passes through the dome and is imaged via the Cassegrain telescope onto a spinning (rotating) reticle. The detector (usually un-cooled Lead Sulphide) then converts this *chopped* IR signal into an electrical signal. A *pick-off* is used on the reticle to enable phase sensitive detection to allow the error signal to yield pitch and yaw. An automatic gain control (AGC) is used to prevent saturation of the electronic amplifiers and filters. The gimbaled head allows field-of-regard (FOR) typically in excess of 90°.

Several different reticle designs have been developed to optimise their tracking capability with the one of the simplest referred to as the *rising-sun* reticle, see Figure 3-2. It consists of a *null-phase* portion that only transmits 50% of the radiation, to set the AGC within the seeker and generate the phase with respect to the pick-off. The other section alternates between 100% and 0% transmission to produce an amplitude modulated carrier. The closer the image is to the axis the smaller the amplitude of the square wave produced. Hence this produces a time-referenced waveform that provides spatial information of the image with respect to the optical axis of the seeker (centre of the reticle).

Legitimate targets are distinguished from background IR sources by the degree of amplitude modulation. Large sources, such as clouds, produce little (if any) modulation, as no single hot spot can be identified as the reticle rotates through its target sensing section.

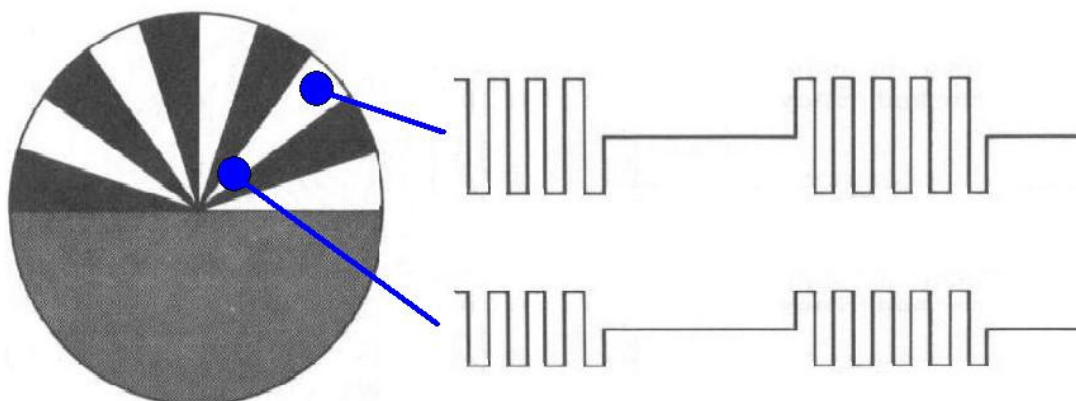


Figure 3-2 : Rising-Sun Reticle showing Amplitude Modulation and Null-Phase Sector

The un-cooled Lead Sulphide (PbS) detectors usually used in this generation of seekers have a peak sensitivity at $< 3\mu\text{m}$. These systems therefore typically operate in the near-IR 2-2.7 μm atmospheric window (see Figure 3-3), which tends to limit such missiles to rear engagements as the detector can only discern the hot metal parts of the engine and the hotter water emission in the plume.

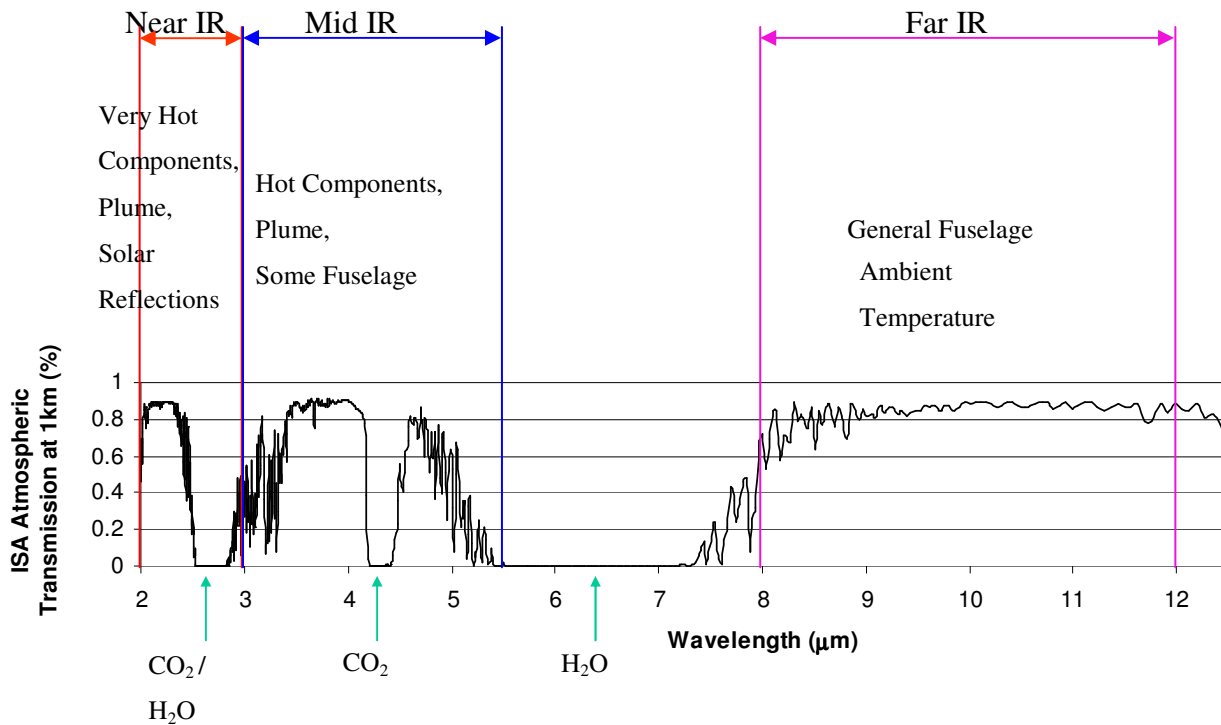


Figure 3-3: Typically Atmospheric Transmission with IR Emitters

Improvements to the rising-sun design included adding curved radials to the reticle to reduce the chance of being spoofed by straight edge IR emitters such as the horizon (see Figure 3-4).

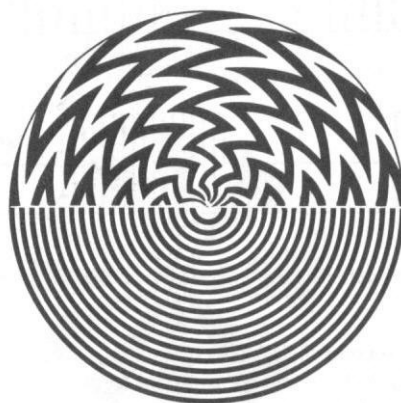


Figure 3-4: Improved First Generation Reticle

An example of a 1st generation IR missile is the Strela-2 (SA-7 ‘Grail’). Originally fielded by the Soviet military in 1968, the SA-7 is one of the simplest versions of this type of weapon (see Figure 3-5). Widely proliferated, it poses a major threat to aircraft without any countermeasure (CM) systems, although, it is limited to rear aspect engagements. It has an impact fuse and has a minimum engagement altitude of 50m. These types of weapon are often referred to as a man-portable air defence systems (MANPADs).



Figure 3-5: SA-7 a First Generation Seeker System (source [FAS07])

Once this type of seeker has manoeuvred the missile body so that the target is in the centre of its FOV, it suffers from axial insensitivity and starts to *hunt* back and forth. This is a result of the seeker effectively losing all fine directional information on the target because of a lack of amplitude modulation at the centre of the reticle. This leads to poor hit probabilities for engagements with even a small level of crossing rate. This axial insensitivity was removed by rotating the optical axis as used in second generation systems.

3.2.2 Second Generation Seekers

Second generation seekers (often referred to as *Con-Scan*) used a stationary reticle with a rotating optical system to yield a square wave on axis and hence remove the axial insensitivity of the first generation systems. This can be seen in Figure 3-6, where the secondary mirror is tilted and the primary and secondary mirror are rotated. This yields a *nutation* circle image motion on the stationary reticle.

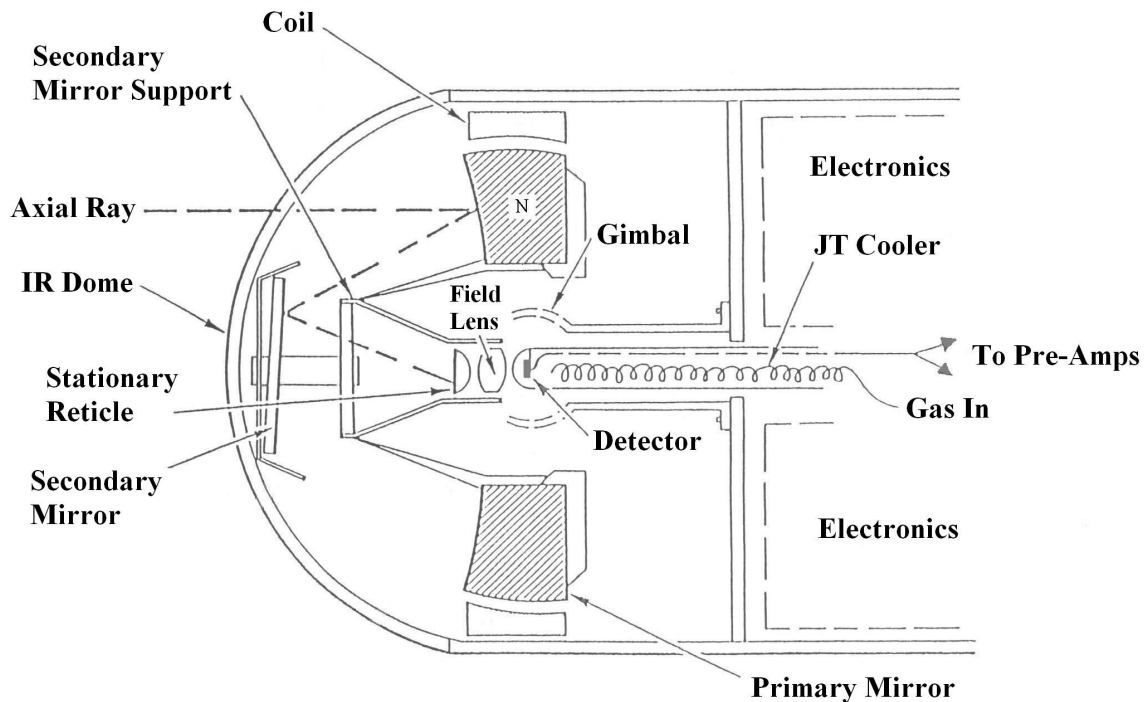


Figure 3-6: Second Generation Seeker Schematic

The reticle in the second generation system is usually referred to as a wagon wheel reticle and can be seen in Figure 3-7. When the target is on-axis a centred nutation circle is produced, yielding a constant square wave (with no frequency variation – this is the *tone* played into the earpiece of many systems). As the target moves off-axis a frequency modulated waveform is produced. Again a pick-off from the rotating optical system is used to enable the computation of the axial error in terms of pitch and yaw.

More sensitive detector materials were also introduced to facilitate all-aspect tracking. These cooled detectors, used materials such as Indium Antimonide (InSb) for detection in the mid-IR 3-5 μ m atmospheric window (see Figure 3-3). Operating at longer wavelengths allowed cooler parts of the engine, hot parts of the airframe, and the cooler CO₂ emissions in the exhaust plume to be detected, thus allowing wider angles of engagement. There are many options for cooling the detector, arguably the most common method is via a Joule-Thomson (JT) cooler with a small bottle of Argon or Nitrogen or dry air.

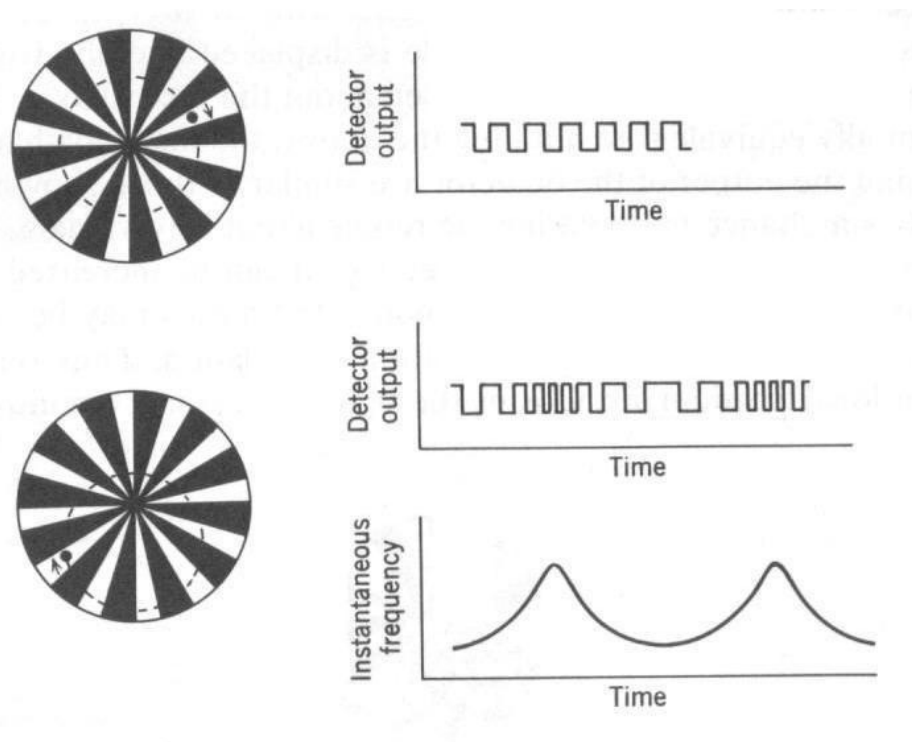


Figure 3-7: Wagon Wheel Reticle Showing Frequency Modulation Outputs

An example of 2nd generation system is the ubiquitous AIM-9L (Sidewinder) see Figure 3-8. Other examples of this type of system in the MANPADS role are the US Redeye and basic Stinger and the Soviet Strela-3 (SA-14). The Chinese QW-1 (Vanguard) is also probably this type of generation system, as is the Pakistani-built version Anza Mk-1.



Figure 3-8: AIM-9L a Second Generation Seeker System (source [FAS07])

There is however another type of second generation (con-scan) seeker as typified by the French MANPADS Mistral. This still uses a nutation circle but does

not have a reticle and instead has four detectors arranged in an *open-cross* formation to yield the frequency modulation (FM) output (see Figure 3-9). Again when the target is on axis, the system produces a square wave (four equi-spaced detector outputs); whereas, when the target is off axis, a frequency modulated square wave is produced (unequal spacing of the detector outputs).

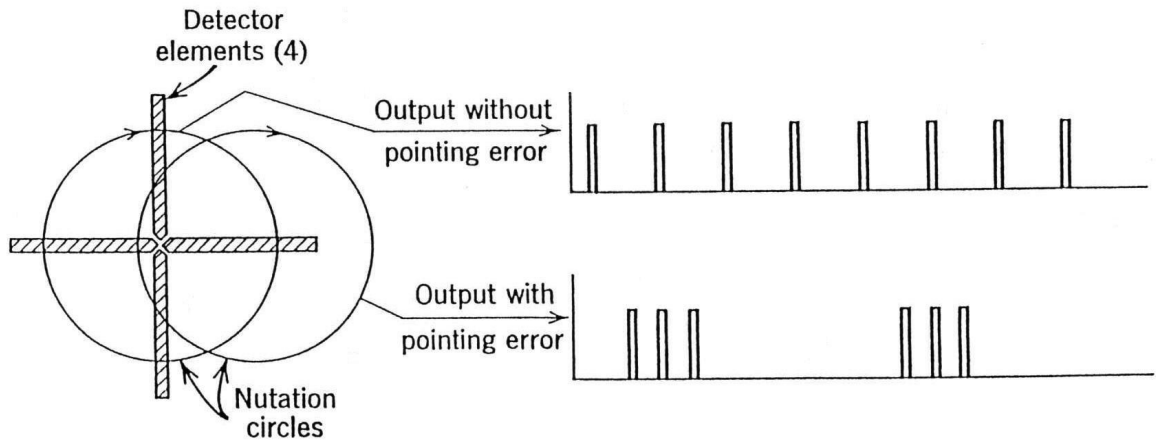


Figure 3-9: Open-Cross Detector Showing Frequency Modulation Outputs

The Soviet Iгла (SA-16 Gimlet) and Iгла-1 (SA-18 Grouse) are possibly this type of seeker as is the Chinese QW-2 and the Pakistani built Anza Mk-2.

3.2.3 Third Generation Seekers

The third generation seeker systems are often referred to as *Pseudo Imaging Systems* as they rely on creating a simulated image of the target by moving the IR signal over the detector. This is achieved by rotating a couple of offset mirrors or Risley prisms (see Figure 3-10) to produce a specified pattern on the detector. The shape of the scan pattern varies according to the relative rotation rate and direction of rotation of the mirrors or prisms.

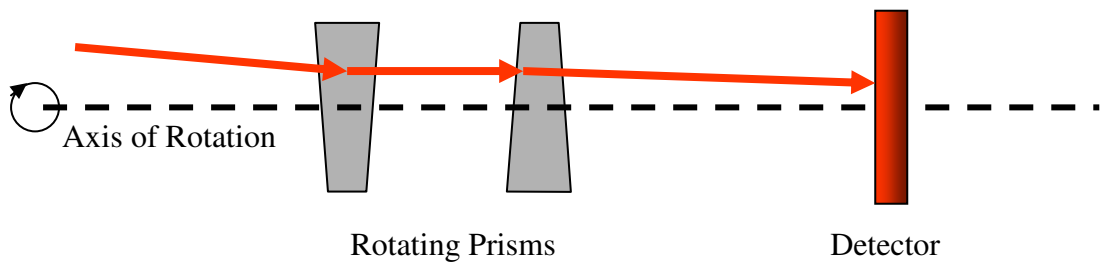


Figure 3-10: Risley Prisms to Generate Pseudo Image Scanning

Scan patterns are optimised to meet various specifications although the most widely used is the Rosette scan due to its re-visiting the axis after each *petal* of the rosette (see Figure 3-11).

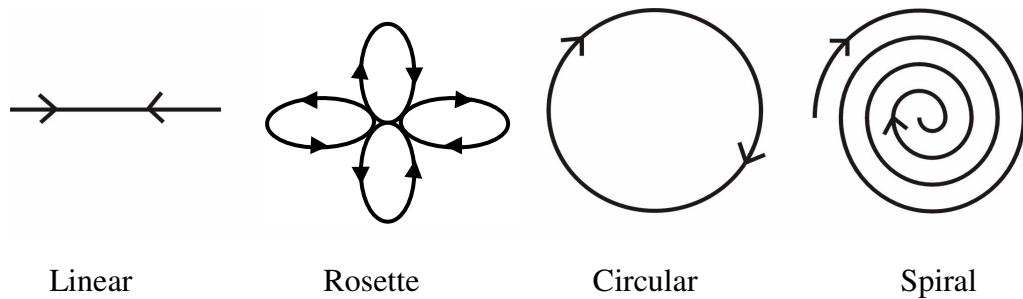


Figure 3-11 : Resley Scan Patterns

The major advantages of this type of system are increased lock-on range and robustness to countermeasures in part due to the smaller instantaneous field-of-view of the detector. An example of a 3rd Generation IR missile is the MANPAD Stinger-RMP (reprogrammable microprocessor). It has more robust flare rejection mechanism including using a dual mode IR/UV detector in its rosette scan. The UV detector looks for a negative contrast signal as the airframe blocks the Rayleigh scattered solar radiation. The IR signal from the plume has to coincide with the recovery of the UV signature for a *valid target enable*. The IR detector is JT cooled with Argon and is operational in less than 5 seconds. See Figure 3-12.



Figure 3-12: Stinger-RMP a Third Generation Seeker System (source [FAS07])

It is also claimed by some that the Soviet SA-16/SA-18 are also an example of this generation of seeker by virtue of the fact that a UV detector is used in its countermeasure (guard) channel.

3.2.4 Fourth Generation Seekers

The fourth generation of seekers are characterised by multi-element detectors that produce an image of the target on the focal plane. Often referred as Imaging Infrared (I^2R) seekers, the individual detectors can either be arranged linearly, with a scanner to produce an image, or as a staring focal plane array. A further development of this technology is likely to see the use of *multi-colour* infrared seekers thus increasing their defence against IRCMs. Although more robust and less susceptible to jamming, array seekers are currently far more expensive to produce than all the earlier generations and have not proliferated to the same extent. Image size and computing power is also an issue with this generation of seeker. Obviously the smaller the number of pixels in the image the easier the computation task but the poorer the resolution on the target (see Figure 3-13).

Figure 3-13 is an illustration of a typical target at range on a staring array whilst Figure 3-14 is an illustration of how advanced multi-colour detectors may extract spectral information from, for example, the plume.

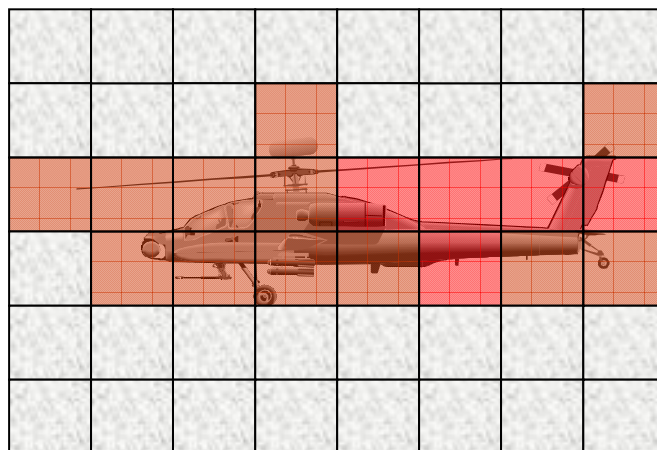


Figure 3-13: Illustration of a Typical Target on a Staring Array

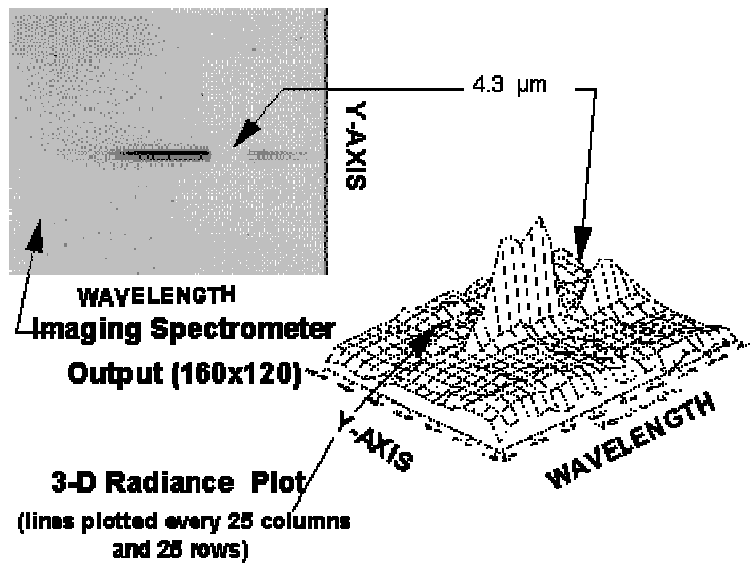


Figure 3-14: Spectral Output of a Typical Plume

There are many examples of 4th generation IR missiles being produced. On the MANPAD front, the US Stinger Block-2, which was to be fielded circa 2000, was consist of a 128x128 or 256x256 3-5 μ m Indium Antimonide (InSb) staring focal plane array, primarily to increase its acquisition capability (especially in ground clutter). Currently though, it is fair to say that most 4th generation systems are in the air-to-air role, for example:

- (a) The German IRIS-T allegedly uses a scanning array of two staggered 64 element linear rows of InSb detectors working in the 3-5 μ m mid-IR region. It has an 180° FOR and an active Laser fuse.
- (b) The Israeli Python-4 has a stabilized seeker slaved to the pilots helmet mounted sight with 60° off-boresight capability and allegedly uses a two colour all aspect IR staring array. (Python-5 is claimed to be a Hughes 128x128 staring focal plane array in 3 IR bands).
- (c) The UK ASRAAM uses a 128x128 staring array of InSb detectors working in the 3-5 μ m mid-IR region. It has an 180° FOR, can be cued by the pilot's helmet and has demonstrated the ability to select an aim point on the target aircraft. It has an impact and active Laser fuse.

(d) The US AIM 9X (Sidewinder-next generation) is currently in its last year of *Engineering and Manufacturing Development*. It is alleged to have the same staring array as ASRAAM and is cued by the pilot's helmet sight. It claims its adaptive and advanced processing gives it superior target acquisition and IRCM rejection capabilities.

3.3 Missile Tracking Techniques

The aim of a tracker is to measure errors or deviations from the bore-sight and send signals to the control system to reduce these errors to zero. Mainly, there are two types of imaging trackers, Gated Video Tracker (GVT) and Correlation Tracker.

3.3.1 Gated Video Tracker

The Gated Video Tracker (GVT) evaluates each resolution element within the FOV against some target criterion and maintains a stable sensor-to-target line-of-sight (LOS). Initially, the target is pre-acquired by some means. Once the target is acquired, the tracker locks-on to it and maintains the LOS. It has a closed area around the target where a tracking-gate is applied which works on the target edges and selects a rectangle around it. The gate can be made up of more realistic contours matching the target shape. The aim-point changes as missile-to-target range reduces. As the target comes closer it is more resolvable. The aim-point goes for higher contrast areas within the target such as a shining canopy in the visible or hot tailpipe in the case of IR detectors [DUD93]. Several methods for target location estimation have been developed. The most common of these is the centroid tracker.

3.3.1.1 Binary Centroid Tracker

The binary centroid of a segmented image is analogous to the centre-of-mass of a discrete distribution of unit masses. Consider the segmented image shown in Figure 3-15, where each pixel has been assigned a value of 1 if it corresponds to the target, and a value of 0 otherwise. It converts the image into a binary go-no-go video-map. The binary centroid tracker is an attractive option for applications that require a low-cost tracker with only modest performance capabilities. Most early imaging trackers used binary centroid because high-performance digital hardware was not available [DUD93]. Binary centroid tracking algorithms work well for situations where targets have high contrast with respect to background.

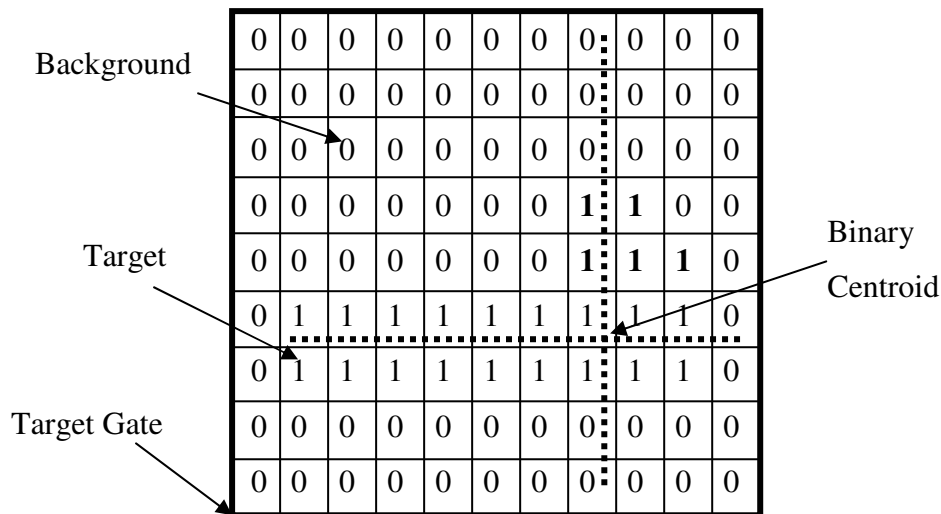


Figure 3-15 : Binary centroid of target image

3.3.1.2 Intensity Centroid Tracker

The architecture of the intensity centroid is similar to that for the binary centroid, but it does not employ the video-map to classify target and background pixels. Instead, it uses intensity information directly in the centroid calculation. This means that pixels with higher intensity values will be given more weight as compared to the pixels with low intensity values. One important application of the intensity centroid algorithm is high-accuracy point-target tracking [DUD93]. However, the accuracy of the intensity centroid tracker is extremely sensitive to the size of the target-gate. If the target-gate is large, then pixel values containing mostly noise are included in the centroid calculation, which degrades the accuracy [DUD93].

3.3.1.3 Threshold Intensity Centroid Tracker

The accuracy of the intensity centroid tracker can be improved if a video-map is used to eliminate pixel values not clearly associated with the target. The video-map acts like a pixel-level gating function in the centroid calculation. This type of intensity centroid is some times called a threshold intensity centroid [DUD93].

3.3.2 Correlation Tracker

The GVT is effective with a low-clutter background. For an image full of background clutter or other IR sources, then correlation trackers may be used. They are more

complex than the GVT and need prior knowledge of the desired target. In correlation tracking frame images are compared with a desired target image which is stored in memory. The offset produced due to matching generates the tracking error signal. The tracker points in the direction of the best match. The correlation tracker needs larger memory and faster computation capability. They are generally used for high value targets [DUD93].

3.4 Missile Guidance

The missile guidance is used to increase the Single Shot Kill Probability (SSKP) of a warhead. An unguided warhead will typically have excessive miss-distance. It is mainly due to number of factors including: the incorrect direction at launch, wind and weather disturbances in the flight path and the movement of the target. The solution to all of these limitations is to use guidance system to reduce the miss-distance and hence improve the SSKP [ROU00]. Missile guidance provides steering commands to the missile control surfaces so that the missile can successfully intercept the target. The selection of the guidance technique largely depends upon the size and speed of both the target and the missile. Missile guidance against large slow moving or quasi-static targets is comparatively simple. However, against small, fast and highly manoeuvrable targets we would need to have sophisticated and rapidly responding missile to enable a successful interception. There are basically three categories of guidance. These are Line-of-Sight guidance, homing guidance and navigation guidance. A further category of guidance, which combines more than one type of guidance, is called compound guidance.

3.4.1 Line-of-Sight Guidance

The Line-of-sight (LOS) guidance is the simplest method and most widely used for guidance against targets moving in straight lines. It needs a high sustained turn-rate to successfully track manoeuvring or crossing targets. A missile using the LOS-guidance has a complex launcher but the missile itself is simple. The LOS-guidance is further divided into two types. These are the Command-to-LOS (CLOS) guidance and the LOS-beam-rider (LOSBR). In CLOS systems, the operator visually acquires the target and guides the missile into the target either by radar or an optical tracking link. CLOS systems are not usually susceptible to countermeasures designed for IR missiles. Examples of CLOS systems are the British Blowpipe and Javelin systems. In LOSBR

an operator tracks the target and maintains a “cross-link” on the point of desired impact. The missile tracker calculates angular deviation from the centre of the beam. A steering command is generated in the missile which guides the missile to the target. The beam riders are difficult to jam once they have been launched. The examples of beam-riders are the Swedish RBS-70 and British Starstreak HVM.

3.4.2 Homing Guidance

In homing guidance the tracker is on the missile itself so it is called “two-point guidance”. The homing guidance is a closed-loop system in which the target data and missile position are observed continuously and steering commands are sent to the missile control surfaces. For moving targets, a feedback system is needed to constantly record the target position which is called guide-on-the-target (GOT). The homing missile sensor is called a “homing-eye”, “homing-head” or more commonly the “seeker-head”. The seeker-head tracks the target by detecting energy emitted from, or reflected by the target. There are three forms of homing guidance available. These are the active-homing guidance, which self illuminate and track their target, semi-active which guides onto energy reflected off the target which was transmitted by some other source which could be on the launch platform and finally passive-homing guidance which tracks emissions coming out from the target like “heat seeking” and “anti-radiation”. The US Stinger and Russian SA-7 SAM’s are the examples of the passive-homing guidance.

3.4.3 Navigational Guidance

In navigational guidance (NG), the missile carries the guidance-computer which obtains information concerning missile position from instruments or sensors which are also installed on the missile. The NG directs the missile onto a location in space planned in advanced and stored in memory. The most common type of navigational guidance is Inertial Navigation system (INS) which generally used in cruise missiles [ROU00].

3.4.4 Compound Guidance

Each type of guidance has its own advantages and limitations. To have an optimized guidance system which suits the specific requirement, combinations of different guidance systems at different stages of flight can be used. Missiles are designed with

two or more guidance systems working in parallel or in sequence. One such example is use of Inertial Navigation (IN) during the cruise phase and then shifting to homing guidance near the terminal phase.

3.4.5 Guided Missile Trajectories

The path a guided weapon follows from its launch point to the target is called its trajectory [ROU00]. Following are the types of trajectories which a missile can follow.

3.4.5.1 Straight-line Trajectory

In the straight-line trajectory a straight path between launcher point and impact point is established before launch, as seen in Figure 3-16. The straight-line trajectory is suitable for fixed or slow moving targets at short ranges. In some cases this technique may be used for the initial flight path of a missile which subsequently follows a ballistic trajectory.

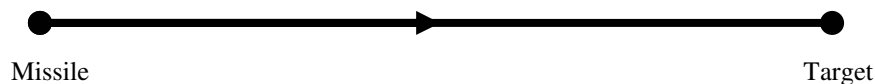


Figure 3-16 : Straight-line Trajectory

3.4.5.2 Line-of-sight Trajectory

The Line-of-sight (LOS) trajectory is shown in Figure 3-17. At any time the LOS is the line joining the observation point (launcher) to the position of the target at that instance. A missile following the straight-line trajectory may require little ability to accelerate laterally. Whereas, the LOS missile will normally follow a curved trajectory requiring considerable lateral acceleration (LATAX) capability. The LOS trajectory is commonly used in short range missiles [ROU00].

3.4.5.3 Proportional Navigation Trajectory

Generally, homing guidance missiles use proportional navigation trajectory. It establishes a sight-line from the missile to the target at all times as shown in Figure 3-18. The rate-of-turn of the sight-line is used to move the missile controls. The rate-of-change of the flight-path is directly proportional to the rate-of-turn of the sight-line [ROU00]. In proportional navigation the tracker is on the missile so it does

not need to have any link with launcher. The proportional navigation trajectory is used for fast moving aerial targets in air-to-air or surface-to-air modes.

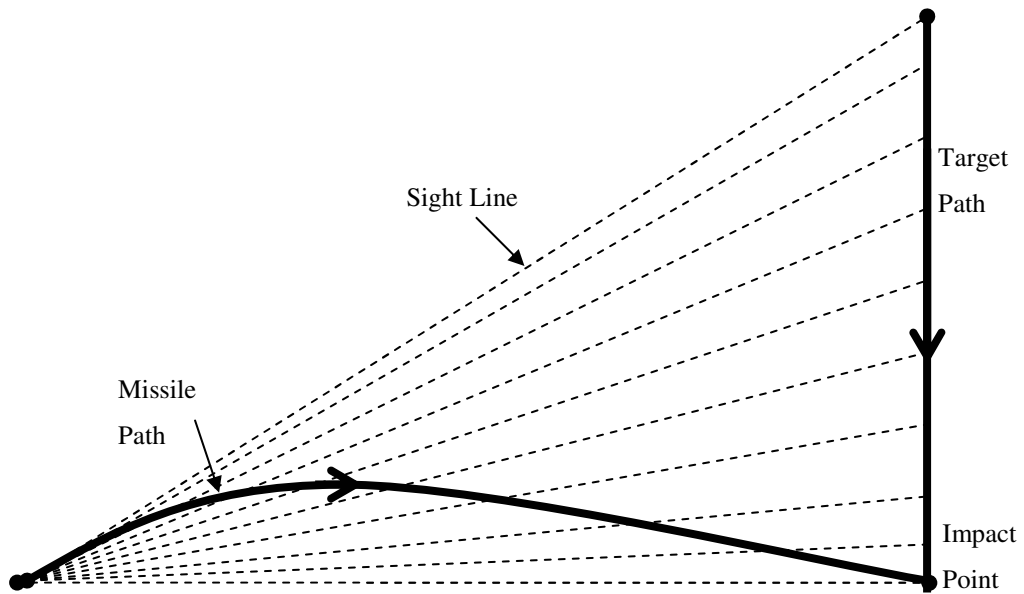


Figure 3-17 : Line-of-sight Trajectory

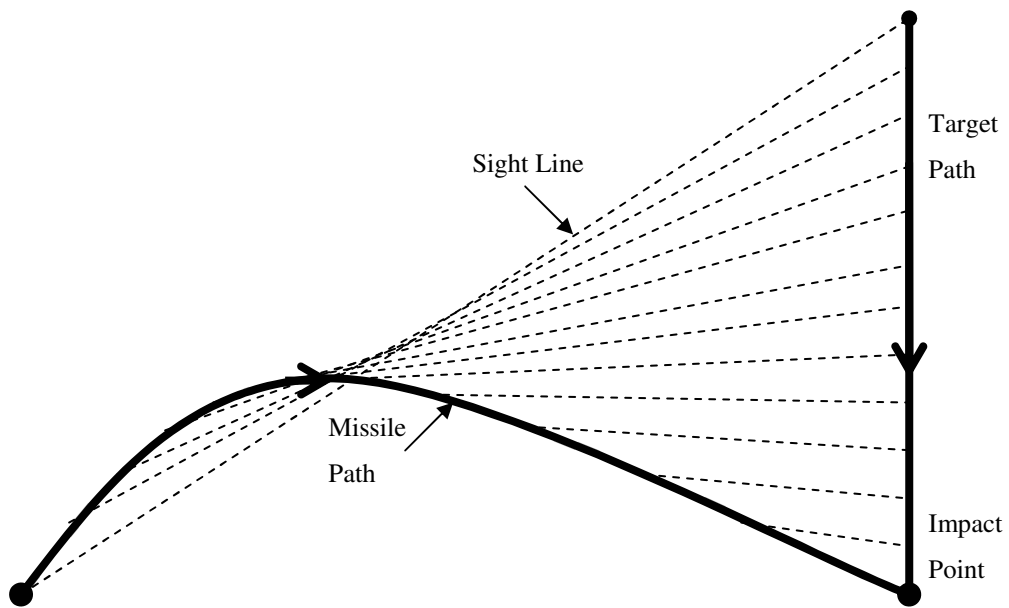


Figure 3-18 : Proportional Navigation Trajectory

3.4.5.4 Pursuit Course Trajectory

Perhaps the oldest and simplest type of flight path is that of the pure pursuit case also called "*hound-and-hare*" course [LOC55]. In pure pursuit course, the missile always

looks towards its target as a dog chasing a cat and never plans ahead to intercept the target. The sight line at any one instance can be found by drawing a tangential to the flight path of the missile at that interval. Figure 3-19 shows the pure pursuit course trajectory.

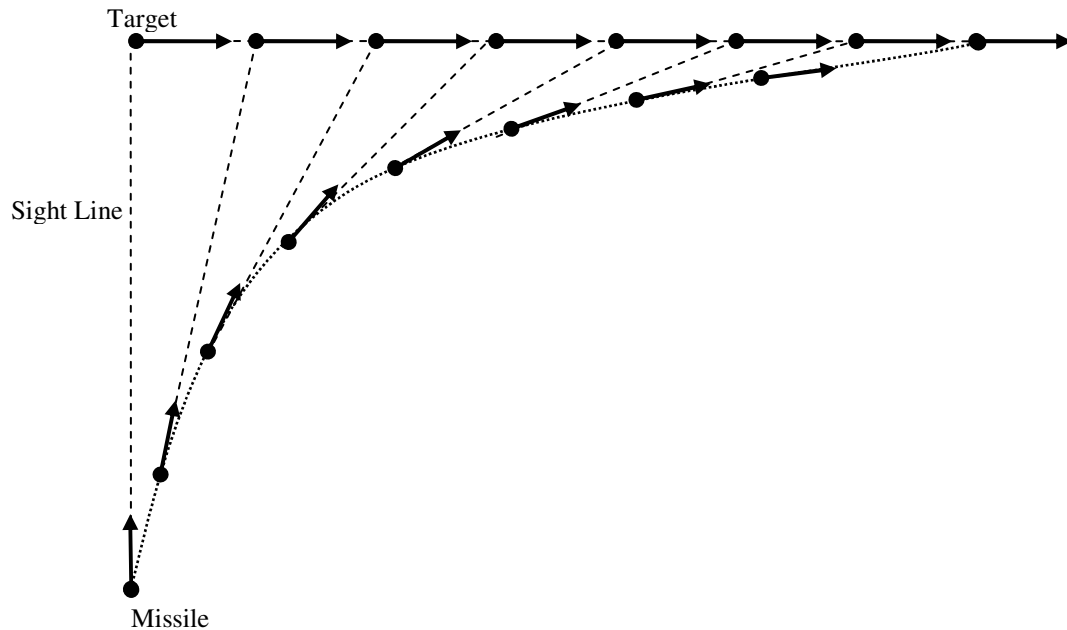


Figure 3-19 : Pure Pursuit Course Trajectory

3.4.5.5 Cruise Trajectory

Cruise is a pre-selected or defined path on which the missile moves at constant speed and height for most of its journey from launcher to target. It is, generally, used for long range cruise missiles. For long distances, the missile may go through a number of phases involving change from one height to another and perhaps a change in speed, but then each phase will be a segment of cruise trajectory [ROU00].

3.4.5.6 Ballistic Trajectory

Ballistic trajectory is the free fall trajectory caused by only the gravitational force as no motor or force is applied to create thrust or LATAX. Inside our atmosphere it is difficult to follow this trajectory, but in space where there is no aerodynamic drag a missile can follow ballistic trajectory [ROU00].

3.4.6 Proportional Navigation Guidance

The origin of proportional navigation guidance (PNG) is probably from the naval tradition of using this navigational technique for avoiding the collision of ships at sea with stationary or moving ships [GAR80]. In ships it is used for avoiding collision whereas, in missile it is used to encourage collision. In December 1950, the Lark missile was the first system developed using PNG, since then it has been the most widely used guidance system in all radar, infrared and TV guided missiles [ZAR02]. In short range homing missiles PNG is the most widely used guidance technique. PNG uses the LOS-rate between the missile and the target and the closing velocity (or time to go) as the basis for the steering commands. It generates command acceleration proportional to the LOS-angle-rate in an effort to form a collision course. PNG is faster and more efficient than LOS-guidance as it looks ahead of the target and reduces the intercept time and the demands on lateral acceleration. Still, it is not very effective against highly manoeuvring targets but it is simple to implement and does not require information about target range and location.

3.4.6.1 Augmented Proportional Navigational Guidance

As mentioned above, PNG has its limitation against highly manoeuvring targets. Augmented-PNG (APNG) is a modified version of PNG for highly manoeuvring targets. It is a higher-order guidance law which uses knowledge of the target range, velocity and acceleration. In APNG the total lateral acceleration requirements are much less as compared to PNG. Therefore, for strategic applications APNG is a more efficient guidance law than PNG [ZAR02].

3.4.6.2 Proportional Navigation Law

Proportional navigation law states that the rate-of-change of the missile heading or the trajectory is directly proportional to the rate-of-change of the sight-line between the missile and the target [GAR80].

$$\dot{\theta}_m = k \dot{\theta} \quad (3-1)$$

where, $\dot{\theta}_m$ is the rate-of-change of the missile trajectory

$\dot{\theta}$ is the rate-of-change of the sight-line

k is the navigation constant

To understand proportional navigation we can take two cases using Equation 3-1. In first case, if the value of the navigation constant is kept as unity ($k=1$), the rate-of-change of the missile trajectory will be equal to the rate-of-change of the sight-line. That implies that at any one instance a tangent drawn to the missile flight path must remain coincident with the sight-line. A tangent to flight-path indicates the instantaneous direction of the flight path at any one point in time. The type of trajectory caused by this is the pure pursuit course. In the pure pursuit course, as the missile is not anticipating the target future position, it needs to put in more efforts in terms of lateral acceleration towards the end of the flight path near impact. On the other hand, if the value of navigation constant is kept at four ($k=4$), then the rate-of-change of the missile trajectory will be four times the rate-of-change of the sight-line. The sight-line rate will reduce as the engagement proceeds. As a lead is established, the missile manoeuvres more in the beginning and it needs to turn less towards the impact. That implies that the overall missile lateral acceleration requirements will be less. Figure 3-20 shows the difference between the pure pursuit course and proportional navigation.

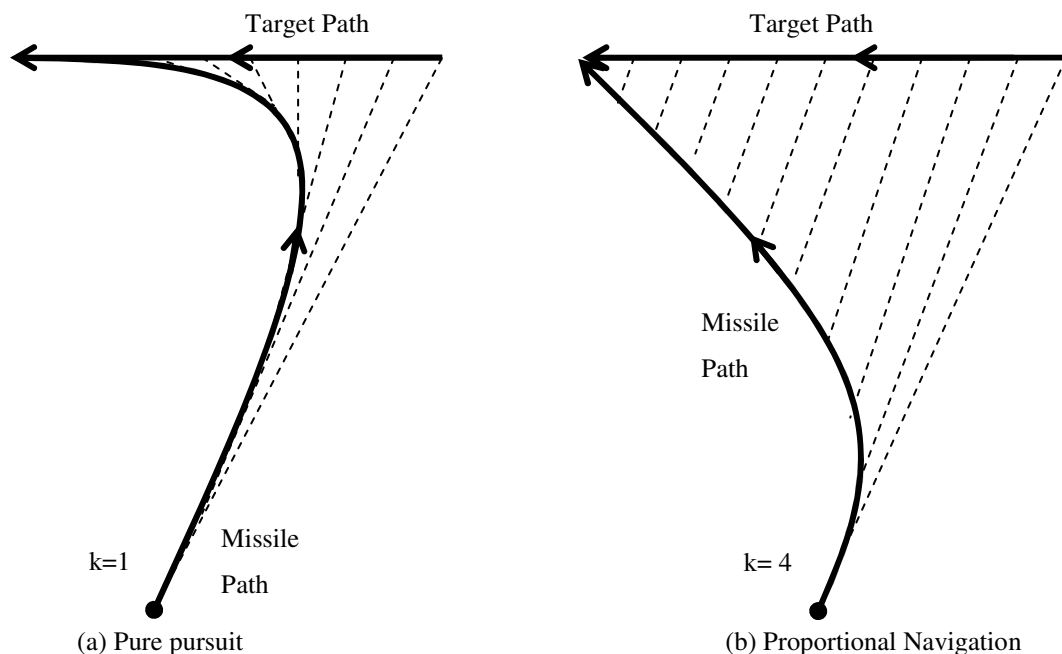


Figure 3-20 : Pure pursuit and Proportional navigation explained

3.4.7 Pursuit Course Guidance

One of the simplest ways of intercepting a target is to keep pointing at the target with missile having a greater speed than that of the target. Pursuit course guidance is the special case of proportional navigation, in which the navigational constant “ k ” is kept at unity ($k=1$). This means the missile always aims towards the instantaneous location of the target and never attempts to aim ahead as in the case of proportional navigation as shown in Figure 3-21 (a) and (b).

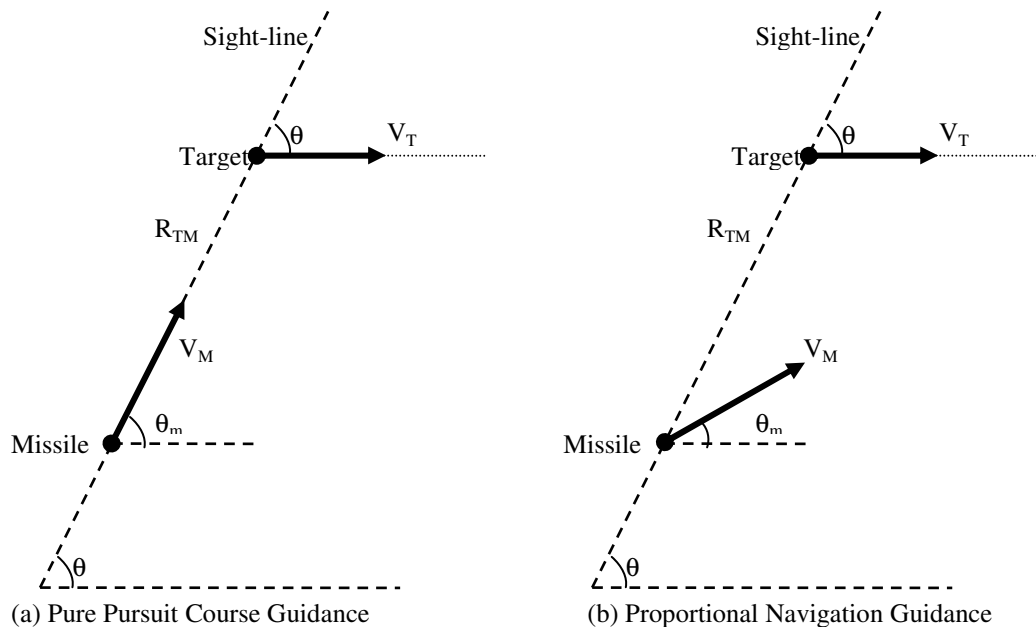


Figure 3-21 : Pure Pursuit Course Guidance

In Figure 3-21(b) by using components of the missile velocity and target velocity (parallel and perpendicular to the sight-line) we can write the following two equations [LOC55]:

$$\dot{R}_{TM} = V_T \cos(\theta) - V_M \cos(\theta - \theta_m) \quad (3-2)$$

$$\dot{\theta} = -\frac{V_T \sin(\theta) + V_M \sin(\theta - \theta_m)}{R_{TM}} \quad (3-3)$$

- where, R_{TM} is the missile to the target instantaneous distance
- V_T is the target velocity
- V_M is the missile velocity
- θ is the angle target is making with sight-line

θ_m is the angle missile is making with horizontal reference or the direction of the target velocity

By integrating Equation 3-1 we get

$$\theta_m = k\theta + \theta_o \quad (3-4)$$

Where, θ_o is the initial angle of missile trajectory. If k is unity and θ_o is zero then Equation 3-4 becomes:

$$\theta_m = \theta \quad (3-5)$$

Which is the condition for pure pursuit course guidance. Figure 3-21(a) shows this special case of proportional navigation. Putting $\theta_m = \theta$ in Equations 3-2 and 3-3 we can get the equations for pursuit course guidance as [LOC55]:

$$\dot{R}_{TM} = V_T \cos(\theta) - V_M \quad (3-6)$$

$$\dot{\theta} = -\frac{V_T \sin(\theta)}{R_{TM}} \quad (3-7)$$

Dividing Equation 3-6 with Equation 3-7 and rearranging we get [LOC55].

$$\frac{\dot{R}_{TM}}{R_{TM}} = (p \operatorname{Cosec} \theta - \cot \theta) \dot{\theta} \quad (3-8)$$

Where “ p ” represent the velocities ratio V_M/V_T and by integrating Equation 3-8 we get [LOC55].

$$R_{TM} = K \frac{(\sin \theta)^{p-1}}{(1 + \cos \theta)^p} \quad (3-9)$$

where, constant $K = \frac{(1 + \cos \theta_o)^p}{(\sin \theta_o)^{p-1}}$.

This equation of R_{TM} is for decreasing range [LOC55].

3.5 Missile Controls

The commands generated by the missile guidance system are fed to the control surfaces for moving the missile in the desired direction in three dimensional spaces. The up/down, left/right and forward/backward movement of the missile are achieved with translation in three axes orthogonal to each other and combined with rotation

around these three axes of *pitch*, *yaw* and *roll*. These six movements are independent of each other and are specified as six degrees-of-freedom (6DOF). Considering three orthogonal translation axis along the body of the missile as shown in Figure 3-22, the up/down rotation along lateral axis is called “*pitch*”, the circular movement along body axis is the “*roll*” and the left/right movement along the vertical axis is the “*yaw*” movement.

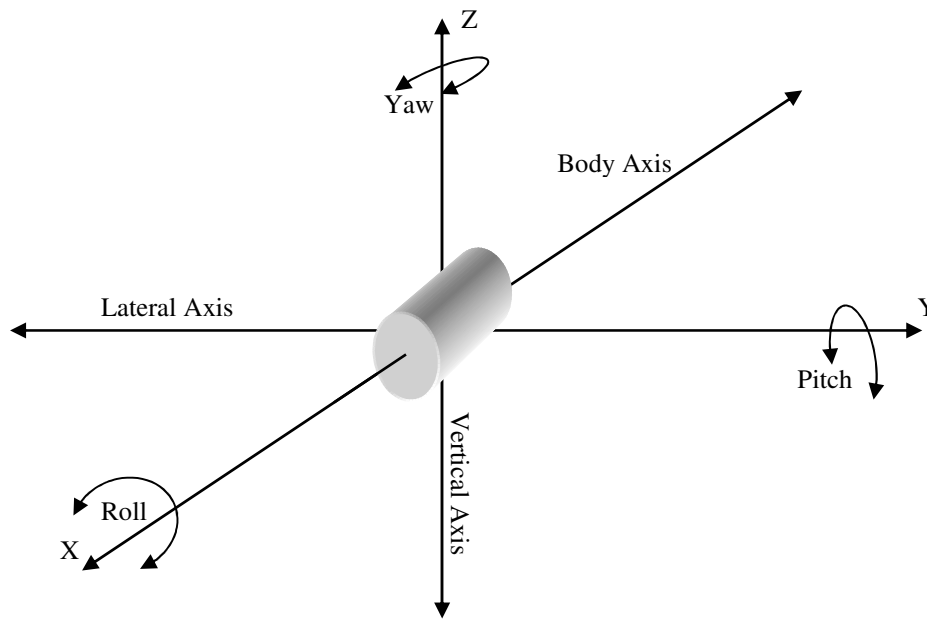


Figure 3-22 : Missile six degrees-of-freedom

3.6 Missile Aerodynamics

The atmosphere is not homogeneous and has different pressure and temperature regions. Missile performance and manoeuvrability is affected by atmospheric conditions. In the following paragraphs some of these effects related to missile modelling and performance are discussed.

3.6.1 Aerodynamics Drag

The total aerodynamic drag produced due to the movement of the missile in the air is sum of three factors; the skin friction, the pressure drag and the drag induced due to lift [ROU00]. The drag force applied on the surface of the object flying in the air is proportional to the square of the velocity ($F_D \propto V^2$). The force produced due to the aerodynamic drag can be written as [AND00]:

$$F_D = DV^2 \quad (3-10)$$

Where,

$$D = \frac{1}{2} \rho C_D A \quad (3-11)$$

- F_D is the force due to the aerodynamic drag
 V is the velocity of the missile relative to the air
 ρ is the density of the air
 C_D is the drag coefficient
 A is the cross-sectional area

However, it is important to know that at speeds greater than Mach 1, the drag coefficient is velocity dependent and behaviour of the drag changes.

3.6.1.1 Skin Friction

Skin friction is caused by the viscosity of the fluid through which the object is passing. The viscosity causes the shearing of the boundary layers which generates friction. The higher the viscosity the higher the friction produced. Air is not very viscous so the shearing forces are not very large, but due to the overall shearing force produced from a big surface area, the skin friction may contribute considerably to the over all missile drag.

3.6.1.2 Pressure Drag

The sharp corners of the missile or sudden changes in the cross-sectional shape due to manoeuvre etc. will cause wakes which generates a force at the back of the surface thus causes drag. The body of the missile should be a smooth rounded streamline surface to keep pressure drag low.

3.6.1.3 Lift Induced Drag

Trailing vortices are produced at the back of lift generating surfaces due to down-wash and up-wash motion of the air. This motion causes a drag which is called lift induced drag.

3.6.2 Lateral Acceleration of the Missile

Lateral acceleration (LATAX) is the sideways acceleration applied in two dimensions (i.e. pitch and yaw) to steer the missile in the desired direction. LATAX is usually

produced by aerodynamic forces acting on control surfaces. The LATAX depends upon the missile velocity and the distance between the missile and the target. The LATAX requirements generally increase with an increase in the sight-line angle. For small angles, the LATAX requirements are reasonable but for larger angles between 50° to 90° the LATAX requirements are much more severe. LATAX is a very important factor in the performance of missile. The design of any missile guidance system depends upon its lateral acceleration capabilities. Generally, surface-to-air and air-to-air missiles require high LATAX capabilities as they require high manoeuvrability to catch fast flying targets. In command guidance system the lateral acceleration tends to increase towards impact. Whereas, in proportional navigation the LATAX demands tends to decrease as it reaches the target provided the target does not manoeuvres.

3.7 Missile Fuses

Lethality of the warhead depends upon its lethal radius, the radius of a hypothetical sphere around the warhead within which any target will receive fatal damage. In reality, warheads are directional, so their lethal zone is typically a lobe shape instead of a sphere. The purpose of a fuse is to activate the warhead once the desired target is within its lethal radius. The effectiveness of the warhead therefore depends upon the performance of its fuse. There are mainly two types of fuses, the impact fuse which is the simplest and the more advance and complex proximity fuse. The most common proximity fuses used are radio proximity and active laser fuse. They do not need to impact the target but, trigger once the target enters the volume of space surrounding the missile. A delay is implemented to allow the target to come inside the lethal volume. Proximity fuses have a limitation in that they can inadvertently operate from for example the proximity of low level terrain, buildings or ship masts which are not the intended targets.

3.8 Summary

The first generation “*spin-scan*”, second generation “*con-scan*” and third generation “*pseudo-imaging*” based seeker’s output can be modelled using different techniques. However, in my work I have implemented the fourth generation “*imaging IR*” seeker using virtual reality modelling techniques. The gated-video tracker (GVT) and correlation trackers are used for generating error signals. In my work I have

implemented the binary and intensity centroid tracker algorithms. The IR homing guidance was implemented using pursuit course guidance which is the special case of proportional navigation guidance (PNG). The missile lateral acceleration is implemented based on the missile speed and load factor. The details of all these algorithms are given in Chapter-8.

3.9 Conclusion

Between 1981 and 1998, the IR guided missiles accounting for approximately 55% of worldwide combat aircraft losses [PAR04]. The threat from surface-to-air and air-to-air missile to the flying platforms is real. The biggest threat to aircraft is the MANPADs. IR homing missiles are fire-and-forget passive systems. They require no special fire control system. They are relatively cheap to manufacture and easy to operate. The new generations of IR guided missiles have an all-aspect attack capability and an improved immunity to flares.

4 INFRARED COUNTERMEASURES

4.1 Introduction

During the Russian invasion of Afghanistan, the Mujahideen downed 269 Soviet planes with 340 shoulder fired SAMs [BOL04]. In the last 25 years, there have been 35 recorded attacks on civilian aircraft using shoulder fired SAMs [BOL04]. While SAMs and AAMs represent a serious threat to combat and civilian aircraft, they can be defeated by the selection of appropriate countermeasures and evasive manoeuvres. Ideally, the launch of a missile should be avoided, if this is inevitable then, exploit the known weaknesses of the missile system to defeat it [TAY05].

4.2 Defence against Heat Seeking Missiles

There is a wide range of IR seeker missiles available in the world including the latest high sensitivity, smart seekers and ideally, an IRCM system must counter all these. However, there is a high probability of meeting a less capable threat of the more basic technology as compare to the latest state-of-the-art seekers. Defence against heat-seeking missiles involves the measures taken to make the missile exceed its design performance limitations so that it can either not be launched at all or, if already launched, it cannot successfully intercept its target. Anti-missile defence, therefore, can be sub-divided into two categories, namely pre-launch defence and post-launch defence.

4.2.1 Pre-Launch Defence

The aim of the pre-launch defence is to deny the enemy the missile launch envelope (MLE). This could be achieved, for example, by moving fast and using terrain to avoid being tracked.

4.2.2 Post Launch Defence

If the pre-launch defence fails, then the enemy will be successful in gaining and holding his position in the MLE and a missile launch will now be inevitable. There are several methods of defeating a missile after launch. First, to defeat the missile's guidance system by executing a high turn rate in an effort to get out of the usually narrow FOV of the missile. Second, to present false targets such as the sun or the use of flare decoys. The sun is a massive IR source, it radiates approximately as a black-

body of 5900 K. The sun is, therefore, a natural flare and one possible post-launch passive-countermeasure. The target aircraft is to fly into the sun so that the missile approaches from the tail aspect; since the missile views both the aircraft and the sun, it tends to lock onto the stronger source (the sun). Coupled with this measure the aircraft is advised to execute a hard turn when the missile draws closer. Although, modern advance missiles possess the ability to reject the sun and conventional flares, still, the flares are effective and inexpensive countermeasure against most basic technology IR threats and will continue to improve and have a major role in the future [PAR04]. The third method is to apply IR jamming techniques to the missile seeker head such as the directional-IRCMs.

4.3 Infrared Signature Suppression

The proliferation of shoulder fired IR guided SAMs makes any aircraft in the air a potential target. Measures are required to counter this threat and increase the survivability of the platform in a hostile environment. Infrared signature suppression (IRSS) is the process of reducing the IR signature of the target and thus reducing the vulnerability of the target to IR guided missiles. The most effective defence against IR guided missile is to avoid detection by the IR threat. This could be done by three main techniques:

- (a) Hiding or camouflaging sources of heat or IR energy from the threat detector.
- (b) Suppressing the IR signatures of the platform to blend the target into the background so that the threat seeker cannot distinguish between the target and the background.
- (c) Creating a screen between the target and the threat thus eliminating the threat's ability to lock-on the target.

The most dominant source of heat on military targets is usually its engine exhaust. Although we cannot entirely hide or cool this source of radiation, it can be made more difficult for the missile to detect or lock-on the target or even just to reduce the lock-on range. The reduced lock-on range obviously increases the platform survivability. To reduce IR signatures the aim must be to either decrease the temperature of the body or the emissivity of the surface or if possible, both

simultaneously for better results. A few IRSS techniques are; thermal insulation, low emissivity paints, optical blockage, smoke screens, camouflaging nets, surface film cooling and exhaust gas cooling etc. Applying IRSS could reduce the susceptibility of the platform to IR guided threats.

4.3.1 Suppressing Heat Source

The basic aim of any IRSS is to reduce the thermal difference or thermal contrast between the target and the background. As all military targets comprise more than one source of heat generation (engine, exhaust plume, aerodynamic heating and skin etc.), there is, therefore, no point in reducing the signature of one component to zero and leaving other significant sources untouched. The aim of IRSS must be to first reduce the most dominant heat source and then the next dominant and so on until as much as is possible has been achieved within the allowed budget [DAV02]. Suppressing the engine's hot exhaust may be the most effective way of reducing IR signature of a hot target. The IR signature of large aircraft can be reduced by as much as 80% by shielding or ducting the engine exhaust or mixing ambient air with the hot exhaust, however, this may adversely affect engine performance, aerodynamic drag, weight and balance [BOL04], [SUL97] and [DIX05].

4.3.2 Reducing Emissivity

A reduction in the overall radiation of a target could be achieved by reducing the emissivity of hot areas. However, reducing the emissivity will increase the reflectivity, so depending upon the waveband of the missile we need to look for the optimized values for emissivity and reflectivity. IRSS can not make target completely invisible in the IR spectrum but can reduce the IR signature to some degree. Camouflaging is the process of reducing the target reflectivity for protection in the visible band and suppressing the emissivity in the IR band. Camouflaging makes it more difficult for the missile operators to visually track the target during the pre-launch phase and also for the missile tracker to lock-on to the target. IR paint can be used to reduce an aircraft IR reflectivity and visual profile [TAY05].

4.4 Infrared Countermeasures

The IRSS can reduce the IR signature, it can, therefore, reduce the detection and lock-on ranges, but once detected cannot provide adequate protection against missiles

under all operating conditions. Therefore, Infrared countermeasures (IRCMs) have been essential in deceiving the IR threat homing mechanism. Ideally, these measures should make the missile miss its target, but if it is not possible, then they should at least increase the miss-distance to lessen the effects of the missile warhead. The aim is, therefore, to implement IRSS as much as possible and then use IRCMs for further protection. Depending upon the type of platform, large wide body civil or military aircraft, fast small size fighter aircraft, slow moving helicopters or ground military vehicles, the appropriate countermeasures, against the individual type of IR missile threat, are different. Using flares as alternate IR source in the missile FOV, or a laser to blind the missile seeker are a few common countermeasures against heat seeking missiles.

The IRCMs may be active or passive. The active countermeasures are usually on-board systems that, for example, use modulated IR sources to provide a time-varying signal to generate false guidance commands for the IR threat. Systems such as Directional IRCM (DIRCM), Large-aircraft IRCM (LAIRCM) and Close-Loop IRCM (CLIRCM) etc. are the active countermeasures that defeat the IR threat by directing a high intensity modulated source of radiation at the missile seeker. On the other hand, the conventional passive countermeasures are mostly off-board expendable flares with very high intensity IR source resulting from a chemical or pyrotechnic reaction. The burning of Magnesium powder provides very high IR signature which cause the IR guided missile to consider it as the primary target and the platform can move out of its path. On most of the high performance fighter aircraft, slow moving transport aircraft and helicopters, the flare decoys are considered to be one of the primary defences against heat seeking missiles [VAI94].

4.5 Off-board IRCM Flares

Flares have been used for over 45 years to successfully defeat heat seeking missile [TAY05]. Flares are inexpensive as compared to other countermeasures and their cost is tiny as compared to the cost of the platform itself. Conventional flares defeat heat seeking missiles by producing a hot source in the missile's FOV. The missile seeker's basic logic is confused by the presence of intense IR energy within its FOV and causes missile to break-lock to this as if it seems the actual target. Conventional flares are generally very effective against early generation missile systems. However, the advancements in flare technology have significantly increased their capabilities

against advance heat seeking missiles [TAY05]. The fundamental requirement for the flare is to be launched in the FOV of the seeker to deceive the seeker and divert it from the real target. In the following paragraphs different types of flares are discussed.

4.5.1 Conventional Flares

The conventional flares are considered to be hot (2000-2200 K) pyrotechnic “point sources” traditionally derived from pellets of Magnesium, Teflon and Viton (MTV) [POL93]. The MTV flares, such as the M-206 and MJU-7B, burn hot and bright in a single temperature range. Their IR signature is more intensified than that of the host aircraft. They are effective for decoying early generation IR threats, such as SA-7, that do not feature any counter-countermeasures [KNO06].

4.5.2 Multi-spectral Flares

The later 2nd and 3rd generation missiles containing counter-countermeasures operating in different or more than one waveband in the IR spectrum, have significantly reduced the effectiveness of the MTV flare types. New materials have been developed using combination of hydrocarbons, propellants and other materials, operating at lower temperatures (about 800 K) [TAY05]. These flares emit radiation in two or even three temperature bands and are known as dual-spectral or multi-spectral flares. These flares operate at about 800 K and much more closely resemble the IR signature of the host aircraft. Still multi-spectral flares are ineffective against modern pseudo-imaging seekers [CHO05]. The DMC69 A1 Array flare is a spectrally balanced IR flares developed by Valley Associates Institute, Ontario, Canada. The temporal and spectral responses can be specially designed to match any particular aircraft’s spectral signature and threat scenarios [ASS07]. In Figure 4-1 the spectral response of an aircraft is compared with array flare and the conventional MTV flare.

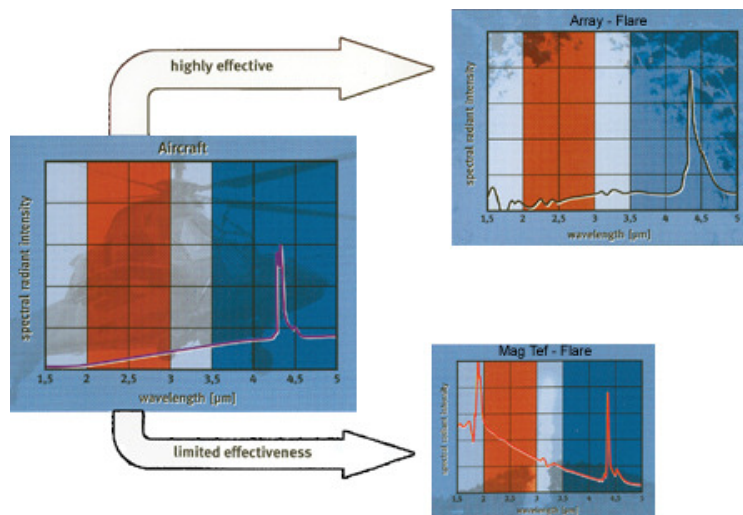


Figure 4-1 : Spectrally balanced array Flares (source [ASS07])

4.5.3 Special Material Decoy

The special material decoys (SMDs) are the metal coated wafers fabricated from pyrophoric materials have now been developed to provide a lower and tailored temperature “big area cloud” rather than conventional hot “point source”. They are dispensed in air stream in bundles which react with atmospheric oxygen and releases heat at temperature up to 820 K that means the decoy burns much closer to an aircraft’s engine temperature than the 2000 K generated by an MTV flare [KNO06]. They have no visible signatures, thus they some time called invisible flares. Invisible flares can be effective against pseudo-image seekers. They are preferred for low-altitude use where chances of a fire hazard from convention flares are higher. The application of conventional bright visible flares could cause panic in the passengers on commercial aircraft and this could be avoided by using invisible flares [CHO05]. The liquid pyrophoric IR flares are developed by the Bristol Aerospace, Minitoba, Canada [AER07]. These flares expel a liquid that burn on contact with the air creating an aircraft-size IR signatures. As shown in Figure 4-2, these flares are electrically ejected from the dispenser and the base of the flare remains connected through a wire to the dispenser. Once fully expelled, the pull on the friction wire ignites a gas which starts the dispersion of the pyrophoric fluid into the air stream where it ignites spontaneously with the air. Pyrophoric flares have demonstrated superior performance compared to convention pyrotechnic flares [AER07].

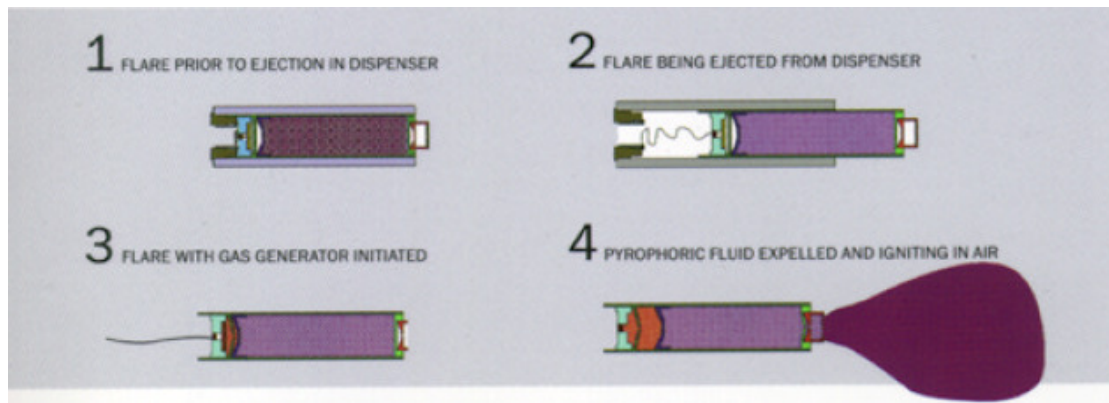


Figure 4-2 : Liquid Pyrophoric Infrared Flares (Courtesy: Bristol Aerospace, Canada)

4.5.4 Electronically Configurable IR Towed Decoy

A towed decoy is dispensed and will therefore follow the same profile as that of the aircraft to remain within FOV of missile seeker. The payload consists of foils of a pyrophoric material. It can be tailored to create IR signature behind the decoy which spectrally matches the IR signature of the host aircraft's exhaust plume.

4.5.5 Kinematics or Fly-along Flares

Fly-along flares, as the name implies, are the decoys which can fly along at a distance from the launching aircraft to remain in the FOV of the missile seeker. They can be self-propelled by a rocket motor or towed along by some attached wire. They are aerodynamic in shape with a lower drag coefficient. These flares are typically more effective against heat seeking missile equipped with a forward-bias countermeasure that employ relative motion and rapid sight-line variations as the discrimination technique.

4.5.6 Flare Performance Factors

The performance of a flare to deceive a missile threat depends upon its design factors. These factors are explained in the following sub-paragraphs:

- (a) **Peak Intensity.** For effective deception, a decoy must exceed the intensity of the platform to be protected. The intensity of the hot metal parts of the host platform are taken as the reference for flare specifications [POL93]. A typical range for a conventional flare is 0.5 to 1 MW of power for each

1000 W sr⁻¹ of in-band radiant intensity [POL93]. A typical range of various airborne platform signature levels are shown in Table 4-1.

(b) **Rise Time.** The flare decoy dispensed from a moving platform must reach an effective level of intensity prior to leaving the seeker FOV. An aerodynamic deceleration as great as 300 ms⁻² is possible once flares are dispensed from an airborne platform [POL93]. Typically, the missile field-of-regard is less than 200 meters at time of deployment. This means the effective operational intensity level must be achieved within a fraction of a second [POL93].

(c) **Spectral Response.** Ideally the spectral characteristics of the flare must match that of the platform to be protected. However, most decoys create higher temperatures in comparison to the target to overcome their smaller size and this does not match with the spectral characteristics of the platform. The spectral matching requirements severely affect the flare's performance. Spectral matching often requires that the relative signal level of the decoy in the missile wavelength band must be within the normal variations of the platform characteristics (see Figure 4-3). This could be achieved either by controlling the flare burn temperature or by selecting the flare material having relatively high emissivity in the missile band and significantly lower emissivity in those bands where the target intensity is low [POL93].

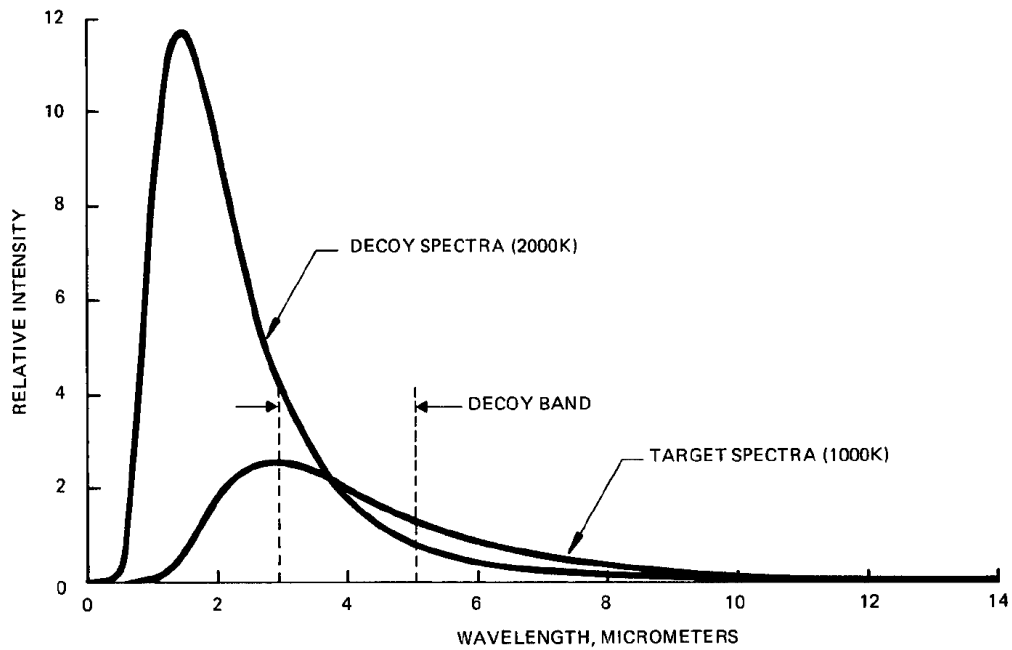


Figure 4-3 : Typical flare decoy/target spectra. (from reference [POL93])

(d) **Burn Time or Function time.** The flare must remain present within the FOV so that the missile should not reacquire the target or otherwise, a second flare is to be deployed. The ideal minimum burn-time is that in which the protected aircraft takes until it is no longer in the missile FOV due to the effective separation of the flare and aircraft. For low altitude applications, the burn-time must be planned accordingly to avoid a fire hazard on the ground [POL93].

(e) **Ejection Velocity and Direction.** The flare may be ejected where it can easily be seen by the missile seeker and then separate from the target so that it remains within the missile kinematics tracking limit. The flares ejection direction should be selected to generate the greatest possible angular separation rate consistent with the missile tracker capability.

(f) **Aerodynamic Characteristics.** Especially in the case of aircraft flares, the aerodynamic characteristics of a flare strongly influence the flare separation profile. It should have some ballistic density so as to avoid rapidly falling out of the missile's FOV [POL93].

Table 4-1 : Typical signature levels of airborne platforms (from reference [POL93])

Aircraft Type	Intensity (Watt sr ⁻¹)	
	2-3 μm	3-5 μm
Rotary Wing	10-100	100-300
Fixed Wing (propeller)	20-200	200-500
Jet Fighter	50-1,000	100-10,000
Jet Transport	100-1,000	100-5,000

4.5.7 Flare Limitations

No system can be ideal, so the flares also have some limitations. Flares are not effective against all generations of missiles. They are typically ineffective against laser-beam riders and radio-frequency (RF) command guided missiles. A flare can cause an undesirable increase in the visible and IR signatures. A limited number of flares can be carried on board. Conventional flares are not suitable for low level dispensation due to fire hazards on the ground in populated areas. Conventional and advanced flares have little prospect for countering imaging seekers.

4.5.8 Flight Guard Self Protection System

Flight Guard is the anti-missile protection system for passenger aircraft. It is developed by ELTA, Israel Aircraft Industry (IAI). It fires invisible gas flares or dark flares which are invisible to the naked eye but confuse the missile heat seeker and send the missile off course. The invisible flares reduce the chances of panic among the passengers of the civilian aircraft and also reduce the risk of causing fire once dispensed at low levels during landing and take-off. This system is in service on aircraft and helicopters of the Israeli Air Force [ELT07].

4.5.9 Wide-body Integrated Platform Protection System

The wide-body integrated platform protection system (WIPPS) is an advanced missile warning and threat adaptive countermeasure system developed by L-3 AVISYS, Texas USA. It consists of a programmable electronic warfare processor, advance dispensers and a multi-function display. It dispenses advanced IR flares decoy. WIPPS can be integrated with DIRCM for back up threat coverage [AVI07].

4.5.10 Comet IRCM Pod

Comet is an advanced IRCM pod being developed by Raytheon, USA for the A-10 and C-130 aircraft. It is based on an IR towed decoy technique. It is suitable for fast moving jets and transport aircraft that spend little time in the threat area. It slowly

dispenses pyrophoric material behind the jet to create a realistic engine plume signature that can defeat IR guided missile. It can engage multiple targets in pre-emptive mode with no cueing required. It is fully covert in the visible spectrum, creates continuous false targets to turn the IR threat away from the host aircraft. It contains six canisters of IR decoy material to protect the aircraft for 30 minutes [RAY07]. It generates a plume tailored to mimic the aircraft exhaust plume signature by controlling the dispersal rate from a precision dispenser system.

4.6 Active IR Countermeasures

IR jammer causes missiles to break-lock by confusing their guidance system by feeding more IR energy into seeker detector. Unlike passive IRCMs, such as flare decoys, which present a second bright IR source to deceive the IR missile seeker, the active IRCMs use beams of energy produced by an arc-lamp or laser to exploit knowledge of the seeker to defeat their homing process [ROC06b]. In the last decade, various active countermeasure systems have been developed against heat seeking missiles. These systems are summarized in Table 4-2 and explained in the following paragraphs.

Table 4-2 : Active IR countermeasure systems for military aircraft

TYPE	MODEL	YEAR	MANUFACTURER	PLATFORM
DIRCM	AN/AAQ-24(V) NEMESIS	2001	Northrop Grumman	Small aircraft, Helicopters
LAIRCM	AN/AAQ-24(V)13	2002	Northrop Grumman	Large aircraft
ATIRCM	AN/ALQ-212(V)	2003	BAE	Small aircraft, Helicopters
TADIRCM	AN/ALQ-212(V)	future	BAE	Tactical aircraft
CLIRCM	-	future	Lockheed Martin	Small aircraft

4.6.1 Advanced Threat Infrared Countermeasures

Advanced threat infrared countermeasures (ATIRCM) is a non-laser based multi-spectral IR jammer. It has two steer-able heads which uses Xenon arc lamp jammer to counter near-IR and mid-IR threats. The ATIRCM gets a cue from the missile approach warning system (MAWS) which consists of four missile sensor heads that detects UV radiations from the missile rocket engine [ROC02].

4.6.2 Directional IRCM

Traditional IRCM jammer uses wide-angle heat lamps to counter missile seekers, but these do not radiate enough energy in all directions to allow all-aspect jamming. Directional IRCMs (DIRCMs) either use IR arc-lamps or lasers to create a field of IR energy designed to confuse the missile seeker. They focus the IR energy directly onto the incoming missile. The lasers based DIRCM can generate more jamming power density than conventional IR-lamp IRCMs. DIRCMs are the most effective defence against modern heat seeking missiles. The laser fired on the seeker could affect its optics and detector. Laser countermeasures will play an increasing role in the defence of aircraft and thus enhancing its survivability. Modelling DIRCM needs pointing and tracking performance of the DIRCM and the effects of a high intensity source on the missile sensor. It needs to see the interaction between the target signature, the laser countermeasure, the IR seeker and the signal processing algorithm. The sequence of events in a DIRCM is that the MAWS is used to alert and give the direction of the threat missile. The countermeasure tracker tracks the incoming missile and a turret based laser source points on to the incoming missile.

Laser jamming is currently the most advanced form of directional IRCMs. They can be extremely effective against first and second generation missiles and can divert the missile by substituting a modulated signal transmitted by the laser. A multi-band laser is required for protection against a variety of missile seekers operating in various IR bands. A laser based jammer needs high accuracy in its pointing. They typically use a turret to slew the laser beam [ROC06b].

4.6.3 Large Aircraft Infrared Countermeasures

Large aircraft infrared countermeasures (LAIRCMs) are similar to directional IRCM specially developed for large transport aircraft, such as C-5s, C-17s and C-130s. The LAIRCM system has been designated AN/AAQ-24(V)13. LAIRCM is optimized for aircraft that present a large IR heat source (in both area and intensity) for incoming missiles and a very different IR signature compared with smaller platforms. A large aircraft's greater IR signature allows missiles to acquire and track from longer ranges, which means this type of applications ideally demands an IR-type MAWS [ROC06b]. Current generation IR missile seekers have very narrow FOV. The four to eight dispersed engines on a large aircraft, spanning 60 to 100 feet, offer several targets.

This makes the job of the LAIRCM more difficult, because it must jam an incoming threat well enough to prevent it from reacquiring another engine [ROC06b].

4.6.4 Tactical Aircraft Directional IRCM

The tactical aircraft directional infrared countermeasure system (TADIRCM) has been developed by the Naval Research Laboratory (NRL) USA, mainly for Navy tactical fixed and rotary wing platforms. The system uses a suit of two-colour IR sensors to passively detect the signature of the threat missile plume [SAR03]. The missile boost signature is segregated from urban and background clutter by using sophisticated processing techniques and a cue is generated for the directed jamming system. A high resolution IR camera is then used to generate track on the target. A modulated laser beam creates false targets in the missile seeker may causing optical break-lock (OBL). Its performance was tested in live fire and optical break-lock was achieved in each trial against advance SAM and AAM [SAR03].

4.6.5 Closed-loop IR Countermeasures

The LAIRCM, DIRCM and ATIRCM all are open-loop systems. In an open-loop countermeasure system the laser modulation is pre-determined, so it must be designed to counter any of the likely threats. On the other hand, the closed-loop infrared countermeasure (CLIRCM) system, which are not yet available are intended to capture retro-reflections from the seeker's reticle that can help to identify the attacking missile [CHO05]. The advantage of close-loop system is to focus all the laser energy in the appropriate pass-band and optimise the jamming modulation. CLIRCM allows the jammer to adapt in real-time to the threat missile seeker processing scheme, maximizing the effectiveness against known and unknown threats. CLIRCM is the next generation of IRCM. It will provide protection at about half of the cost of the existing open-loop IRCM systems [SAW01]. CLIRCM technology has been under development at the Air Force Research Laboratory (AFRL), Dayton, OH, USA under LIFE programme [SAW01].

4.6.6 Mobile Tactical High-energy Laser

Possibly, the ultimate solution for protection against all types of missile is the mobile tactical high-energy laser (MTHL). It uses a megawatt-class Deuterium Fluoride chemical laser weapon housed in a turret. HORNET (hazardous ordnance engagement

toolkit) is a palletized variant of MTHEL being developed by Northrop Grumman for a ground based defence against MANPADs [CHO05]. The advertised performance of a single HORNET site indicates capability to defend against salvos of three missiles out to a range of at least 5 km, and against single missile protection out to 10 km [CHO05]. The primary advantages of MTHELs for SAM defence are the ability to counter every current and future seeker technology. However, due to the lasers limitations, it can not operate under all weather conditions and also eye safety is a cause of concern for using high-power laser in populated areas [CHO05].

4.7 Missile Approach Warning System

Almost, all of the IRCM systems either off-board flare decoys or IRCM jammer need an early warning to take evasive action against the missile threat. A missile approach warning system (MAWS) alerts the platform to any incoming missile threat so that defensive action may be initiated. MAWS detects the launch plume of a missile and provides launcher location information. It operates in the “solar-blind” region of 230 to 280 nano-meters. It detects the ultra-violet (UV) emissions present in the missile exhaust plume. The MAWS works in UV region of electromagnetic spectrum, as there are few manmade and natural sources, including high-intensity lamps, aircraft afterburners, corona discharges and lighting. The missile is small in size and fast moving as compared to the aircraft hence engagement times are usually very short, the MAWS performance therefore is a key factor in the over all effectiveness of IRCM systems and the survivability of the aircraft.

In recent times UV MAWS have been utilized by the military to provide warning of missile fire and approach. MAWS performance is a key feature in the overall effectiveness of the aircraft protection system [BOL04]. Newer dual mode/band IR MAWS using focal plane array technologies and advanced image processing techniques are being used to give better false alarm rates and more accurate information regarding the position of the approaching missile [CHO05].

To avoid being detected by the UV MAWS, the missile launch UV efflux smoke may be camouflage or, alternatively, the other man-made UV sources, such as the high-intensity UV search lights, may be used to decoy missile rocket plume UV signature.

4.8 IR Counter-countermeasures against IRCM Flares

The actions taken by the target aircraft to deceive the incoming IR seeker missile are called the IRCMs. To remain effective, modern missiles apply techniques to counter these IRCMs. Such techniques are called IR counter-countermeasures (IRCCM). To distinguish the flare decoy from the target the missile seeker analyses the incoming signal from the target and the flare. The missile can differentiate flares from targets on the basis of the following techniques:

- (a) **Flare Rise-time.** At any instance, a sudden rise in irradiance above the aircraft signature level could be considered by the missile as the presence of a flare decoy.
- (b) **Fast Separation Rate.** A sudden increase in the sight-line rate caused by the flare separating from the host aircraft could be indicated to the missile seeker of the presence of a flare decoy.
- (c) **Direction Biasing.** Prevention of the seeker optics from tracking the unwanted source, such as a flare, which separates in a given direction for example the forward biasing the seeker FOV.
- (d) **Two-colour Discrimination.** The missile seeker use two-colour sensors to distinguish the aircraft from the flare. This compares the spectral signatures of the hot decoy and the relatively cool target. As shown in Figure 4-3 on page 53, their signatures are approximately equal in 3-5 micron band. However, their signatures do not match in the rest of the spectrum. The flare, being very hot, is much brighter at shorter wavelengths and slightly less bright at the longer wavelengths [POL93]. If the missile seeker also has a detector in other IR waveband then it could easily distinguish between the flare and the aircraft. This can be used by the missiles against conventional flares.
- (e) **Target Gate.** The target gate applied in the gated video tracker (GVT) algorithm is a smallest possible rectangle around the target or in some cases it is even applied along the contour of the target to make the target gate a more realistic shape. It acts as a built-in IRCCM as it improves the performance of the tracker by reducing the computational process to its minimum level and also helps in rejecting IR decoy flares or background noise.

(f) **Optical Filters.** Narrow-band optical filters are used in seekers optics to block a jammer or noise from unwanted wavelengths [CHO05].

4.9 Improvements in Flares Design

To counter missile counter-countermeasures the following improvements can be made in the flares design.

(a) **Slow Rise Time.** To counter the missile's ability to differentiate between the target and the flare due to the sudden change in intensity level, the flare rise-time needs to be kept slow. However, the flare must reach the desired intensity level while still within missile's FOV to deceive the seeker.

(b) **High Intensity.** The automatic gain control (AGC) feature of the missile can be deceived by making the flare intensity very high, so that its modulation capability will reduce by applying the AGC.

(c) **Kinematics.** The ability of the missile to detect a change in the separation rate due to the flare's sudden separation can be overcome if the flare can fly along side the aircraft for a period of time or even moves ahead of the aircraft. This can be achieved with the aerodynamic or self-propelled flares.

(d) **Large Area.** Instead of a high temperature point source flare, the IR signature of a large area can be produced by using pyrophoric material that can burn once in contact with the atmosphere.

(e) **Spectrally Tailored.** The hot MTV flares can easily be countered by the missile seeker due to spectral difference in the IR signature from that of the target aircraft. To overcome this, the flare's material is modified such that it resembles the IR signature of the host aircraft.

4.10 Terrorist Missile Threat to Commercial Airlines

The efficient use of IR guided missiles against airborne targets was first seen in the Korean War. Since then IR guided missiles have been extensively used in various conflicts. In the last decade alone, IR guided missiles were responsible for more than 50% of all aircraft losses world-wide [SAR03]. IR guided missiles are getting much harder to defeat by any current method as they are becoming more lethal and stealthy

[PAR04]. Recent events of terrorist missile attacks on commercial airlines, have given a new aspect to this problem. The civilian aircraft are wide-body and easy targets. They are most vulnerable to terrorist SAMs threat near airports during takeoff and landing. Figure 4-4 shows an envelop of 6 miles by 50 miles along the runway (i.e. 300 square miles area around the runway) where generally it is below 10,000 to 15,000 feet altitude during a typical takeoff and landing approach [PLE03].

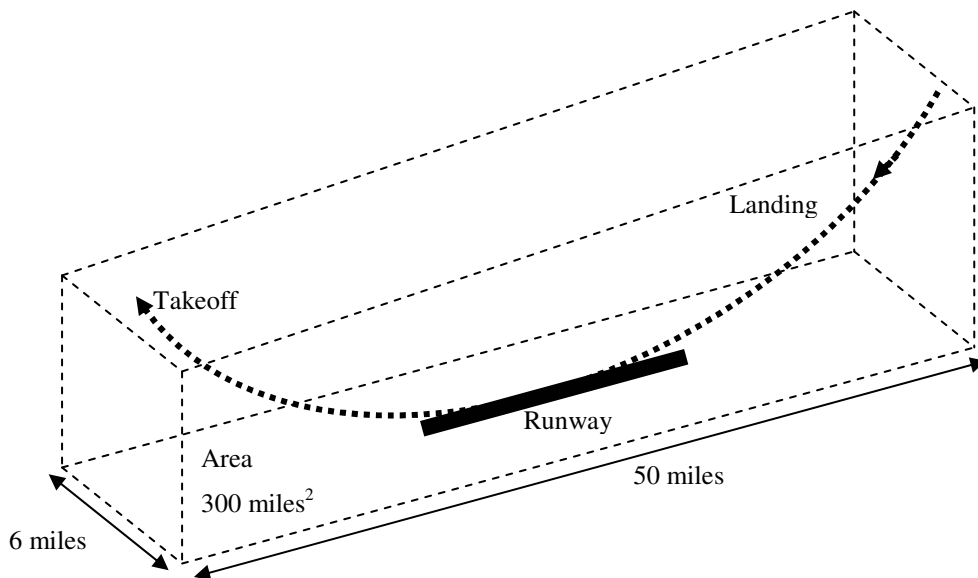


Figure 4-4 : MANPAD Threat Area on Takeoff and Landing (source [PLE03])

The existing LAIRCM systems installed on military transport planes and also on VIP aircraft may not be considered a viable solution for protection of commercial airliners. The cost of existing LAIRCM system ranges from one to three million dollars per aircraft which seems beyond the budget of commercial airlines. The use of standard flares by civil airlines during takeoff and landing presents a fire hazard on the ground as most civil airports are in populated areas. The laser based DIRCM may offer a more effective defence against modern shoulder-fired SAMs. However, its weight, size, cost and reliability, may not make it attractive for commercial airlines. Another option is to apply IRSS measures on civil airplanes. This could be effective in mitigating the missile threat but cannot completely eliminate the threat. It may also adversely affect engine performance or increase aerodynamic drag. An immediate and complete solution to counter the terrorist missile threat to civil airliners is not currently available [BOL04]. In February 2003, the US government passed a bill “Commercial Airline Missile Protection Act” to attempt to mitigate this threat [BOX03], [CAT01] and [SHE03]. In July 2004, three companies Northrop Grumman,

BAE systems and United Airlines were each given two million dollars to determine whether existing technology could be used to counter the terrorist threat. They have come up with some economical solution for commercial airliners. Table 4-3 summarizes the various infrared countermeasures systems developed for the protection of commercial airliners.

Table 4-3 : IRCM systems developed for the protection of commercial airliners

MODEL	YEAR	MANUFACTURES	BASED UPON	PLATFORM
Guardian	Nov, 2005	Northrop Grumman	LAIRCM	Airliner
Jet-eye	Nov, 2005	BAE	ATIRCM /TADIRCM	Airliner
CAPS*	2005	United Airlines	Many subsystems	Airliner
Hornet	2004	Northrop Grumman	Tactical high energy laser	Ground based
Matador	Nov, 2005	BAE	IR-lamp based	Airliner
Vigilant Eagle	Jun, 2005	Raytheon, USA	High-power microwave	Ground based
MUSIC	2003	EL-Op Israel	Multi-spectrum laser jammer	Airliner
Flight Guard	Jul, 2005	Elta, IAI, Israel	Flares based	Airliner

* NOTE: CAPS sub-systems are WIPPS (widebody integrated platform protection system), AVISYS L-3 Communications Integrated systems (aircraft integration), ATK (AN/AAR-47(V)2 missile warning system), Thales airborne systems (MWS-20 TA missile warning system), Symetrics Industries (AN/ALE-47 countermeasures dispenser) and Alloy Surfaces (special material decoys)

4.11 IRSS and IRCM System Analysis and Evaluation Software

Extensive efforts have been made at various levels to develop more efficient IRSS and IRCM systems. The parameters of IRSS/IRCM systems are often classified. It is difficult to get detailed specifications and design information from open sources and the published articles available, through open sources, only give guidelines and an idea about the latest technologies. A few examples available in the literature are Naval Threat and Countermeasures Simulation (NTCS) [VAI94],[VAI00] and [DAV02], tactical helicopter IRSS [SUL97], turbojet engine IRSS [DIX05] and IR camouflage [GIL01]. Also, the Advanced System Group, USA has developed a generic model for IRCM system evaluation [FOR01].

4.11.1 DSTL Fly-in 2000 Model

DSTL (UK) started working on IRCM effectiveness against imaging IR seeker anti-air missiles in 1986. In 1990 the fly-in model was developed. In 1997, a Windows-NT and C++ based model was generated and then Fly-in 2000 was created. It simulates the

engagement of an aircraft, equipped with IRCM, by a missile with an imaging IR seeker. It contains the background, aircraft, clouds, sun, countermeasures, atmosphere, scene generation, sensor, image processing and the missile dynamics. The background was generated using an IR camera on a trial aircraft. Aircraft models were created using commercially available wire-frame models of military aircraft. The temperature and emissivity information was added on each facet. The spatial frequency was based on the detector pitch and photon flux. Target tracking algorithms, Automatic Target Acquisition and Guidance System (ATAGS) and Advance Anti-air Acquisition Algorithm (PentA) were used. ATAGS uses edge and feature extraction whereas PentA uses a neural network state-of-the-art algorithm potentially found in modern seekers. The image processing module operates on grey levels. Target tracking data is used to steer the missile. The missile motion is controlled by the missile aerodynamic. The Flyin-2000 improvements over earlier versions includes the capability to model multi-colour arrays, the atmospheric attenuation model is upgraded from LOWTRAN to MODTRAN, the plume is represented in a better way and the system is made more user friendly so that a non-expert user can operate it [COX04].

4.11.2 Tactical Engagement Simulation Software

The Tactical Engagement Simulation Software (TESS) has been developed by Tactical Technologies Inc. Ontario, Canada (TTI) for analysis of passive infrared guided SAM and AAM systems. It includes a missile warning system, DIRCM and conventional and propelled flares. The missile seeker has several flare detection techniques such as two-color band signal processing, rapid changes in signature intensity and line-of-sight rate change dynamics [TES07]. To counter an IRCM, an appropriate IRCCM feature, out of five available techniques, can be incorporated in tracker. These are rate-hold, angle-hold, rate-bias, angle-bias or un-biased. It also has a ground based launcher to simulate MANPAD operation [TES07].

4.11.3 Chemring Countermeasures CounterSim

CounterSim is an aircraft decoy assessment model (ADAM) developed and maintained by Chemring Countermeasures, High Post, UK [WAL06]. It simulates engagements between IR homing missile and various airborne platforms. It can simulate scenarios with or without countermeasures deployed. The model can be used

for improving chances of platform survivability by examining decoy deployment tactics to enhance its effectiveness. The optimization of payload and dispensation sequences can be done by running simulations. CounterSim has been further developed to allow the modelling of any environment, land, sea or air, and has the ability to model RF seekers and countermeasures as well as IR.

4.12 Summary

Like every system, heat seeking missiles have limitations. The sensitivity of the sensor, atmospheric attenuation, background clutter (hot terrain and bright lit clouds), FOV limits, solid angle limits, seeker tracking rate limits are features which could be explored in to defeat these missiles. Predominantly, two generations of IR homing missiles are currently in operation. First generation missiles can often be defeated by standard flares, however, second generation missiles are more difficult to defeat. The conventional flares available today are simple to make and easy to operate. Unlike active IRCMs, flares do not need sensors for tracking the threat and can be dispensed pre-emptively in a hostile area or on cue from a MAWS. The new flare materials are effective against later generation missiles but their performance in a reactive mode may be limited against the earlier generation missiles. To cover the entire range of missile threats, flares must consist of a cocktail of flare materials [TAY05]. The latest IR decoys are visually covert and safe to operate in populated areas. Low and slow flying platforms, along with commercial airliners, are especially vulnerable on takeoff and landing, where flares are not suitable because they lack the airspace to disperse and also because of the fire hazard posed by traditional flares [ROC06a].

To defeat IR guided missile the directional IRCMs emit directional energy to jam the missile seeker. The laser based DIRCM systems are probably more capable of protecting airborne platforms than the conventional flares and arc-lamp based jammers. For the majority of current IR missile threat types the single-turret laser based countermeasure systems would have good effectiveness against single missiles but still can not fully protect against all possible missile threats [CHO05].

Rapid advancements in IR missile seeker technology has made it necessary to continuously develop new countermeasures to increase the survivability of aircraft in hostile environments. With the proliferation of more advanced IR staring-array seekers the threat to military and civilian aircraft is increasing every day.

4.13 Conclusion

In light of the increasing terrorist SAM threat to civil and military aircraft, we cannot overstate the need of a high-fidelity low-cost PC based IR signature scene modelling and simulation capability which could be used for development, testing and evaluation of Infrared Countermeasure systems. As the missile threat evolves, so will be the development of improved countermeasures and their techniques to protect the aircraft [RIT03]. If laser based directional IRCM systems prove more capable of protecting aircraft, than punching out dozens of flares, this will be the place to be in airborne electronic warfare [ROC02].

Although, the Directional-IRCM, Large-aircraft IRCM, and Close-loop IRCMs are the modern IRCM systems, however, in this work presently only the IR expendable flares have been modelled. An effort has been made to model the conventional MTV and aerodynamic flares. Their temporal and spectral responses, dispensation mechanism and ballistic trajectory are modelled. The details of these are given in Chapter-7. The typical targets for MANPADs threat are the fast-jet aircraft, the slow-moving helicopters and the large aircraft such as the C-130 or Boeing-737 etc. Although in Chapter-7 the 3D models of these aerial targets are altered to suit the IR signature modelling. However, in Chapter-9, the IRCM analysis has only been performed on fast-jet aircraft to demonstrate the IR signature using virtual reality modelling techniques. With minor changes the same algorithm can be used for IRCM analysis of other aerial targets. Although, the target generator can simulate different manoeuvres such as landing, take-off, spiral descent etc, the IRCM analysis are performed in straight-and-level and in-level turn modes only to validate the results of IRCM analysis with that of the CounterSim. Chapter-7 explains the 3D modelling sequences and the IRCM analysis results are discussed in Chapter-9.

5 SIMULATION AND MODELLING

5.1 Introduction

To help understand the tactics and performance of IR sensors and countermeasures against them, the use of modelling and simulation can be an invaluable tool. High-fidelity and time efficient engagement modelling using third and fourth generation missiles or focal planer array seekers using sophisticated counter-countermeasure routines is a challenge and an area where technology investments is needed [TAY05]. In this chapter, the computational power and flexibility of modern personal computer will not only be discussed, but how they will be used to implement an infrared signature model which allows for easy interpretation of the IR physical characteristics in terms of fast computer graphics hardware features. The aim of this chapter is to understand the importance of modelling and simulation and the powerful features of modern graphics hardware.

5.2 Simulation and Modelling

Simulation is the creation of an artificial situation or stimulus that causes an outcome to occur as though a corresponding real situation or stimulus was present [SMI99]. The task of executing simulation can provide an insight understanding of the physical processes that are being modelled. With the rapid advancements in realism and greater fidelity in modelling and simulation technology, simulation has become one of the primary solutions for military training and testing of real weapon systems. Researchers are exploring and developing better solutions for military simulators.

5.2.1 Types of Simulation

Depending upon the application, the simulation could be divided into three main categories.

5.2.1.1 Hardware-in-the-loop Simulation

If an actual system or sensor is part of the simulation process then it is called hardware-in-the-loop (HWIL) simulation. It involves generation of signals in the form they would have at the point where they are injected into the system. It is performed in test chambers with simulated targets and backgrounds and with controlled

environmental conditions. Generally, it is done for the evaluation and testing of some existing system.

5.2.1.2 Human-in-the-loop Simulation

Another type is the human-in-the-loop (HITL) simulation or operator interface simulation. It generates displays and output readings on operator consoles in response to the modelled situation without the generation of actual signals. The operator can interact during the simulation through input devices like a key board, mouse or joy stick etc. It is performed generally for the testing or training of the operators. This type of simulation may be based on an actual sensor or just a mathematical model. The car simulator used by driving schools or the flight simulator for training of pilots are examples of HITL simulations. Clearly, in this type of simulator the operator can crash his simulated aircraft or car without being hurt. Also, to some extent, modern interactive computer games can be put in this category.

5.2.1.3 Computer Simulation

The computer simulation is that in which no actual systems or hardware are involved and all is done on a computer using mathematical models. Generally, it is used for comparison of several sensor designs or to evaluate the expected performance of a proposed design. This could be used for the evaluation of strategies and tactics. The validation of the results of a computer simulation is mainly based on the accuracy of the models used. The accuracy of a model can be validated only by extensive comparison with measured data or with some already validated accurate model.

5.2.2 Uses of Simulation and Modelling

The simulation and modelling of IR systems has grown side-by-side with the growth of both IR technology and computer technology over the past decade or so [SCH95]. The IR simulators help military planners to specify systems accurately and economically. It enables manufacturers to design, develop, and produce systems on time and within budget that may meet performance requirements. It allows end-users to test and verify system performance. The following are a few applications of simulation and modelling.

5.2.2.1 Simulation as a Replacement of Live Tests

The military IR systems in use and those under development are going to be more complex and expensive. Therefore, their costs and the cost of performing live tests is also likely to increase. Modelling and simulation presents an attractive alternative to the costly fire/fix/fire approach of live field trials. It can reduce costs and save time in the development cycle of any IR system. Additionally, models may help resolve issues which cannot be adequately investigated by live field testing. Limitations such as range constraints, safety concerns, inability to test in all intended environments and inability to accurately replicate the threat could be overcome by simulation and modelling. Also the availability of spy satellites, surveillance ships and other means of intelligence have made simulation a suitable alternative to avoid the leaking of sensitive test parameter data into enemy hands.

5.2.2.2 Simulation for Training

Simulation for training exposes operators to situations that allow them to improve their skills. Simulation can allow the realistic evaluation of the performance of operators, equipment and techniques under circumstances that do not yet exist. Simulation can also allow the realistic training of individuals under conditions that, in real life, might kill them.

5.2.2.3 Simulation for Test and Evaluation

Simulations for test and evaluation make sure that the equipment is fit for the purpose of doing the job for which it was designed. It is used for system performance prediction, pre-flight trajectory prediction or post-flight analysis. For system performance prediction a wide variety of scenes and times of engagement must be used. The pre-flight predictions are performed in a well known area and the variations used are based upon the area, day and time of the test. An envelope of expected conditions for the flight is compiled and the expected trajectory is estimated. For post flight analysis the exact conditions are recorded and the best match is made with some reference data.

5.2.3 Application of Modelling and Simulation in Military Systems

In today's high technology environment, virtual reality is used in all walks of life. The vast application of virtual reality in video games, walking through models and

animated movies has made the pace of advancement much faster [SIM00]. Defence industry is becoming increasingly dependent on the development of state-of-the-art modelling and simulation tools. It is a potential means of cutting the cost of live trials and enables the testing of extreme scenarios which are otherwise difficult or even impossible to produce in the real world. Extensive use of modelling and simulation has been seen in battle field simulations, war game exercises, flight simulators and the test and evaluation phase of missile development. Various examples of modelling and simulation in military applications are available [KIS99] and [LIM99]. The Ship IR/Naval Threat and Countermeasures Simulator (SHIPIR/NTCS) was developed by W.R. Davis Engineering Ltd. for the Canadian department of national defence. Later it was adapted by the US Naval Research Laboratory and also considered as the NATO-standard ship signature model [VAI96] and [VAI99a]. Similarly, IR-Scene Projector (IRSP) of the US Army Redstone Technical Test Centre [MAN02], Tactical Guidance Research and Evaluation System (TiGRES) of NASA for Air-to-Air missile simulation [KAP94] and Modelling Simulation Animation and Real-Time control (MoSART) of Arizona State University, USA [LIM99] are a few examples of IR modelling and simulation.

5.2.4 Low cost PC Based Systems

The advancements in the computational capabilities of Personal Computers (PCs) has been so rapid that a job which a few years ago, was difficult for the expensive high-end proprietary workstations to perform, can now be done easily by a low cost PC [BEC02]. The military simulation community has taken advantage of low cost PC technology and has developed close to reality simulators for ground vehicles and combat training systems. Such examples are given in the references [SIM00], [WRI01] and [GON03]. Similarly, low cost PC based IR scene generators have been developed by various agencies. Examples are given in references [SHE98], [LIM99a], [LI99], [CUR01] and [CHR03].

5.2.5 Military Simulators Developed around COTS Software

Many military simulator developers have taken advantage of this trend by using commercial modelling applications to provide an integrated infrared/electro-optical three dimensional modelling environment. The following are a few examples of such systems [source : internet]:

- (a) Real-time IR/EO Scene Simulator (RISS) of Amherst Systems Inc., Northrop Grumman, New York, USA provides a set of integrated tools for development, test and evaluation of IR/EO sensor systems.
- (b) Tactical Engagement Simulation Suit (TESS) developed by Tactical Technologies Inc. Ontario, Canada is an IR guided weapon system engagement simulator for passive infrared surface-to-air and air-to-air missiles.
- (c) Nytric Ltd. Ontario, Canada, Missile System Simulator.
- (d) MIRAGE Dynamic IR Scene Simulator of Santa Barbara Infrared Inc. (SBIR), CA, USA.
- (e) IR Target Generator (IRTG) and Target IR Simulator (TIRS) of CI Institute CA, USA.
- (f) IR Scene Projector (IRSP) of Dynetics Alabama, USA.
- (g) Aerial Target IR Simulator and Naval Target and Countermeasures Simulator (NTCS) developed by W.R. Davis Engineering Ltd. Ottawa, Ontario, Canada.
- (h) Vega Prime IR Scene developed by MultiGen-Paradigm, CA, USA.
- (i) IR Scene Generator of Raytheon Missile Systems USA [AMM99].
- (j) Multi-Service Electro-optics Signature Code (MuSES) and PRISM of ThermoAnalytics, Inc., MI, USA.
- (k) Paint-the-Night (PTN) IR Scene Simulator developed by Night Vision Electronic Sensors Directorate (NVESD) CECOM.
- (l) Cameo-Sim broad scene simulator developed under DSTL (UK) MoD.
- (m) GCI ToolkitTM is a physics-based multi-spectral scene simulator developed by Photon Research Associates, Inc., NM, USA.
- (n) Sensor Vision is terrain visualization tool for visible through to IR bands developed by MultiGen-Paradigm CA, USA.
- (o) SIMTERM is a PC based computer simulator of thermal imagers developed by Inframet Inc., USA.
- (p) CounterSim is simulation software developed by Chemring Countermeasures, High Post, UK for study and evaluation of expendable countermeasure.

5.2.6 Commercial Modelling Tools

Commercial tools are now available for building virtual three-dimensional worlds for use in flight simulators, computer games, or web pages. Driven by this large commercial market, these tools have become enormously sophisticated yet relatively easy to use. These tools are available with various add-in features and costs in thousands of dollars. The following are a few examples of such tools collected from internet sites:

- (a) Terra Vista of TERREX, Terrain Experts Inc. AZ, USA.
- (b) World Perfect, a terrain and content generation system and Virtual Reality Scene Generator (VRSG) both developed by MetaVR Inc. Massachusetts, USA.
- (c) VegaTM for real-time simulation, Cloud ScapeTM, Creator Pro, Site Builder 3-D and Creator Terrain Studio (CTS) are commercial modelling tools of MultiGen-Paradigm, CA, USA.

5.3 Computer Graphics Hardware

Graphics hardware is far faster, smaller, cheaper and more capable than twenty years ago and we do not need to be a genius to predict that it will continue on that path in the future [ENG00]. The hardware acceleration is the performance of the rendering steps by the hardware outside the central processing unit (CPU) and without the help of the software. In general, any thing that can be done with hardware can also be done with software and vice versa. With improvements in hardware graphics more and more rendering steps are shifted from software based CPU rendering to fully graphical processing units (GPU) based hardware acceleration. Earlier only shading and texturing were hardware accelerated. Presently, a graphics card has full hardware transformation and lighting support.

5.3.1 Applications of Hardware Graphics

The only home application of high end graphics cards is the gaming environment. Computer games are the only consumer application that actually takes advantage of the graphics card capabilities. However, the latest generation Microsoft Windows Vista[®] offers a hardware accelerated user interface that will require a 3D graphics card. Also, professional applications like computer aided design (CAD), video

editing, image synthesis, visual simulations, image processing, virtual reality, scientific visualization and flight or car simulation also require fast 3D graphic cards.

5.3.2 Advantages of Hardware Graphics

In 1965, the co-founder of Intel[®] Corporation, Gordon E. Moore, roughly stated that the density of transistors in a microchip doubles every 18 months. In recent years, the graphics hardware performance has increased more rapidly than that of CPUs. This is mainly due to the vast entertainment and 3D gaming market which is the biggest user of the advance graphics [SIM00]. The intense competition between various vendors, the cost of 3D graphics cards have been kept relatively low and the pace of innovation has been high. Hardware graphics or GPU has many advantages over CPU or software based graphics [PUR02].

- (a) High speed imaging compared to a conventional CPU.
- (b) More advanced or rapid development of GPU technology than CPUs.
- (c) As CPUs are designed for high performance on sequential operation, it is becoming difficult to use additional transistors to improve performance. Whereas, GPUs can use additional transistors much more effectively.
- (d) GPU optimized for high parallelism of vertex and fragment.
- (e) GPUs are readily available and easily up gradable.
- (f) Compatible with multiple operating systems and hardware structures.
- (g) Improved performance by dynamic simulation on GPU.
- (h) Reduce computational load on CPU.
- (i) GPU can run entire ray-tracing, thus rendering process accelerated.
- (j) Hardware computer graphics goal is to provide maximum performance at the lowest cost.
- (k) Eliminates the GPU-CPU communication bottleneck.

5.3.3 Computer Graphics Card

The graphics card is also called video card, display adapter, graphics adapter or 3D accelerator. Early age graphics cards were mere interfaces to draw the image on the screen and all other jobs were done by the CPU. With the advancements in hardware technologies, more of the 3D graphics pipeline load is shifted from the CPU to the

graphics card, thus leaving the CPU free to do other important jobs. This is mainly due to the improvements in technology and the drop in prices [MUR03]. The early graphics cards were monochrome and could display text of specific resolution and point size. Then resolution and refresh rates improved gradually. The colour pallets were increased and then 3D rendering followed. Graphic cards are improving almost exponentially, to the point that high-end consumer gaming PCs are often faster than graphic workstations purchased less than six months ago for two to four times the price. In fact games are the driving force behind the development of real-time 3D graphics hardware [SIM00]. The major components of a computer graphics card are: Graphical processing Unit (GPU), video random access memory (VRAM) and video basic input/output system (video BIOS). Fig illustrates the functional block level diagram of the graphics card.

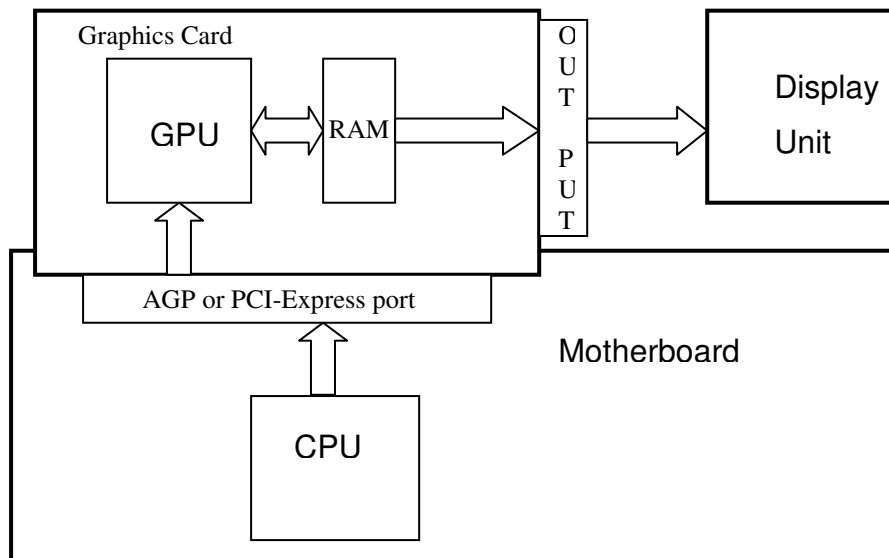


Figure 5-1: Functional block diagram of graphics card

5.3.3.1 Graphical Processing Unit

The graphical processing unit (GPU) is an independent microprocessor installed on a graphics card. The GPU is the heart of the graphics card. The main attributes of the GPU are the core clock rate and the number of pipelines. Depending upon the rendering pipeline, the GPU may contain different functional units such as: vertex shader unit, pixel shader unit, texture mapping unit and or raster operator unit etc. The GPU is very efficient at manipulating and displaying graphics. Current GPUs are faster than CPU at graphics. A modern GPU is a highly specialized self contained computational unit, acting basically as a computer with in the computer.

5.3.3.2 Video RAM

The GPU has its own independent memory installed on the graphics card called Video RAM (VRAM). It is independent of the RAM of the motherboard. The VRAM works hand in hand with the GPU to help in bandwidth-intensive applications such as 3D games. The typical VRAM sizes are 128, 256 and 512 MB.

5.3.3.3 Video BIOS

The video basic input/output system (Video BIOS) interfaces the GPU to the motherboard and the display system. The GPU is connected to the CPU through the accelerated graphics port (AGP) or the PCI-Express interface (peripheral component interconnected express). The output images are exported to video display unit (monitor). The typical output ports are the D-sub type VGA, composite video, component video, digital video interface (DVI), or s-video etc. For analogue displays the random access memory digital-to-analogue converter (RAMDAC) is used which converts the digital signals into analogue signals. However, due to the growing availability of digital computer displays, the RAMDAC is slowly disappearing from the graphics card.

5.3.4 Integrated Graphics Processor

The “integrated graphics” processor allows a computer to perform video graphics functions without a separate graphics card. It is a build-in graphics processor on the motherboard. The overall cost of the integrated solution is much less than the discrete graphic card solutions and also has lower power consumptions. Thus are commonly used in laptop computers or some low- and mid-range desktops. Intel[®] “*Extreme Graphics II*”, Intel graphics media accelerator (GMA) series such as GMA-900 and GMA-X3500 are few examples of the integrated graphics solutions [INT07]. The integrated graphics processor shares the computer main memory with CPU on same bus, which imposes a performance penalty. They usually have inferior 3D performance compared with dedicated graphics cards. Although, they are suitable for most applications, but they are not usually a good choice for the gaming enthusiast or professional applications [INT07].

5.3.5 Graphics Hardware Manufacturers

Major chip producers are ATI Technologies[®] and Nvidia[®] Corporation. Nvidia[®] is a chipmaker only, focusing its attention solely on designing and producing graphics processors while leaving the production and sale of retail cards to its board partners. ATI[®] on the other hand, makes their own cards and is quite active in the retail market as well. Nowadays, a PC-based graphic card has outperformed the thousand-pound “high-end” graphics workstations of several years ago. Few examples of the graphics cards from Nvidia[®] are the GeForce3 Ti 500GPU, GeForce4 Ti 4600GPU, GeForceFX series, GeForce6 series and now the latest GeForce7 series. ATI[®] Radeon[®] X1950 is the latest ATI product and can sample more textures per pass than the GeForce[™] latest card. Other than these, the Parhelia and P-series of Matrox[®] and Wildcat of 3DLabs[®] are famous in the market place [SCO01]. GeForce3 (Nvidia) and Radeon 8500 (ATI) replace fixed-function vertex and fragment (including texture) stages with programmable stages. Minor chipset producers are S3 Graphics (Chrome Series) XGI Tech Inc (Volari) and Tech Support (Rapton). The market leader in graphics solutions are the Intel[®], ATI[®] and Nvidia[®]. The VIA tech, SiS, Matrox Graphics, XSI and 3Dlabs also have their products in market.

5.3.5.1 Nvidia[®] GeForce[™]

GeForce[™] is the Nvidia[®] GPU series for the main stream desktop PC user. It is the most feature-rich cost effective and highly integrated GPU. The first GeForce[™] was GeForce 256 and was launched in August 1999. It was designed and marketed for the gaming community of personal computer users. The latest in the GeForce series is the GeForce[®] 7950 GX2 launched in June, 2006. It is 48 pixel pipeline PCI Express[®] chip and also has SLI[™] (Scalable link Interface) support for linking two video cards together to produce a better output. Nvidia nForce[®] is the chipset for AMD Athlon[®] and Duron[®] microprocessors and Nvidia Quadro[®] Plex is a professional workstation class GPU used for computer aided design (CAD) and digital content creator (DCC) applications. Nvidia Gelato[®] is rendering software designed to create stunning images for applications in film and broadcast.

5.3.6 AGP and PCI Express

This started with the industry standard architecture (ISA) bus, then in the early 90’s the era of the peripheral computer interconnection (PCI) came with 132 MB/sec

bandwidth. In the mid 90's the accelerated graphics port (AGP) was developed specifically for graphic cards. It was 32 bits which offered a bandwidth of 533 MB/sec in its initial version of AGP 2X and subsequently the AGP 4X and finally AGP 8X was the latest version with a bandwidth of 2.133 GB/sec. Recently PCI-Express, formally known as 3rd Generation Input Output (3GIO), has been developed by Intel[®] Corporation. PCI-Express is a 32-bits local bus with bandwidth of 2.5 GB/sec. It is a two way serial connection. Where 3D performance is concerned, PCI-Express offers at best minimal advantages over AGP. PCI uses a parallel connection and shared bus protocol. AGP uses serial connection and point-to-point protocol. PCI-Express also uses a serial connection and point-to-point protocol. It is general purpose and has dual-channels. PCI express is two time faster than AGP 8X.

5.3.7 Nvidia[®] SLI Technology

In 2004, scalable link interface (SLI) technology was introduced by Nvidia. SLI technology is a revolutionary approach to scalability and increased performance. SLI can deliver as much as two times the performance of a single GPU. It combines two graphics cards in a single system and doubles the graphics performance [NVI06]. Nvidia SLI can output in both digital and analogue formats for the highest image quality. It needs a PCI Express motherboard and Nvidia based PCI Express graphics cards, joined by the Nvidia SLI connector. It takes advantage of the increased bandwidth of the PCI Express to automatically accelerate applications through a combination of intelligent hardware and software solutions.

5.4 Graphics APIs

The application programming interface (API) is either the set of instructions written to interface two programmes and make the job of the programmer bit easier, or it is a software interface to the graphics hardware. The two main standard 3D APIs for real-time graphics programming are Direct3D[®] from Microsoft[®] and OpenGL[®] (a standard originally based on SGI's GL API) [MUR03].

5.4.1 OpenGL[®]

In 1992, OpenGL[®] was introduced by Silicon Graphics Incorporated (SGI). It became industry's most widely used and supported 3D and 2D graphics API. With more than sixty hardware developer licences, it is considered the mother of all APIs and is a

premier environment for developing portable interactive 2D and 3D graphics applications. OpenGL[®] is supported on all the major computer platforms including; AIX[®], HP-UX[®], IRIX[®], Linux[®], Mac[®], OS X[®], Microsoft[®] Windows[®] 2000, Windows[®] XP and Solaris[™]. The top manufacturers of real-time 3D graphics cards; 3DLabs, ATI and NVIDIA have released products supporting the OpenGL 2.0 specifications and OpenGL Shading Language. OpenGL 2.0 is the latest core revision of the OpenGL graphics software. Its specifications were finalized in September 2004 by the ARB (architecture review board), however, it was introduced in 2003. OpenGL 2.0 API represents a revolution in graphics by providing high-level access to the programmable features of modern GPUs. It can create photo-realistic real-time 3D graphics. OpenGL 2.0 is a direct compiled model, which means that a given graphics hardware/driver combination will take its OpenGL source code and compile it directly into machine code that runs on the graphics hardware. OpenGL is backward compatible and is fully universally licensed throughout the graphic hardware developers' community. OpenGL is constantly evolving state-of-the-art functionality to efficiently support a wide array of applications from consumer games to professional design applications. OpenGL provides high-level access to the programmable features of modern graphics processors. It creates photo-realistic, real-time 3D graphics.

5.4.2 Architecture Review Board

The OpenGL architecture review board (ARB) is an industrial consortium that governs the specifications of OpenGL[®]. It was formed in 1992. The nine promoting members of the board are; 3DLabs, Apple, ATI, Dell Inc., IBM Corporation, Inter Corporation, Nvidia Corporation, Sun Microsystems Inc., and SGI.

5.4.3 Difference between Direct3D and OpenGL

Direct3D[®] and OpenGL[®] are both graphical API packages used extensively in many graphical systems. The Direct3D[®] is a proprietary standard API and includes a software renderer and a hardware abstraction layer for accelerated rendering. It is designed by the Microsoft[®] Corporation for hardware 3D acceleration on their Windows[®] platforms and X-Box[®] family of video game consoles. Every time more hardware features are added, a new version of Direct3D is released. The latest version is DirectX 9.0c. On the other hand, OpenGL[®] is an open standard API available on

Windows[®], Unix[®], Apple Macintosh[®] and other platforms. It is independent of the platform.

5.5 Realism

Realism is required for simulation, entertainment, advertising, research, education and command and control applications. Ideally, the simulation would require interaction between all of the photons and atoms in a scene, to correctly and accurately represent real life phenomenon. However, it is not currently possible to perform this level of simulation [FER01]. Therefore, to approximate these phenomena a variety of tricks or special effects are used and with the advancements in computer graphics technologies, the demand for realism is also increasing. Ideally, a system must produce an image as accurately as possible (photo-realistic) and also as quickly as possible (at least 25 images/sec for movie-realistic) but accomplishing both of these goals at the same time is a big challenge. The aim of any realistic imaging simulation is to produce images that capture the appearance of real objects and scenes. Generating visually realistic images are an art form and not a science because physical accuracy is not necessary to produce visually realistic images. The following are the different types of realism.

5.5.1 Physical Realism

In physical realism, the image has to be an accurate point-by-point representation of the spectral radiance values in a scene [FER01]. Physics based rendering algorithms can create an accurate simulation of light travelling from the objects to the viewer. It can be of great use in engineering and design applications. However, for human consumption physically accurate rendering is usually an excess as it is beyond the human visual processing limits. Also, it is extremely computationally expensive and it is difficult to display the results as its dynamic range usually exceeds the capabilities of the existing display devices [FER01].

5.5.2 Photo Realism

Photo realism means generating an image that is indistinguishable from a photograph of a scene. The aim is to produce an image that appears the same as the photograph, even if the physical energy coming off the image is different from the actual scene. Although, photo-realistic rendering algorithms can be faster than physically realistic algorithms, it is still computationally expensive [FER01].

5.5.3 Functional Realism

To overcome the issues of physical realism and photo realism, an approach is needed to produce images which can allow an operator, for example, to do the required task as efficiently as they would have done in the real world [FER01]. Functional realism uses wide range of rendering styles depending upon its need. One example is the rendering techniques used in flight simulators. In this application images are not physically accurate nor are they photorealistic but they are functionally realistic because they provide the user with much of the same visual information they would get if they were flying a real plane [FER01].

5.6 Computer Graphics Rendering

Computer graphics is the art of creating realistic images on the computer and rendering is the last step in the 3D computer graphics pipeline. It gives the final appearance to the models and animation. Rendering is the process of converting three-dimensional geometric descriptions of graphical objects into two-dimensional images. Rendering could be photorealistic or non-photorealistic. The photorealistic rendering is based on photo-realism and the real world. Whereas, the non-photorealistic rendering is usually based on artistic paintings or drawings.

5.6.1 Rendering Pipeline Stages

Every rendering method has its own steps. However, the following are the stages which are usually common in all rendering pipelines:

- (a) **Object Models Generation.** All objects 3D models are generated in local space and then transformed in to the world space with respect to other objects present in the world space.
- (b) **Viewing Specifications.** Depending upon the viewer angle or eye space, the 3D scene is projected onto a 2D plane.
- (c) **Lighting Conditions.** Calculating shading information based on the position of lights in the environment and the surface properties.
- (d) **Hidden Surface Removal.** The polygons or parts of the polygon not visible in viewing or eye space are clipped. Also parts of objects that are too close or too far away are also removed or clipped.

- (e) **Fragment Rasterization.** The next step is converting scene into 2D raster image (pixels or dots) for out put on a video display.
- (f) **Texturing and Colouring.** Texturing is the association of one or more images to a polygon and then colours are assigned to the visible surfaces.
- (g) **Anti-aliasing.** Anti-aliasing reduces undesirable visual artefacts due to insufficient sampling of textures or shades and motion blur.
- (h) **Animation.** Time varying changes if motion is desired.

5.6.2 Types of Rendering

Many rendering algorithms have been researched and system used for rendering may employ a number of different techniques to obtain a final image. The rendering engines are either real-time or non-real time engines. Scan-line rendering, ray casting, radiosity and ray tracing are the main techniques.

5.6.2.1 Scan-line Rendering

A scan-line rendering engine draws an imaginary line from the viewer's eye through a single pixel on the screen and into the imaginary 3D scene to determine what elements would be visible. It scans one by one all pixels in the view window and colours them accordingly.

5.6.2.2 Ray Casting

Ray casting is primarily used for real-time simulations. It cast a ray from the object to the point of view and the angle of incidence of the light rays from the source(s) of light to the view point. Based on the intensities the value of each pixel in the scene is calculated.

5.6.2.3 Ray Tracing

Ray tracing is an extension of the same technique developed in scan-line rendering and ray casting. In ray tracing the samples are imaginary rays traced backward from each pixel on the monitor into the three dimensional model, thus considering only the light that enters the eye. In ray tracing the angles of reflection and refraction are calculated every time light hits any object. It is primarily beneficial when complex and accurate rendering of shadows, refraction or reflection are issues.

5.6.2.3.1 Advantages and Disadvantages of Ray Tracing

Ray tracing is a very versatile technique. It can cover characteristics of direct illumination, shadows, specular reflections and refractions through transparent objects accurately. The ray tracing technique is computationally expensive and slow even for scenes with only moderate complexity. Ray tracing does not cover diffuse inter-reflections (diffraction and scattering), therefore, only the objects that are illuminated directly are rendered accurately and areas or objects not directly illuminated are pitch dark, which is clearly not the same as in the real world. Ray tracing cannot reproduce secondary illumination effects from diffuse surfaces and tends to simulate light reflecting only once off each diffuse surface. The ray tracing scene must be lit by some light source for it to be visible. As it does not cover secondary illumination, the phenomenon of IR radiation can not be shown with the help of the ray tracing.

5.6.2.4 Radiosity

Radiosity in computer graphics was first introduced in 1984; however, in the 60's methods for simulating the radiation heat transfer was developed by thermal engineers. They modelled the emission and reflection of radiation and produce more accurate inter object reflections. This produced a model for conservation of thermal energy in a closed environment. Radiosity is the rate at which energy leaves a surface. It is the sum of the rates at which the energy reflects or transmits from that surface or other surfaces. All energy emitted or reflected by every surface is accounted for by its reflection from or absorption by other surfaces. Unlike ray tracing which is a direct illumination algorithm, radiosity is a global illumination algorithm. In radiosity any light that hits a surface is reflected back into the same medium. This means any light source as well as other objects acting as secondary illumination sources. Radiosity is closer to nature and represent a scene more realistically as compared to ray tracing; however, it deals with only diffuse or dull surfaces.

5.6.2.4.1 Advantages and Disadvantages of Radiosity

Radiosity is very realistic for diffuse surfaces. It is simple and easy to implement but cannot handle point sources or specular reflections from shiny surfaces. It is computationally expensive and slow. Radiosity operates on finite areas called patches.

5.6.3 Illumination Techniques

The physical material properties of the surface and the light conditions will determine the colour or appearance of any specific pixel in any image. The local or global illuminations are used to determine how a surface reflects and transmits light.

5.6.3.1 Local or Direct Illumination

Local illumination is that in which only the light coming directly from the light source themselves is considered in the shading. It predicts the intensity, spectral characteristics, colour and distribution of light.

5.6.3.2 Global Illumination

Global illumination not only considers the light directly coming from the source but also reflections and refractions from other surfaces and objects present in the scene. When light hits a surface, depending upon the material of the surface, part of it is absorbed in the material and the rest is scattered out into the same environment. A rough surface tends to reflect light back in all directions, called diffused reflection. On the other hand a very smooth surface (like a mirror) reflects light in one direction and this is called specular reflection.

5.6.3.3 Direct vs. Global Illumination

The direct illumination is that which consider the light falling on a surface only due to the light that has taken a path directly from a light source. Whereas, global illumination consider both direct as well as indirect illumination due to the reflections of the light from other objects. Direct illumination can render both mathematically derived objects and polygons. It can be modified to render soft shadows but it is very tricky. The ray tracing is slow. Direct illumination is suitable for cases with point light sources and perfectly shining objects. However, in the real world it is difficult to have all things shining. On the other hand, global illumination techniques simulate multiple reflections of light around a scene. In global illumination a scene may be lit simply by its surroundings even without a light source present in the scene.

5.7 Virtual Reality Modelling Language

Virtual reality modelling language (VRML) is an open and flexible platform for creating interactive three-dimensional (3D) scenes or virtual worlds. VRML is easy to

use as it is a text based object-oriented programming language written in World Wide Web (WWW) oriented format. It uses file extensions such as “*wrl*”, “*wrz*” and “*wrl.gz*” etc. In 1994, during a European web conference, Tim Berners Lee used the term “virtual reality makeup language” when he emphasised the need for a 3D World Wide Web standard. In the same year, a group of artists and engineers produced the VRML-1 specifications which were based on a subset of the Open Inventor™ file format of Silicon Graphics Institute (SGI®). They also changed the name to virtual reality modelling language (VRML). This first version of VRML could only create static worlds. It was replaced with VRML-2 with animation features added. In 1997, VRML-2 was adopted by the International Standard Organization (ISO) and was referred as VRML97. Although, X3d is the successor of VRML97, (with added features of humanoid animation, non-uniform rational B-splines (NURBS) and geographical reference VRML etc.) still VRML97 is the current and functionally complete version of VRML that is still popular with education and research oriented applications.

VRML can specify objects and backgrounds with vertexes and edges of polygons with surface colour, texture, shininess, transparency and many more physical properties applied on it.

5.7.1 Military Vehicles 3D Virtual Reality Models

Due to the vast 3D modelling community, there are several sites available on the internet which offer free downloads of 3D models of military vehicles in VRML format. Even if the models are available in some other modelling formats, they can easily be translated into VRML format using translation software. Table 5-1 shows a list of a few such sites which provide 3D virtual models of military vehicles and other objects required to develop a scene.

Table 5-1 : Virtual Reality Models available on the internet

Organization	WWW Address
OCR Incorporated	http://www.ocnus.com/models/Military/
3D World Club	http://www.3dworldclub.com/browse.aspx
3D Caffe™	http://www.3dcafe.com/index.php
Amazing 3D Graphics	http://www.amazing3d.com/services/aircraft1.html
CSC Modelling and Simulation Centre of Excellence	http://www.cscmodeling.com/homepage.htm
Yaap Hanger VRML Models	http://www.topedge.com/panels/aircraft/hangar/yaaphavr.html
Global Security.org	http://www.globalsecurity.org/military/systems/aircraft/index.html
Federation of American Scientists	http://www.fas.org/man/dod-101/sys/ac/index.html
Free models index	http://www.amazing3d.com/modfree.shtml

5.7.2 Open Inventor™ vs VRML

Open Inventor™ is an object oriented 3D graphical library written in C++ programming language. It is built on top of OpenGL® and provides a high-level interface to OpenGL®. Open Inventor™ is developed and maintained by Silicon Graphics Institute (SGI®). Open Inventor™ and VRML are quite similar. Open Inventor™ has node classes that exactly match the node definition in the VRML specifications. The VRML specifications were written on the bases of Open Inventor™. Many new features were added in VRML which were not available in Open Inventor™. Later on, these additional features developed in VRML were also available in Open Inventor™ latest version 6.0. Open Inventor™ includes a rich set of objects such as cubes, polygons, texts, materials, camera and lights etc. It has a built in viewer and editor for editing virtual worlds [JAN03].

5.8 Virtual Reality Toolbox

Virtual reality (VR) toolbox is a software package developed by “The MathWorks Institute”, for use with MATLAB® and Simulink® [VIR04]. It provides a solution for interacting with virtual reality models of dynamic systems in engineering applications. VR-toolbox enables the programmers to create virtual worlds or 3D scenes and animate them in the Simulink® environment. Using VR-toolbox, a developer can interact with the virtual world and change the position and other properties of objects while running the simulation. To enable programmers to model

or develop virtual worlds and to view their results, the VR-toolbox contains a VRML editor or builder and VRML viewer.

5.8.1 V-Realm™ Builder/Editor

The V-Realm™ is a virtual reality builder/editor programme developed by Ligos Corporation, USA. It is part of the VR-toolbox of The MathWorks Institute [VIR04]. The V-Realm™ is used to create complex shapes and landscapes for virtual worlds. It helps in applying material properties, texture-mapping and animations on the virtual worlds. In V-realm™ builder the user can create and edit the VR worlds in VRML97 code. It is a much faster way of editing and takes away the time consuming hand coding process. It is graphical user interface (GUI) based editor in which the user can quickly alter existing nodes and fields or add more nodes while viewing the results instantaneously. It has a cut-copy-paste edit facility which makes the job of editing very easy and fast. V-realm builder contains objects, textures, transforms and material libraries which can easily be called at any time. It can import Open Inventor, VRML-1.0, 3D studio, SGI wave-front and true space files.

5.8.2 Virtual Reality Viewer

VR-toolbox contains a virtual reality viewer (VR-viewer) that enables the developers to visualize the virtual worlds. Alternatively, on a PC platform, the results of a virtual world can be viewed on VRML enabled internet browsers using TCP/IP protocol [VIR04]. The VR-viewer provided with VR-toolbox is a Windows based viewer with a menu bar and toolbar and navigation panel for moving and rotating the objects. It also has a feature for capturing the static virtual scenes and recording the animations.

5.8.3 MATLAB VRML Interface

The VR toolbox provides an interface between MATLAB and virtual reality. To interact with the virtual world from MATLAB, it associates all transform and rotation and material properties with MATLAB source code. In VRML the world coordinates systems are used. It is a right hand Cartesian coordinates system with positive Y-axis pointing up and positive Z-axis coming out of the screen towards the viewer. It differs from MATLAB coordinates which takes positive Z-axis as upward and negative Y-axis out of the screen. Figure 5-2 explains both VRML and MATLAB coordinate systems. To translate VRML coordinates to MATLAB, it has to be rotated 90°

clockwise on the X-axis [NIE00]. The units used in VRML and MATLAB are meters for the dimensions and radians for the angles. To interact with nodes and fields of the virtual world from the MATLAB environment, it is necessary to give unique names to all nodes in the virtual world.

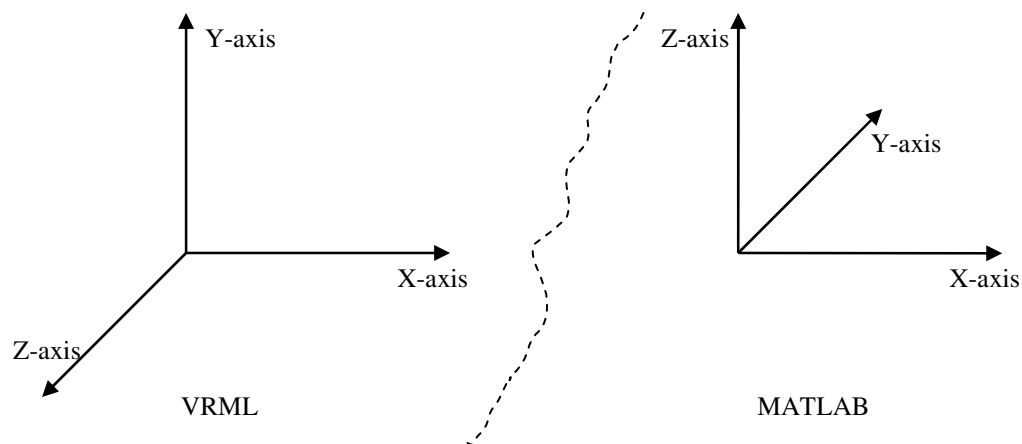


Figure 5-2 : MATLAB VRML Coordinates System

5.9 MATLAB[®] Aerospace Blockset

Aerospace Blockset is a Simulink[®] block set of MATLAB[®] which comprises of aerospace system design, integration and aircraft simulations. It consists of a variety of core components to assemble a broad aerospace system. Its library contains the environmental models, 6-DOF motion equation models, 3-DOF motion equations model, aerodynamic model, flight trajectories, propulsion and actuator models. It also has utilities such as Direction Cosine matrix, Euler angles, quaternion and also the unit conversion functions. The Aerospace Blockset can be used with Real-Time Workshop[®] to generate code for the real-time execution of programmes for prototyping and hardware-in-the-loop (HWIL) applications.

5.10 Microsoft Flight Simulator

Microsoft Flight Simulator[®] is a video game developed by Microsoft[®] Corporation for their Windows[®] platform. It is one of the best known and most comprehensive flight simulators in the video game category. It started in 1982 as a simple small aircraft simulator and now it uses 3D graphics and graphics hardware acceleration to present state-of-the-art results. The latest version is Flight Simulator-X, released in late 2006.

It can simulate the flights over any area and environment around whole world in all weather conditions. It includes over 20,000 airports and has a vast library of airplanes from Wright Brothers 1903 Flyer to latest Boeing-777s.

5.11 Unmanned Dynamics AeroSim Blockset

AeroSim blockset is a MATLAB[®]/Simulink[®] block library for developing aircraft dynamic models with visualization interfaces to Microsoft Flight Simulator[®], FlightGear and other products. It was designed by flight control engineers at Unmanned Dynamics, LLC. It includes equations of motion, aerodynamics and propulsion models. It also contains an environmental model such as the atmosphere, wind, turbulence and gravity. It also provides transformation to and from various references. The AeroSim blocksets are built in C-code using simulation block components. It can be used for real-time HWIL simulation applications by generating C-code using Real-Time Workshop[®]. AeroSim can work on Windows[®] platforms with MATLAB[®] and Simulink[®] installed.

5.12 FlightGear Flight Simulator

FlightGear is an open source free flight simulator project available under general public licence. It is a unique project developed by the public, for the public and maintained and upgraded by the public. Anyone can contribute towards expansion and improvements of the code. It is a sophisticated flight simulator frame work for use in a research and an academic environment. The idea of FlightGear came from the problem that commercial PC based flight simulators are proprietary and do not give access to their source code for modification and enhancement. The FlightGear source code is available and can be altered by any person having sufficient understanding of programming. Many people involved in research and education could use the FlightGear frame work on which they can built their own project. FlightGear can run on Windows[®], linux[®], Mac OS-X[®], Solaris[®] and IRIX[®] platforms. FlightGear contains a flight dynamic model and an extensive and accurate world scenery database of over 20,000 real world airports. It also contains an accurate and detailed sky model. It contains a flexible and open aircraft modelling system in which the programmer can model a wide variety of aircraft. FlightGear does not require a sophisticated computer. It can work smoothly on a moderate PC with a reasonable

hardware accelerated 3D card with full OpenGL drivers. On a 1 GHz class CPU, with a GeForce graphics card, frame rates in excess of 60 frames per second are possible.

5.13 Conclusion

Driven by the steadily growing demands of the gaming industry, the performance of modern graphics processors has exceeded the computational power of CPUs both in raw numbers and in their extraordinary rate of growth. Today's GPUs have evolved into very sophisticated, highly programmable processing units. Programmability of consumer level graphics hardware has evolved at an increasing pace. In past many low cost PC based military simulators has been developed which uses COTS software.

Although, Nvidia GeForce and ATI Radon provides the best low- and mid-range hardware graphics solutions in the market. However, in this work, the Intel “*Extreme Graphic II*” integrated graphics processor has been used to keep the cost as low as possible and as well as get sufficient processing power to render scenes using MATLAB VR Toolbox.

VRML and Open Inventor™ are the two most widely used programmes for 3D virtual reality modelling. It is mainly because of the free graphical resources available from Blaxxun™ Interactive Institute and Silicon Graphics Institute SGI® [DUT04]. As MATLAB VR Toolbox uses VRML for virtual modelling thus in this work VRML has been used for developing 3D virtual world for IR signature modelling and simulation. An effort has been made to achieve functional realism using low cost hardware graphics and COTS software. The details of developing 3D virtual IR scene are given in Chapter-7 and 8.

